博士論文

エネルギー収支バランス
に基づく三次元準受動歩行機の歩容安定化

北見工業大学　医療工学専攻

生体メカトロニクス研究室

曹　贏（ゾ　イ）

Gait stabilization of a three-dimensional quasi-passive walker based on energy balance

CAO YING

Abstract

A passive walker can walk down a gentle slope powered only by gravity without any actuator and control. Its similarity to human gait implies that human walking may sufficiently utilize passive dynamics, and passive walkers have high energy efficiency. Therefore, study of passive walking contributes to an understanding of the mechanism of biped walking and to design and control of biped robots.

Stable passive walking can be realized under the condition of appropriate design, appropriate initial state and appropriate slope angle. However, it is difficult to stabilize passive walkers in variable environments, such as a variable slope with different slope angles and elastic coefficient. Therefore, addition of some stabilization control is necessary to stabilize the walking gait of passive walkers. Some researchers have focused on actuation of the hip, ankle and knee. However, most of these quasi-passive walkers can only walk on flat ground. In the previous study, it has been experimentally demonstrated that synchronization of the period of lateral motion T_L with the period of swing leg motion T_S is a necessary condition for stable 3D passive walking, which is used as a necessary stabilization condition and is named period stabilization condition in this research. In the next step, a mechanical oscillator actuated by a stepping motor has been mounted on a 3D passive walker with spherical feet, and can roll in the frontal plane to control T_{L} and to synchronize T_{L} into T_{S}. The movement of the mechanical oscillator is always entrained into the lateral motion of the quasi-passive walker based on forced entrainment realized by Van der Pol oscillator, and the quasi-passive walker can be stabilized on flat ground.

However, the problems of excess or deficiency of input energy from the mechanical oscillator exist under uncertain ground conditions due to the determination method of the amplitude of the mechanical oscillator based on period stabilization condition. In order to solve the problem, This research proposes a gait stabilization method based on energy balance and examines the method numerically and experimentally under uncertain ground condition. In this stabilization method, the target path of the mechanical oscillator is determined based on energy balance and forced entrainment. The energy balance means that the input energy in periodic stable walking is transformed to the dissipation energy and the change in potential energy of the quasi-passive walker during one step. If energy balance is satisfied, the change in kinetic energy during one step is equal to 0, which means that the quasi-passive walker can keep periodic stable walking. The stabilization method based on energy balance has two advantages. First, since energy balance can be satisfied in different ground conditions such as downward and upward slopes, the proposed method based on energy balance can stabilize the gait of the quasi-passive walker under complex and even uncertain ground conditions. Second, the control method does not rely on a specific parameter of gait, so the quasi-passive walker under the control based on energy balance is robust to the sudden change of the gait caused by the change of ground condition. Moreover, the energy transformation and the energy transfer of walking are investigated, and it is found that the input energy is transformed into the mechanical energy consumption and the change in potential energy during periodic stable walking.

In chapter 1, the background of the research is introduced. In chapter 2, simulation model and experimental quasi-passive walker are introduced, and uphill-, level-waking and turn control methods based on stabilization control are proposed. The proposed methods are examined numerically and experimentally, and the results are indicated. In chapter 3, energy efficiency of downhill-, uphill- and level-walking are investigated numerically and compared with other biped robots and human walking. Energy transformation and energy transfer of walking are investigated to show the importance of energy balance for stable walking by using Open Dynamics Engine simulation. In chapter 4, a stabilization algorithm based on energy balance is proposed and examined numerically and experimentally under uncertain ground condition, and a direct method and an indirect method are proposed to calculate the input energy based on energy balance. Moreover, the dynamics of lateral motion of the quasi-passive walker is introduced, and the relation between the amplitude of the mechanical oscillator and mechanical work performed by the quasi-passive walker is investigated analytically based on the dynamics of the lateral motion of the quasi-passive walker. In chapter 5, the proposed methods including direct method and indirect method are examined under uncertain ground conditions. In chapter 6, some conclusions and findings of the research and future work are summarized.

Gait stabilization of a three-dimensional quasi-passive walker based on energy balance

Contents

1. **Introduction……..1**
1.1 Background……..1
1.2 Research about passive walking……...4
1.2.1 Passive walkers……...4
1.2.2 Quasi-passive walkers……5
1.3 Introduction of the thesis……7
1.4 Thesis outline……11
2. Stabilization control based on forced entrainment……..12
2.1 Introduction……....12
2.2 Simulation model and experimental quasi-passive walker……13
2.2.1 Simulation model……..13
2.2.2 Experimental quasi-passive walker……20
2.3 Stabilization control algorithm……..22
2.4 Uphill and level walking……..25
2.4.1 Control algorithm……25
2.4.2 Simulation……26
2.4.3 Comparison of control methods……..30
2.5 Turn control……..33
2.5.1 Control algorithm……33
2.5.2 Simulation and experiment……..38
2.5.3 Comparison of turn and straight walking……..43
2.6 Conclusion……48
3. Energy transfer, transformation and efficiency of walking……...49
3.1 Introduction……49
3.2 Mechanical cost of transport in uphill and level walking……..49
3.3 Energy efficiency and energy transformation……52
3.4 Comparison of energy efficiency under different control methods……...58
3.5 Mechanical energy transfer and transformation……60
3.6 Conclusion……..63
4. Stabilization method based on energy balance……...64
4.1 Introduction……64
4.2 Relationship between the amplitude of the mechanical oscillator and the work performed by the quasi-passive walker…….....…65
4.2.1 Dynamics of lateral motion of the quasi-passive walker with spherical foot sole……65
4.2.2 Simplified model of switching of stance leg…….....….…69
4.2.3 Relationship between the amplitude and the work ……72
4.3 Energy balance in stable walking……78
4.4 Direct method for the determination of the amplitude of the mechanical oscillator……...79

4.4.1 Dissipation energy……79
4.4.2 Potential energy……80
4.4.3 Determination of the amplitude based on input energy……82
4.4.4 Simulation in the condition of a flat ground……84
4.5 Indirect method for the determination of the amplitude of the mechanical oscillator……87
4.5.1 Transformation of the energy balance equation……88
4.5.2 Potential energy……90
4.5.3 Kinetic energy……91
4.5.4 Mechanical work performed by the quasi-passive walker……94
4.5.5 Determination of amplitude based on input energy……97
4.6 Conclusion……98
5. Examination of the environmental adaptability of the quasi-passive walker……99
5.1 Introduction……99
5.2 Examination of the direct method for the determination of the amplitude by simulation ……100
5.2.1 Walk on a constant angle slope……100
5.2.2 Walk on a changeable slope……105
5.2.3 Walk on a flat ground with different coefficients of restitution……111
5.3 Examination of the indirect method for the determination of the amplitude by simulation……115
5.3.1 Walk on a changeable slope……115
5.3.2 Walk on a flat ground with different coefficients of restitution……121
5.4 Examination of the indirect method by experiments……125
5.4.1 Hardware structure……125
5.4.2 Experiment on changeable slope……127
5.4.3 Experiment on a flat ground with different coefficient of restitution……132
5.5 Conclusion……137
6. Conclusion……138
Acknowledgement……141
Bibliography……142
Publications and presentations……148

1. Introduction

1.1 Background

Biped walking robots, which have a similar gait to humans, can walk under complex ground conditions such as uneven terrain, upward or downward stairs or slopes. Biped walking robots can adapt to more complex environments in comparison to other kinds of mobile robots. It is thus expected that biped walking robots can substitute human beings in various environments including dangerous, tiresome or repetitive situations.

Humanoid robots, which are a kind of biped walking robots, have similar appearance and body structure as humans. It is possible for these robots to work in environments where humans live and work. For example, these robots can function in entertainment and public service sectors.

Research of biped walking robots can help us to understand the mechanism of biped walking and also human walking. The mechanism of biped walking can be applied to rehabilitation therapy and biomedical engineering. Moreover, the research of biped walking robots also contributes to the theory and technology of designing lower extremity exoskeletons, rehabilitation devices, and intelligent prosthesis [1]-[4].

However, controlling biped walking robots and stabilizing their gaits are challenging, because biped walking robots are multi-variable, non-linear, unstable, and hybrid dynamic systems. Some successful attempts have been made to build humanoid robots, and one of the most successful examples is the ASIMO of Honda [5]-[7]. In order to ensure stability of walking, the target path of the zero moment point (ZMP), which is proposed by Vukobratović and Stepanenko [8][9], is calculated before walking. If the ZMP remains strictly inside the support polygon of the support foot, the support foot does not turn over on the ground, and thus the robot can be treated and controlled as a fixed manipulator. This method is not only used for ASIMO but also for most of humanoid robots, such as HPR-4C [10] and QRIO [11].

All joint trajectories are planned based on the method using ZMP, and the position of limbs and the angle of joints are controlled with servo motors, like the control method for robotic manipulators. Since electrical motors usually have relatively low

torque but high speed, it is necessary to use reduction gear to increase the output torque of servo motors. However, since reduction gear increases both inertia of the segments and friction of joints, it is difficult to control the actual torque output on the limbs. Moreover, due to the drawback of the trajectory tracking control method, it's hard to utilize the natural dynamics of legs, such as the natural pendulum motion of a swing leg, resulting in low energy efficiency of walking and unnatural gait as compared with human walking. For example, the mechanical cost of transport (C_{mt}), which is an index of measuring the energy efficiency of transport, of ASIMO is 20 times of a human's [12]. The trajectory tracking control method cannot reveal the mechanism of natural dynamics and the energy efficient gait of human walking. Therefore, it is necessary to study the mechanism of natural dynamics of walking to improve the energy efficiency of biped walking robots, and to improve the practical application of biped walking robots.

Research of passive walkers provides a new and different research paradigm of the biped walking robots in comparison to the biped robots mentioned above. Passive walkers are a class of machines which can walk stably on a slightly downward slope without sensors, control, or actuators. Passive walkers display a steady gait, which is energy efficient and incredibly natural like human walking. The research of passive walking mainly focuses on the analysis of passive gait, control method, walking stability, and the dynamics of passive walking.

Passive walker was first studied in depth by McGeer [13]-[15]. McGeer successfully designed and analyzed several planar passive walkers with and without knees. His walkers exhibited stable, natural and human-like walking on a slightly downward slope. Unlike the biped walking robots, which are controlled to follow pre-designed trajectories, passive walkers exhibit natural gaits resulted from the natural interaction between passive walkers and their environment including the slope angle, friction and collision condition etc. McGeer thought that, the passive dynamics, stability and control of biped walking could be learned by studying passive walkers [13], in the same way that the aviation engineers studied aerodynamics from gliders, which are also passive machines. Studies of passive walking may contribute to the

understanding of the mechanism of stability and the energy efficient gait of human walking, as well as the design and control of biped walking robots.

Stable passive walking can be realized under the condition of appropriate mechanical design, appropriate initial state and appropriate ground condition, such as slope angle and coefficient of restitution of ground. [16] However, it is difficult to stabilize passive walkers in complicated environments, such as a variable slope with different slope angles and coefficient of restitution. For this reason, addition of some control and actuation based on the characteristics of passive walking is necessary to stabilize passive walkers under variable ground conditions. Inspired by the simplicity of passive walkers, some researchers have attempted to realize two-dimensional (2D) [15]-[23] and three-dimensional (3D) [24]-[27] passive walking on level ground. These passive walkers with control and actuation are named quasi-passive walkers, which are different from those biped walking robots based on trajectory tracking control such as the common humanoid robots. Although some joints of quasi-passive walkers are actuated and controlled, quasi-passive walkers still preserve the natural dynamics, which means that the interaction between the passive walkers and their environment still exists.

Most quasi-passive walkers proposed by researchers can walk on flat ground only at present. It is necessary to stabilize their gait under more complex and even uncertain ground conditions, because it is difficult to measure the precise ground condition in an actual environment. Here, uncertain ground condition means that the ground information such as the slope angle and coefficient of restitution of ground is unknown. Since the passive walking gait is a result of the interaction between the passive walkers and their environment, the gait contains the information of the environment (or ground condition). If the information can be used to control quasi-passive walkers in an appropriate way, it is possible to stabilize the gait of quasi-passive walkers under complex and even uncertain ground conditions.

1.2 Research about passive walking

1.2.1 Passive walkers

The first passive walker, which had a huge impact on the research of biped walking, was McGeer's 4-legged passive walker that had 4 side-by-side legs with knees but no torso. The passive walker could be treated as a planar biped passive walker and was built for the analysis of gait, dynamics, and stability of walking [13]. Despite the 4-legged design, the passive walker had a gait that was incredibly natural like human walking. Other planar passive walkers were also studied by some researchers. Ikemata et al. built a planar biped passive walker with arc feet, and studied the dynamic effects of arc feet on the leg motion of the passive walker [28].

Two dimensional (2D) research of passive walking was extended to 3D by some researchers [29]-[35]. The first successful 3D experimental passive walker was the Tinkertoy walker built by Coleman et al. [29] without knees, and it was later mathematically modeled and shown stable [29][30]. However, Tinkertoy walker requires large masses to be put on extended booms to obtain sufficient moments of inertia. Collins et al. built a 3D biped passive walker which successfully demonstrated downhill walking [31].

Further research about passive walking has been performed. For example, Coleman et al. studied bifurcation and chaos phenomenon of passive gaits [36]. And Smith and Berkemeier discovered and analyzed a passive quadruped walking mechanism [37].

The research about gait stability of passive walkers and quasi-passive walkers is less encouraging. Although stability of several passive walkers has been numerically predicted by simulations, there are almost no rigorous analytic theories of stability of passive walking, and thus there are almost no rigorous analytic methods to improve stability.

An objective measure of stability is the norm of the largest eigenvalue of the Jacobian of the state transition equation of the periodic walking cycle [13]. The norm of this eigenvalue indicates how fast the disturbances would grow or shrink after a small disturbance which deviates the passive walker from a steady-state periodic motion. If the largest eigenvalue has a norm less than one, the periodic cycle is stable.

According to this analysis method, when the norm of all eigenvalues is far less than one in value, the passive walker has strong stability. In general, typical passive walkers have only mild stability by this measure, because their norm of the largest eigenvalues are usually larger than 0.6 [30][38].

Some researchers treated passive walking as one kind of periodic motion and studied the stability of passive walking using limit-cycle and Poincaré map of the periodic motion [39]-[47]. These methods are essentially same to the one using transition equation proposed by McGeer, and the fixed point of Poincaré map is the periodic solution of transition equation.

1.2.2 Quasi-passive walkers

There have been attempts to realize passive walking on level ground by adding actuation and control while preserving the passive dynamics. Collins and Ruina [24] built a 3D quasi-passive walker which walks successfully on level ground. The quasi-passive walker has passive hip joints and powered ankles, as shown in Fig. 1-1 (a). The ankle motor loads up an ankle spring during the single support phase. When the swinging leg touches the ground, the ankle spring is released. And the released spring generates an ankle push-off that actuates the quasi-passive walker to walk. The quasi-passive walker based on passive dynamics is quite energy efficient. For example, the 12.7 kg quasi-passive walker built by Collins and Ruina [24] uses only 12 W to walk at 0.44 m/s on level ground. The walking energy efficiency of the quasi-passive walker is close to human efficiency [12][24]. Harata et al. reported a biped quasi-passive walker with only knee actuation controlled by a parametric excitation method [48]. Russ Tedrake et al. [25] investigated a 3D biped passive walker “Toddler” with large curved feet and active ankle joints, rolling motions of which are controlled by utilizing a sine oscillator in order to excite the overall lateral motion of the quasi-passive walker, as shown in Fig. 1-1 (b).

Some researchers have focused on pitching control of the upper body based on planar walking models. McGeer added an upper body to his planar walking model and maintained a constant gesture of the upper body by using a PD controller [49]. Wisse

et al. investigated a planar walking model with the upper body constrained to the middle angle of the two legs [46]. Narukawa et al. showed that a planar walking model can walk on level ground efficiently by utilizing upper body and swing leg control [50]. However, few researchers have focused on rolling control of the upper body based on 3D passive walkers. In walking of humans, the upper body not only pitches in the sagittal plane but also rolls in the frontal plane. Kuo reported that upper body control can be utilized to stabilize lateral motion of a 3D passive walker, but his method was energy-inefficient for his walking model and was thus not investigated sufficiently [51].

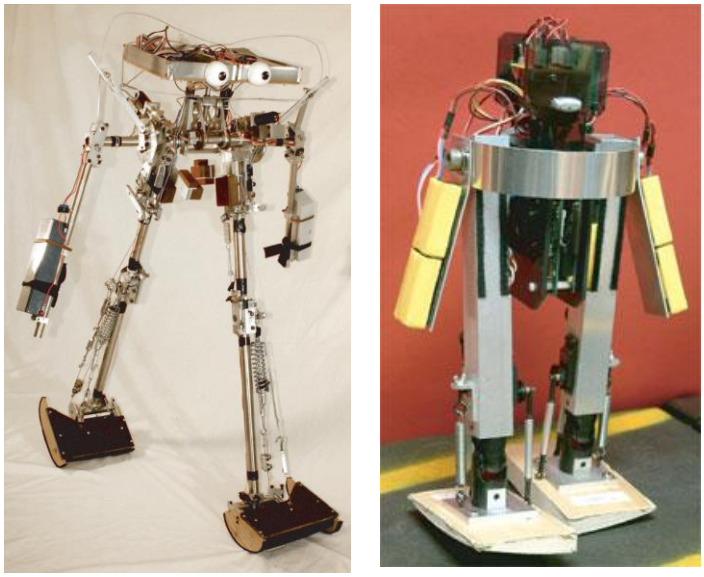

(a) Collins's quasi-passive walker [24]

(b) Tedrake's quasi-passive walker [25]

Fig. 1-1 Two quasi-passive walkers

1.3 Introduction of the thesis

In this study, it has been experimentally demonstrated that synchronization of the period of lateral motion T_{L} with the period of swing leg motion T_{S} was a necessary condition for stable 3D passive walking [32]. In the next step, a 3D passive walker with large spherical foot sole is built to increase the success rate of walking, and a mechanical oscillator actuated by a motor is mounted on the passive walker. The mechanical oscillator can roll in the frontal plane to control T_L and to synchronize T_L into T_S to stabilize the gait of the quasi-passive walker on level ground [52]. The movement of the mechanical oscillator is always entrained into the lateral motion of the quasi-passive walker based on forced entrainment realized by forced Van der Pol oscillator, and the quasi-passive walker can be stabilized on flat ground [52][53]. The control method is named "stabilization control algorithm" in this study.

In this thesis, to improve the environmental adaptability of the 3D quasi-passive walker, a gait stabilization method based on energy balance is proposed and examined under more complex ground conditions including uncertain ground conditions. Here, the environmental adaptability means that quasi-passive walkers can stably walk under variable ground conditions and adapt to the changing ground conditions such as slope angle and coefficient of restitution.

First, uphill walking, level walking and turn control methods are proposed and examined based on the "stabilization control algorithm". Second, the energy efficiency, energy transformation and energy transfer of walking of the quasi-passive walker are investigated. Third, the dynamics of lateral motion of the quasi-passive walker is indicated. Further, the relationship between the amplitude of the mechanical oscillator and the mechanical work performed by the quasi-passive walker is investigated analytically based on the dynamics of the lateral motion. Fourth, based on energy balance and the "stabilization control algorithm", a gait stabilization method is proposed and examined under uncertain ground conditions. The amplitude of the mechanical oscillator is determined by the required input energy in one step.

The gait of quasi-passive walkers can be understood as a result of the interaction between the quasi-passive walkers, their controllers and their environment. The

interaction means that the change of quasi-passive walkers, their controllers or their environment can change the gait of the quasi-passive walkers. By understanding the generation patterns of the gait of quasi-passive walkers, it helps to design appropriate control algorithm for the quasi-passive walkers. The generation patterns of the gait of passive and quasi-passive walkers are shown in Fig. 1-2. The color lines represent the actions of the environment, quasi-passive walkers, and controllers on the gait. The generation pattern of the gait of passive walkers is an open-loop structure, as shown in Fig. 1-2 (a). Passive walkers can exhibit different gaits if the parameters of both environment and passive walkers are changed in stable region, which is generally very small.

In contrast, the generation pattern of the gait of the quasi-passive walker proposed in this research is a closed-loop structure. The controller uses the gait information, which indirectly contains the information of the quasi-passive walker, its environment, and its controller, as shown in Fig. 1-2 (b). Here, the gait information of the quasi-passive walker refers to the information acquired from walking motion, including the attitude of the quasi-passive walker, the periods of swing leg motion, and the angular velocity of the segments of the quasi-passive walker and so on. Although no external sensor is used to detect the information of environment, it is possible to improve environmental adaptability of the quasi-passive walker by using the gait information in an appropriate way. Based on this idea, the periodic lateral motion (the gait in the frontal plane) of the quasi-passive walker has been utilized to entrain the periodic motion of the mechanical oscillator based on forced entrainment to stabilize the quasi-passive walker [52].

This thesis extends the idea to stabilize the gait of the quasi-passive walker based on energy balance under complex and uncertain ground conditions. The energy balance means that the input energy in periodic stable walking is transformed to the dissipation energy and the change in potential energy of the quasi-passive walker during one step. If energy balance is satisfied, the change in kinetic energy during one step is equal to 0, which means that the quasi-passive walker can keep periodic stable walking. The stabilization control method based on energy balance has two

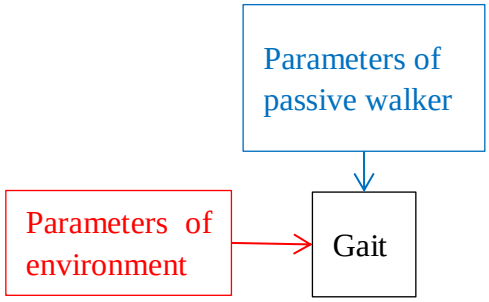

(a) Passive walker

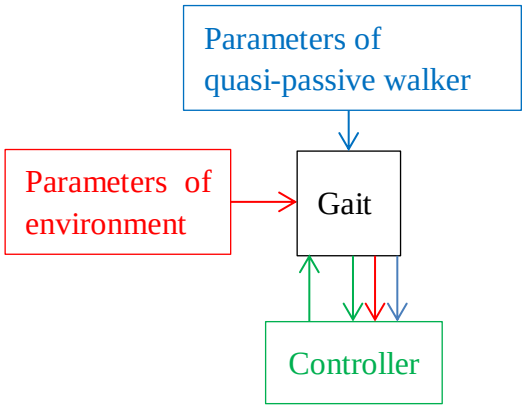

(b) The quasi-passive walker proposed by this research

Fig. 1-2 Generation patterns of the gait of passive and quasi-passive walkers

advantages. First, since energy balance can be satisfied in different ground conditions such as downward and upward slopes, the proposed method based on energy balance can stabilize the gait of the quasi-passive walker under complex and even uncertain ground conditions. Second, the control method does not rely on a specific parameter of gait, so the quasi-passive walker under the control based on energy balance is robust to the sudden change of the gait caused by the change of ground condition.

Two quasi-passive walkers similar to ours are the Tedrake's "Toddler" [25] and the quasi-passive walker proposed by D. Nakanishi et al [54]. "Toddler" was used to test the utility of motor learning, and it is demonstrated that "Toddler" could learn to walk on flat ground by using its passive walking trajectory as the target [12]. Another similar quasi-passive walker proposed by Nakanishi et al. also has curved feet and excites its lateral motion by a sine oscillator. The difference between "Toddler" and the Nakanishi et al.'s quasi-passive walker is that the oscillator moves from side to side on its hip axis in the method proposed by Nakanishi et al..

"Toddler" is stabilized by direct excitation of a sine oscillator. As a result, the entrainment can occur only when the frequency of the sine oscillator is tuned to near the passive step frequency of the quasi-passive walker. Furthermore, the "Toddler" must be initialized in phase with the sine oscillator and the entrainment is very sensitive to disturbance in phase [25].

In contrast, our quasi-passive walker is robust against initial condition and disturbance, because the dynamics of the mechanical oscillator is always forcedly entrained into the dynamics of lateral motion in order to excite or damp the lateral motion of the quasi-passive walker. Even when the gait of the quasi-passive walker is changed in varying environments, the gait of the quasi-passive walker can still be stabilized. Consequently, the environmental adaptability of "Toddler" is worse than ours. More detailed investigation and comparison about the two methods are performed, and the results and analysis are presented in section 2.4 of the thesis.

1.4 Thesis outline

In chapter 2, simulation model and experimental quasi-passive walker are introduced, and uphill walking, level walking and turn control methods based on "stabilization control algorithm" are proposed. The proposed methods are examined numerically and experimentally, and the results are presented.

In chapter 3, energy efficiency of downhill, uphill and level walking are investigated numerically, and compared with other biped robots and human walking. Energy transformation and energy transfer of walking are also investigated using ODE simulation to show the importance of energy balance.

In chapter 4, first, in order to calculate the amplitude of the mechanical oscillator β, the relationship between β and mechanical work performed by the quasi-passive walker is investigated analytically based on the dynamics of lateral motion. Second, energy balance is defined, and the gait stabilization method based on energy balance is proposed. In order to determine the amplitude the mechanical oscillator based on energy balance, a direct and an indirect method are proposed.

In chapter 5, in order to verify the environmental adaptability of the quasi-passive walker under uncertain ground conditions including different slope angles and coefficients of restitution, the proposed stabilization methods based on energy balance is examined numerically and experimentally. The direct and an indirect method are compared with each other by simulation.

In chapter 6, some conclusions of the research and future work are summarized.

2. Stabilization control based on forced entrainment

2.1 Introduction

In this chapter, in order to stabilize the quasi-passive walker in uncertain ground condition, the "stabilization control algorithm" based on forced entrainment is improved to enable the quasi-passive walker stably walk on a gentle upward slope and turn on a flat ground.

In the previous researches [32], it was experimentally shown that synchronization of the period of lateral motion T_L with the period of swing leg motion T_S was a necessary condition for stable 3D passive walking, and the necessary condition is named "period stabilization condition". In the next step, a mechanical oscillator actuated by a motor was mounted on a 3D passive walker with spherical feet, and can roll in the frontal plane to synchronize the period of lateral motion T_L with the period of swing leg motion T_S [52]. The period of the target trajectory of the mechanical oscillator is generated based on forced entrainment. If the movement of the quasi-passive walker is changed by disturbance in walking, the movement of the mechanical oscillator is always entrained into the lateral motion of the quasi-passive walker based on forced entrainment to stabilize the quasi-passive walker. Therefore, the quasi-passive walker is robust against disturbance. The amplitude and phase of the trajectory are planned separately.

The quasi-passive walker can stably walk on a flat ground by utilizing the "stabilization control algorithm" [52]. However, it is difficult to stabilize the quasi-passive walker in uphill walking, because the amplitude of the mechanical oscillator is not large enough, and the input energy is not enough for uphill walking by using the previous "stabilization control algorithm". In this chapter, the determination method of the amplitude of the mechanical oscillator is improved for uphill walking, and the control methods are numerically examined.

Further, in variable environments, the ability to turn is necessary for a biped quasi-passive walker to change walking direction and avoid obstacles. For the purpose of improving adaptability of the quasi-passive walker to varying environments, a turn control method was proposed and numerically examined [55]. However, such method

cannot appropriately apply to our experimental quasi-passive walker, because the target trajectory of the mechanical oscillator becomes discontinuous when the stance leg changes. Because the power of the motor of the experimental quasi-passive walker is limited and the mechanical oscillator cannot follow the discontinuous target trajectory, the experimental quasi-passive walker fails to turn. In this chapter, a novel turn control method is proposed. Proposed method uses the central axis of oscillation of the mechanical oscillator to shift the gravity center of the quasi-passive walker to control turn radius, and enables the quasi-passive walker to turn stably on flat ground. This new method is examined experimentally and numerically.

First, the simulation models, experimental quasi-passive walker and the "stabilization control algorithm" proposed in the previous researches are introduced. Two versions of the simulation models are introduced in this research. Version 1 is the simulation model of the former experimental quasi-passive walker, and version 2 is the simulation model of the current experimental quasi-passive walker, which is improved based on the former quasi-passive walker. Second, control methods for uphill walking, level walking, and turn control are proposed based on the "stabilization control algorithm". The control methods are numerically and experimentally examined.

2.2 Simulation model and experimental Quasi-passive walker

2.2.1 Simulation model

The quasi-passive walker consists of a mechanical oscillator, a motor, a trunk and two straight legs, as shown in Fig. 2-1. The simulation model in Fig. 2-1 is the version 1 of the quasi-passive walker. The quasi-passive walker has three joints: two passive joints connecting the legs with a hip axis, and one active joint driven by a motor that actuates a mechanical oscillator in the frontal plane. At least six generalized coordinates are necessary to describe the dynamics of the quasi-passive walker by Lagrangian mechanics: three coordinates are used to describe the orientation of the stance foot and the other three are used to describe the rotational angles of the three joints. In addition, the quasi-passive walker is a non-holonomic system because the spherical stance-foot rolls on the ground during walking. In order to reduce the

mathematical complexity, Open Dynamics Engine [56] (ODE) (a 3D rigid-body physical simulation engine) is used to conduct simulations.

In order to describe the position and orientation of the quasi-passive walker in ODE simulation, the global coordinate O–XYZ is defined as shown in Fig. 2-1. The orientation of the trunk relative to the coordinate O–XYZ is determined by the sequence of rolling (θ), pitching (γ), and yawing (ψ) about the axes of O–XYZ. The trunk and the mechanical oscillator have the same pitch (γ) and yaw (ψ) angles but can roll independently.

Therefore, the relative roll angle of the mechanical oscillator to the trunk is defined as θ_w. The trunk and the legs have the same roll angle (θ) but different yaw and pitch angles. The pitch angles of the left and right legs are therefore denoted by γ_L and γ_R, respectively, and the yaw angles of the left and right legs are denoted by ψ_L and ψ_R, respectively. Finally, the state vector of the quasi-passive walker is described as shown in Eq. (2.1).

$$q = [\theta, \theta_w, \gamma, \gamma_L, \gamma_R, \psi, \psi_L, \psi_R, \dot{\theta}, \dot{\theta}_w, \dot{\gamma}, \dot{\gamma}_L, \dot{\gamma}_R, \dot{\psi}, \dot{\psi}_L, \dot{\psi}_R] \tag{2.1}$$

The body coordinates of the mechanical oscillator and the trunk are defined as o_1–$x_1y_1z_1$ and o_2–$x_2y_2z_2$, respectively, as shown in Fig. 2-1. The origins of the coordinates o_1 and o_2 are fixed on the centers of masses of the mechanical oscillator and the trunk, respectively. The body coordinates of the legs are omitted in Fig. 2-1. These body coordinates are used in the calculation of rotational kinetic energy of the segments of the quasi-passive walker.

In the single support phase, the spherical stance foot purely rolls on the ground without slip, and the swing leg swings ahead like a pendulum. The swing leg continues to leave the ground until the roll angle θ becomes 0. The double support phase is assumed to be instantaneous, and the motion of the swing foot reaching the ground is regarded as heel-strike. The heel-strike is assumed to be inelastic and without sliding. The frictions of the joints are set to 0 in the ODE simulation.

The pitching motion of the trunk is uncontrollable, but the rolling motion of the mechanical oscillator around the x_1-axis is controllable. The trunk is fixed at the hip

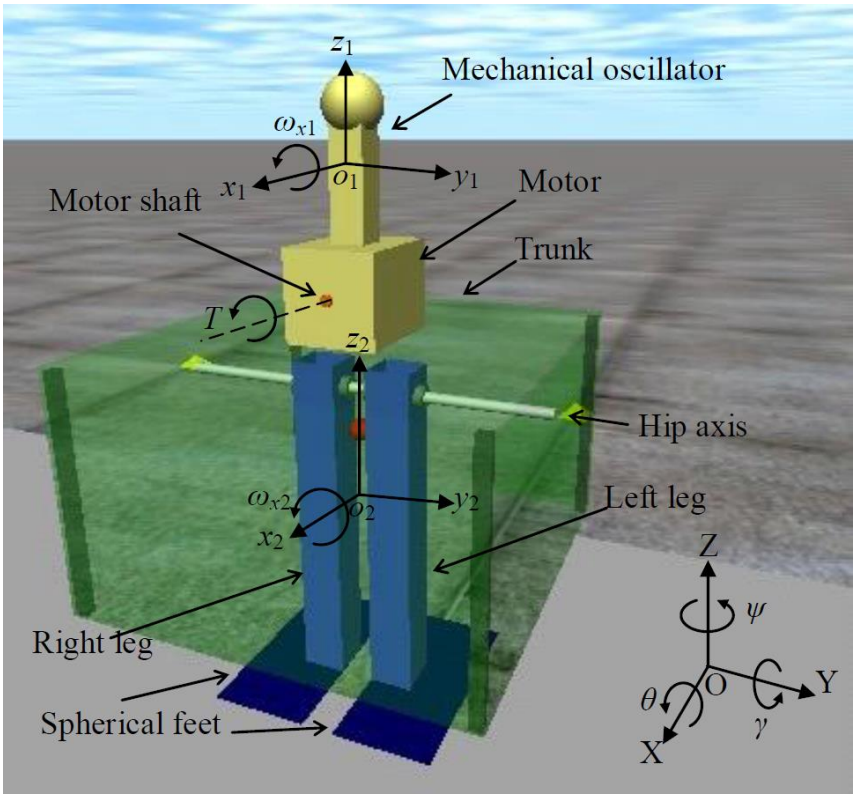

Fig. 2-1 Overview of simulation model of the quasi-passive walker (Version 1)

Table 2-1 Mass of segments of the quasi-passive walker

	Trunk: m_T	Right leg: m_{LR}	Left leg: m_{LL}	Mechanical oscillator: m_o	Total: M
Mass[kg]	9.404	0.9760	0.9760	1.170	12.53

Table 2-2 Moment of inertial of segments of the quasi-passive walker

Moment of inertia [N・m^2]	Trunk: I_T	Right leg: I_{LR}	Left leg: I_{LL}	Mechanical oscillator: I_i
body axis x	0.1940	0.006300	0.006300	0.001399
body axis y	0.1650	0.007968	0.007968	0.001399
body axis z	0.1870	0.002926	0.002926	0.0002760

axis to mount the motor and the mechanical oscillator on the passive walker, and the trunk has the function of ballast to keep the mechanical oscillator upright. The mechanical oscillator is analogous to the upper portion of the human torso above the waist. The mass and moment of inertial of the segments of the quasi-passive walker are shown in table 2-1 and table 2-2. In table 2-2 the moment of inertia of each segment is defined about the body axes *xyz* of the segment, which pass through the center of mass of the segment. The soles of the feet of the quasi-passive walker are spherical. The centers of the spheres are designed to be higher than the center of mass of the quasi-passive walker in order to make the quasi-passive walker stable in a standing posture, as shown in Fig.2-2. Further, the quasi-passive walker is quite robust against disturbances due to the spherical feet.

The geometric design of the feet is symmetric with respect to front and back, but the mass distribution of the feet is not symmetric. The center of masses of the feet are regulated backward to generate a rotation moment around hip axis, and thus the swing leg can naturally swing forward even on a slight upward slope, as shown in Fig. 2-3. The gravitational force of the left leg is represented by G_L, δ_L is the pitch angle of the center of mass of the left leg relative to hip joint, $G_L\sin\delta_L$ is the component force of G_L, τ_L is the rotational torque of the left leg generated by $G_L\sin\delta_L$, the rotation axis is the hip axis, and L_L is the moment arm of τ_L. In experimental quasi-passive walker, the mass distribution of the feet can be changed by putting a weight on each foot.

When the quasi-passive walker walks on a slight upward slope, because of the design of the spherical foot sole, a rotational torque is generated around the contact point between the stance foot and the ground, as shown in Fig. 2-3. The gravitational force works on the quasi-passive walker is represented by G_r, δ_r is the pitch angle of the center of mass of the quasi-passive walker relative to the contact point with ground, $G_r\sin\delta_r$ is the component force of G_r, τ_r is the rotational torque of the quasi-passive walker generated by $G_r\sin\delta_r$, the rotation center is the hip axis, and L_r is the moment arm of τ_r.

In uncertain ground condition, for example an upward slope or soft ground, the quasi-passive walker needs more power to stabilize it, but the power of a real motor is

limited. One method is to decrease the mass of the quasi-passive walker. Therefore, the construction of the trunk of the simulation model is improved, as shown in Fig. 2-4. The simulation model in Fig. 2-4 is the version 2 of the quasi-passive walker. Compared to the version 1, the height of the trunk is decreased, and the arm and batteries are fixed to the trunk to lower the center of mass of the trunk and to increase the moment of inertia about yaw axis. A low position of the center of mass of the trunk can keep the mechanical oscillator upright, and large moment of inertia about yaw axis can improve the stability of the quasi-passive walker about yaw axis. Besides the trunk, other construction of version 2 of the simulation model is the same as the construction of version 1.

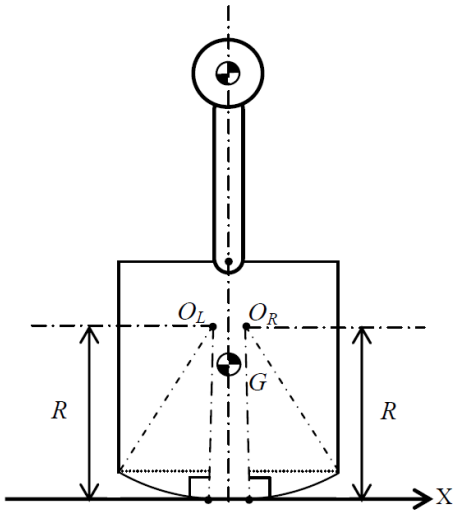

(a)

Fig.2-2 Two dimensional simplified model with curved feet

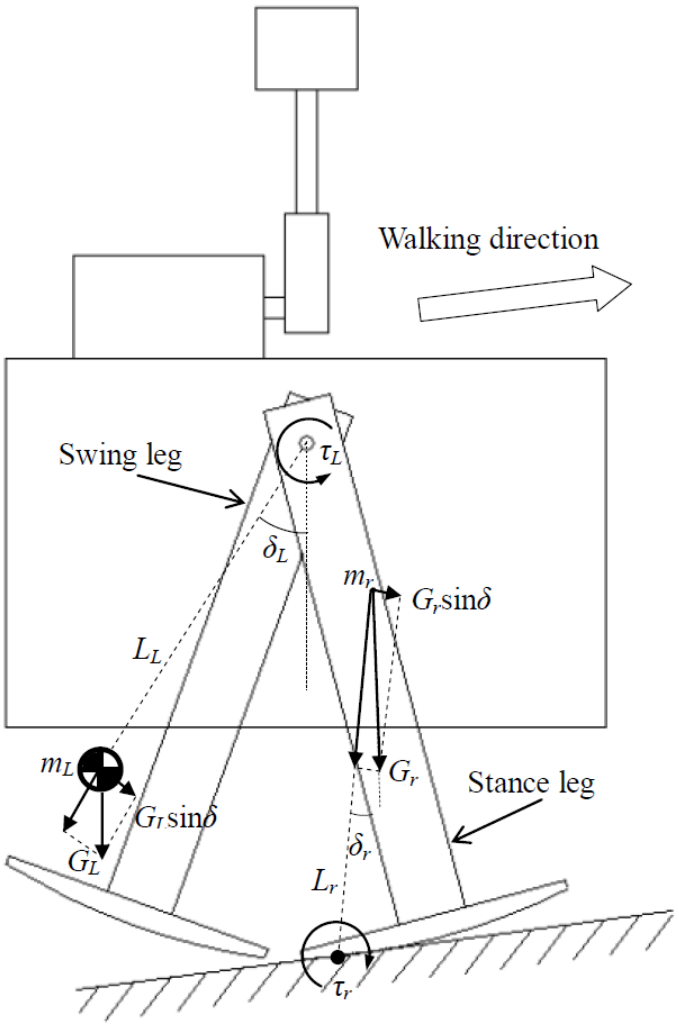

Fig. 2-3 Rotational torques of the legs generated by gravity in uphill walking

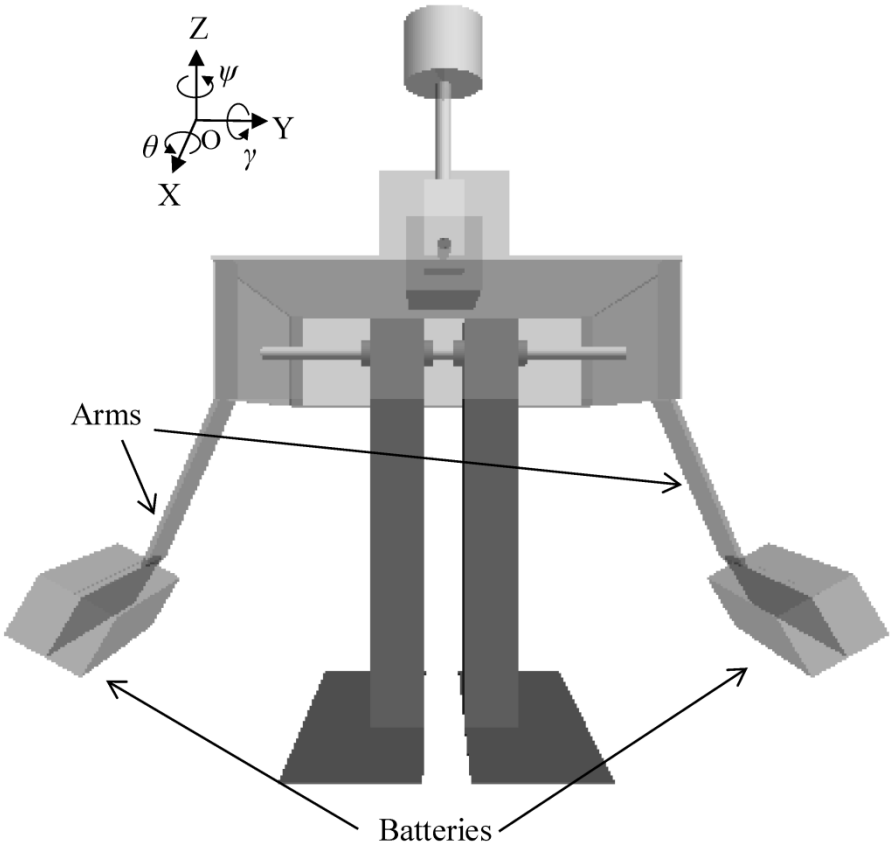

Fig. 2-4 Simulation model (Version 2) with less mass and lower center of gravity than the version 1of the simulation model in ODE simulation

2.2.2 Experimental quasi-passive walker

The construction of the experimental quasi-passive walker is the same as the construction of version 2 of the simulation model. The quasi-passive walker is composed of two straight legs, a trunk, a stepping motor and a mechanical oscillator, as shown in Fig.2-5 (a). In the experiment of turn control, a 1-axis acceleration sensor is fixed on the MCU circuit board to measure the acceleration in the direction which is parallel to the central line of the quasi-passive walker.

The legs are connected to hip axis by two passive joints, and the relative angles between the legs and the hip axis are measured by utilizing two rotary encoders, as shown in Fig.2-5 (b). The center of mass of the feet is adjusted backward by weights so that the swing leg can naturally swing forward even on a flat ground, as shown in Fig.2-5 (b).

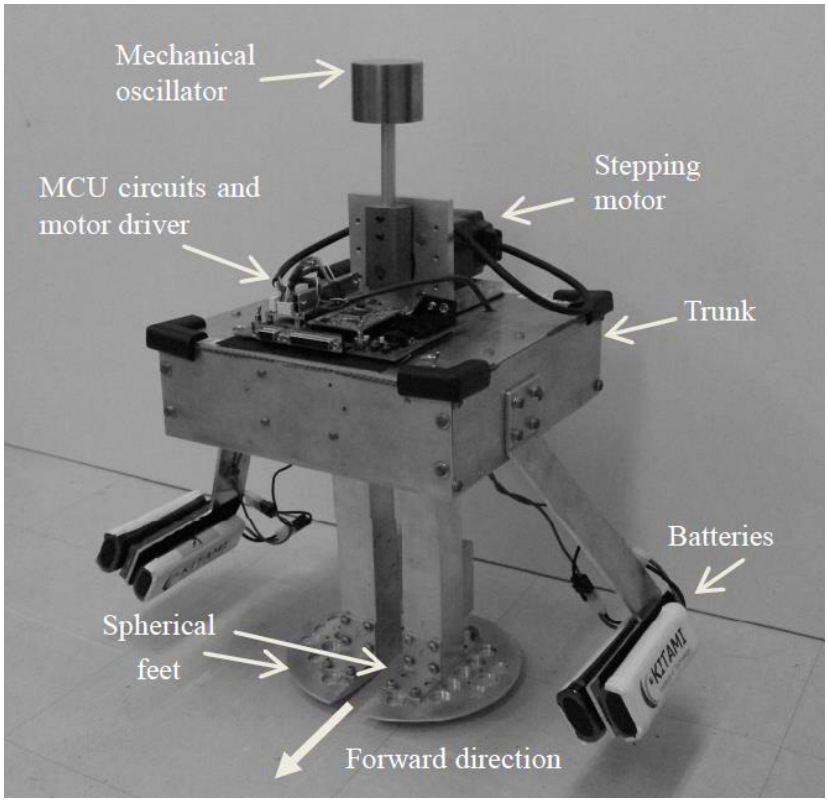

(a) Experimental quasi-passive walker

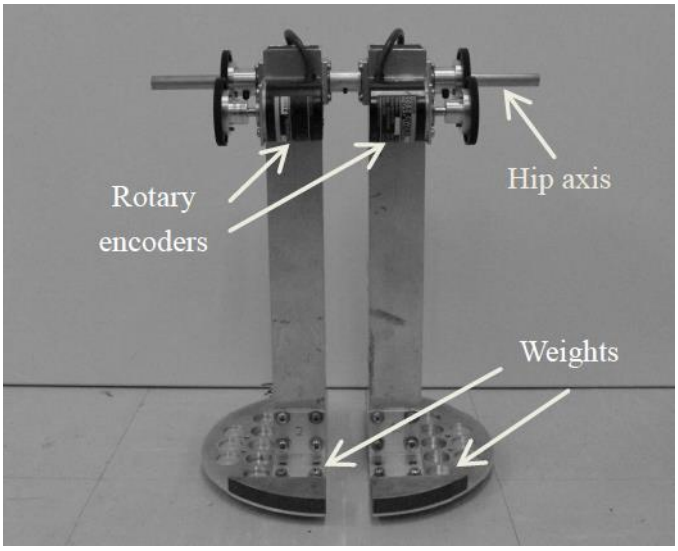

(b) Back view of the legs and the hip axis

Fig. 2-5 Experimental quasi-passive walker based on a passive walker.

2.3 Stabilization control algorithm

In variable environments, a quasi-passive walker will changes its gait and the gait may become unstable because of the disturbance from the environments. If the change of gait caused by environments can be utilized in an appropriate way to stabilize the quasi-passive walker, the environmental adaptability of the quasi-passive walker may be improved. Based on this idea, the periodic lateral motion of the quasi-passive walker in walking is utilized to entrain the periodic motion of the mechanical oscillator based on forced entrainment.

In previous study, it has been experimentally demonstrated that synchronization of the period of lateral motion T_L with the period of swing leg motion T_S is a necessary condition for stable 3D passive walking [32]. The necessary condition is called "period stabilization condition" in this research. In the next step, a mechanical oscillator actuated by a motor has been mounted on a 3D passive walker with spherical feet, and can roll in the frontal plane in order to change T_L and to synchronize T_L with T_S [52]. Because swing leg motion is passive, T_S cannot be changed directly. Thus, T_L is changed and synchronized with T_S by the motion of the mechanical oscillator in the frontal plane. In order to adjust the period of lateral motion T_L, the mechanical oscillator can excite or damp the lateral motion by changing the phase of the mechanical oscillator. The motor of the simulation model is controlled by a simple PD controller to trace the target trajectory of the mechanical oscillator. The target trajectory of the mechanical oscillator θ_{wt} is planned according to the period, amplitude and phase, as shown in Fig. 2-6.

The period of the target trajectory is controlled on the basis of forced entrainment, which is an interesting phenomenon in nonlinear vibrations [57], and forced entrainment is realized on the basis of forced van der Pol equation as follows [52]:

$$\ddot{y} - \varepsilon(1 - y^2)\dot{y} + \Omega_V^2 y = K\theta, \tag{2.2}$$

where the roll angle θ of lateral motion of the quasi-passive walker is input for Eq. (2.2) as a periodic force input. The self-excited angular frequency of Eq. (2.2) is represented by Ω_V, and the angular frequency of θ is represented by ω. If "$\Omega_V \cong \omega$" or

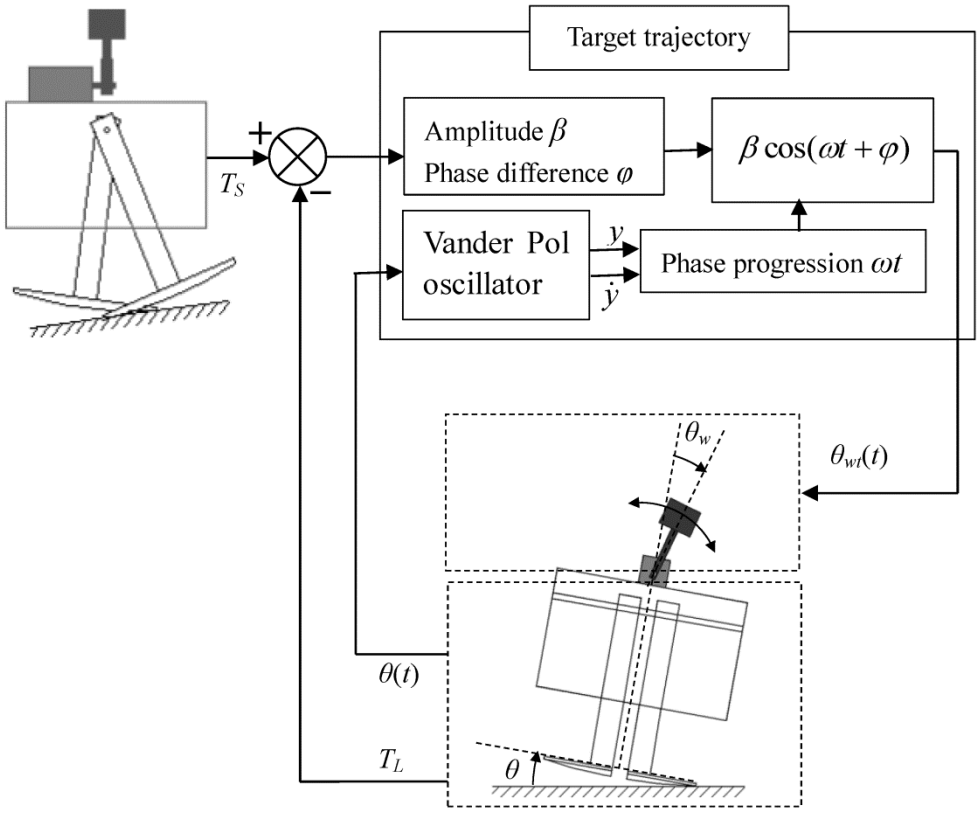

Fig. 2-6 Stabilization control algorithm

"the coefficient K is sufficiently large" is satisfied, the system indicates a phase-locking phenomenon and oscillation of θ entrains the oscillation of y. According to forced entrainment, the periods of y and $\dot{y}$ are synchronized to the period of θ, and the phase of $\dot{y}$ agrees with the phase of θ, and phase difference of $\pi/2$ between y and θ exists. Numerical solutions of y and $\dot{y}$ are utilized to determine the phase progression of θ_{wt}. The period of the target trajectory θ_{wt} is also synchronized with the period of lateral motion θ. The trajectory of θ and θ_{wt} can be approximately expressed as harmonic function as

$$\theta = \alpha \cos(\omega t) \tag{2.3}$$

$$\theta_{wt} = \beta \cos(\omega t + \varphi), \tag{2.4}$$

where α and β are the amplitudes of θ and θ_{wt}, and φ is the phase difference between θ and θ_{wt}. θ_{wt} can be expanded as

$$\theta_{wt} = \beta \cos[\cos(\omega t)\cos\varphi - \sin(\omega t)\sin\varphi]. \tag{2.5}$$

Because of Eq. (2.2) and characteristics of the forced entrainment of Vander Pol oscillator, $y \approx c_2 \sin(\omega t)$ and $\dot{y} \approx c_1 \cos(\omega t)$ are satisfied, and thus the target trajectory θ_{wt} can be determined by the phase progression of y and $\dot{y}$, amplitude β, and phase difference φ as follows[52]:

$$\theta_{wt} = \beta\left(\frac{1}{c_1}\dot{y}\cos\varphi - \frac{1}{c_2} y \sin\varphi\right), \tag{2.6}$$

where c_1 and c_2 are the amplitudes of y and $\dot{y}$.

According to "period stabilization condition", the amplitude of the target trajectory, β, is given by a proportional control (P-control) to synchronize T_L with T_S,

$$\beta = K_P(T_S - T_L) \tag{2.7}$$

where K_P is the proportional gain for the period difference between T_S and T_L. When β is constrained into positive value, the phase difference φ between the target trajectory θ_{wt} and the roll angle of the quasi-passive walker θ is set to $90°$ or $-90°$ in order to increase or decrease T_L most efficiently, respectively [52]. When φ is set to 90°, the phase difference is automatically selected as $90°$ or $-90°$ according to the sign of β,

because –sin90° is equal to sin(−90°) and cos(±90°) is equal to 0.

2.4 Uphill and level walking

The “stabilization control algorithm” can stabilize the quasi-passive walker on flat ground. However, the determination method of the amplitude of the mechanical oscillator by proportional component leads to deficiency of input energy in uphill walking. In this section, the determination method of the amplitude of the mechanical oscillator is improved, and the uphill and level walking based on “stabilization control algorithm” are realized by ODE simulation. Further, the comparison of the control methods of our quasi-passive walker and Tedrake’s “Toddler” [27] are performed by ODE simulation, and the results shows that our control method is more robust against disturbance.

2.4.1 Control algorithm

In uphill and level walking control, the period and phase difference are determined by the same method as the “stabilization control algorithm” shown in section 2.3. The amplitude of the target trajectory β is improved in uphill and level walking control. In “stabilization control algorithm”, according to “period stabilization condition”, β is determined by a proportional algorithm, but that leads to steady state error. Because of the steady state error, it is difficult for the quasi-passive walker to walk from flat ground to an upward slope.

In order to improve the adaptability of the quasi-passive walker in uphill and level walking, β is controlled by a proportional integral (PI) algorithm,

$$\beta = K_P(T_S - T_L) + K_I \int_0^t (T_S - T_L)dt, \tag{2.8}$$

where K_P and K_I are proportional and integral gains, respectively. The PI algorithm can suppress steady state error to synchronize T_L with T_S. Moreover, a simple method is used to deal with integral windup, which will cause large overshoots. Since the power and maximum speed of an actual motor are limited, the maximum value of the amplitude β is limited to 18° in the ODE simulations. If the output is larger than the maximum value, the integral calculation of the I component will be stopped.

2.4.2 Simulation

In order to generate the period of the target trajectory, the forced Van der Pol equation needs a periodical input of θ. The initial condition of the quasi-passive walker is thus set to q= [0.12, 0 …0] so as to let the quasi-passive walker periodically roll first. In the ODE simulation, the quasi-passive walker walked on a path with slope angle changed from 0 °to 3 °and started to walk on the slope of 3 °after 5.59 [s]. The changes in T_L and T_S are shown in Fig. 2-7. The period of lateral motion T_L was synchronized with T_S, and the quasi-passive walker was stabilized despite the change in slope angle. The forced entrainment of lateral motion and motion of the mechanical oscillator is characterized by the roll angle θ and θ_{wt}, as shown in Fig. 2-8. In this figure, θ_w and θ_{wt} are the actual trajectory and the target trajectory of the mechanical oscillator, respectively. As shown in Fig. 2-8, T_L is defined as the period of θ. The stable cycle of pitch angles of the legs is shown in Fig. 2-9. A stance phase and a swing phase of the right leg are also shown in Fig. 2-9. The period of swing-leg motion T_S begins when the pitch angle γ_L matches γ_R, and the end of the period T_S is defined as the moment when γ_L matches γ_R after one period, as shown in Fig. 2-9.

The improved control algorithm enables the quasi-passive walker to walk stably on upward slope, but the control algorithm leads to excess of input energy in downhill walking and the walker tumbles at last. In downhill walking the swing phase lasts until the swing leg touches the downward ground, and the swing phase lasts longer on downward ground than flat and upward ground. Therefore, the T_S increases in downhill walking. According to “period stabilization condition”, the T_L is synchronized with T_S so that the lateral motion of the quasi-passive walker is further excited, which leads to excess of input energy. In order to solve the problem of excess of input energy, it is helpful to consider the energy balance, which is investigated in the later chapters.

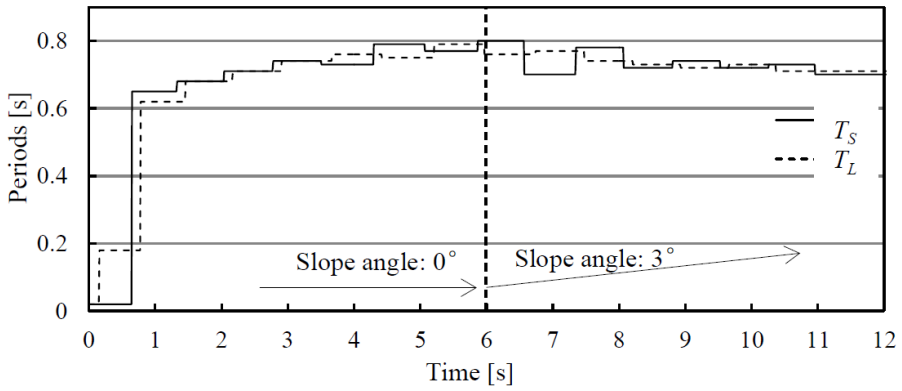

Fig. 2-7 Synchronization of the period of lateral motion T_{L} with the period of swing leg motion T_{S}

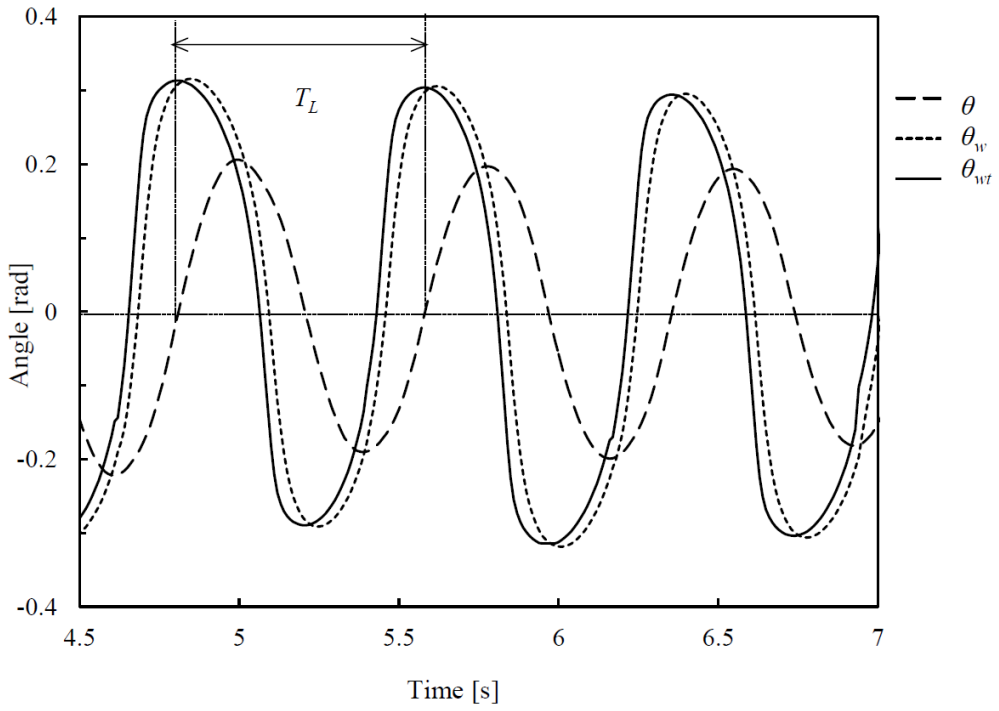

Fig. 2-8 Forced entrainment of mechanical oscillator motion and the lateral motion

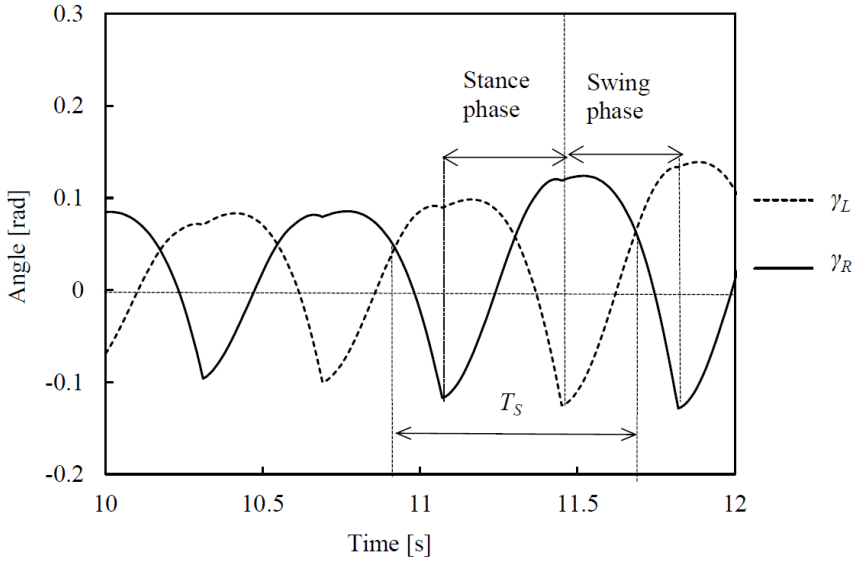

Fig. 2-9 Pitch angles of the legs

2.4.3 Comparison of control methods

A three-dimensional (3D) quasi-passive walker similar to ours is “Toddler” [25] because it has curved feet and its lateral motion is controlled by the rolling motion of ankle joints. The trajectory of ankle’s rolling motion of “Toddler” is a sine function, which is determined by its amplitude and frequency. Its ankle rolling motion entrains the overall lateral motion of the quasi-passive walker for stable walking.

Another similar quasi-passive walker proposed by Nakanishi et al. [54] also has curved feet. The quasi-passive walker excites its lateral motion by an oscillator, which moves from side to side on its hip axis. The trajectory of the oscillator is also a sine function, which is determined by its amplitude and period. The actuation method is similar to “Toddler” by entraining lateral motion into a sine oscillator.

There are two major differences in the control methods between our quasi-passive walker and the above mentioned two quasi-passive walkers. First, the mechanical oscillator of our quasi-passive walker does not entrain the overall lateral motion, but is forcibly entrained into the lateral motion of the quasi-passive walker by using a forced van der pol oscillator. As a result, the forced entrainment always occurs even when the step frequency of the quasi-passive walker changes in variable environments. In contrast, “Toddler” is stabilized by direct excitation of a sine oscillator. As a result, the entrainment can occur only when the frequency of the sine oscillator is tuned to near the passive step frequency of the quasi-passive walker. Furthermore, the “Toddler” quasi-passive walker must be initialized in phase with the sine oscillator and the entrainment is very sensitive to disturbance in phase [25]. Consequently, the environmental adaptability of “Toddler” is worse than ours.

Second, the phase of the sine oscillator is uncontrollable in the mentioned quasi-passive walkers, but the phase of the mechanical oscillator is controllable in our quasi-passive walker. The motion of mechanical oscillator of our quasi-passive walker can excite or damp the lateral motion of the quasi-passive walker to control T_L, by adjusting the phase difference between the motion of the mechanical oscillator and the lateral motion of the quasi-passive walker. This is why our quasi-passive walker is very robust against disturbance in phase.

In order to compare the control methods of our quasi-passive walker and the above mentioned two quasi-passive walkers through ODE simulation, the control method with the sine oscillator [25], $d(t)=A\sin(2\pi t/T_{sf})$, is applied to our quasi-passive walker in level walking. In stable walking with our control method, the amplitude of mechanical oscillator is near 0.3 rad, as shown in Fig. 2-8. Therefore, the amplitude of the sine function A is set to 0.3 rad to compare the results in the similar condition. When the period of the sine oscillator T_{sf} is changed from 0.4 s to 0.75 s the quasi-passive walker can walk stably. A longer or shorter period will cause unstable gait. The lateral motion of the quasi-passive walker and the mechanical oscillator motion in stable level walking are shown in Fig. 2-10. The period of the sine oscillator, T_{sf}, is set to 0.45 s, 0.65 s and 0.75 s in Fig. 2-10 (a), (b) and (c), respectively. Under the control with the sine oscillator, the phase difference between θ and θ_w changes as the period T_{sf} changes. Only when T_{sf} is near 0.75 s, the phase difference is near $\pi/2$, as shown in Fig. 2-10 (c). However, in our control method in level walking the phase difference between θ and θ_w is always constant at $\pi/2$ to excite the lateral motion of the quasi-passive walker, as shown in Fig. 2-8.

Besides, under the excitation of the sine oscillator, the quasi-passive walker becomes sensitive to initial conditions, including initial period and phase of lateral motion of the quasi-passive walker. Therefore the environmental adaptability of the method is worse than that of our method in the model of our quasi-passive walker.

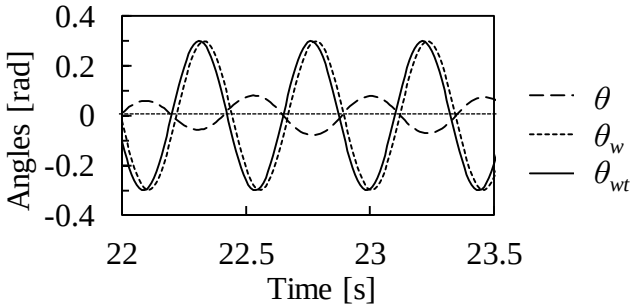

(a) T_{sf} = 0.45 s

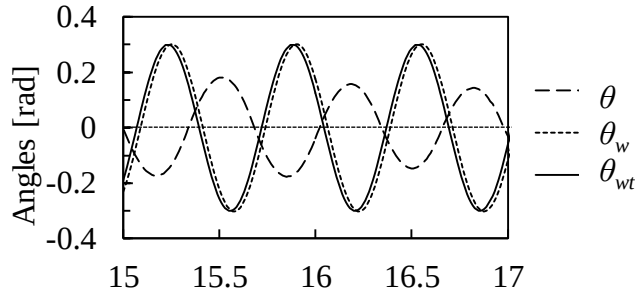

(b) T_{sf} = 0.65

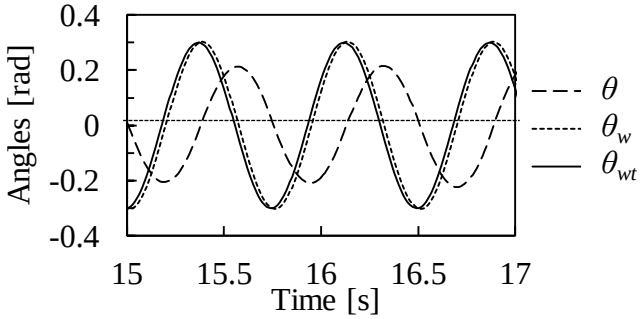

(c) T_{sf} = 0.75 s

Fig. 2-10 Entrainment of mechanical oscillator motion and lateral motion under the excitation of a sine oscillator

2.5 Turn control

In variable environments, the ability to turn is a necessity for a biped quasi-passive walker in order to steer and avoid obstacles, as an example. In order to improve the adaptability of the quasi-passive walker in changing environments, a turn control method has been proposed and been numerically examined [55]. However, the same method cannot appropriately apply to our experimental quasi-passive walker because the target trajectory of the mechanical oscillator becomes discontinuous when the stance leg changes. The power of the motor of the experimental quasi-passive walker is limited, so the mechanical oscillator cannot follow the discontinuous target trajectory.

In this section, a novel turn control method by controlling the central axis of oscillation of the mechanical oscillator is proposed to enable the quasi-passive walker to turn stably on flat ground. This new method is examined experimentally and numerically. Since this method does not need to increase actuators or change the structure of the quasi-passive walker, the turn control and stabilizing methods for straight walking can switch to each other directly. Additionally, the gait of turn is compared with that of straight walking and analyzed in terms of mechanical work and energy.

The simulation model of version 2 and experimental quasi-passive walker are utilized to examine the turn control method. Because the simulation model of version 2 and experimental quasi-passive walker have the same structure and mass distribution, the results of simulation and experiments can be compared to each other.

2.5.1 Control algorithm

A simplified model of lateral motion in turn control is shown in Fig. 2-11, where the trunk and legs are simplified to a block. Line segment *AB* represents the central axis of the block, and line segment *AC* represents the central axis of oscillation of the mechanical oscillator.

The roll angle of the lateral motion of the block is represented by θ, the inclination angle of the mechanical oscillator relative to line segment *AB* is represented by θ_w, the inclination angle of the central axis of oscillation relative to line segment *AB* is represented by θ_1, and the inclination angle of the mechanical oscillator relative to

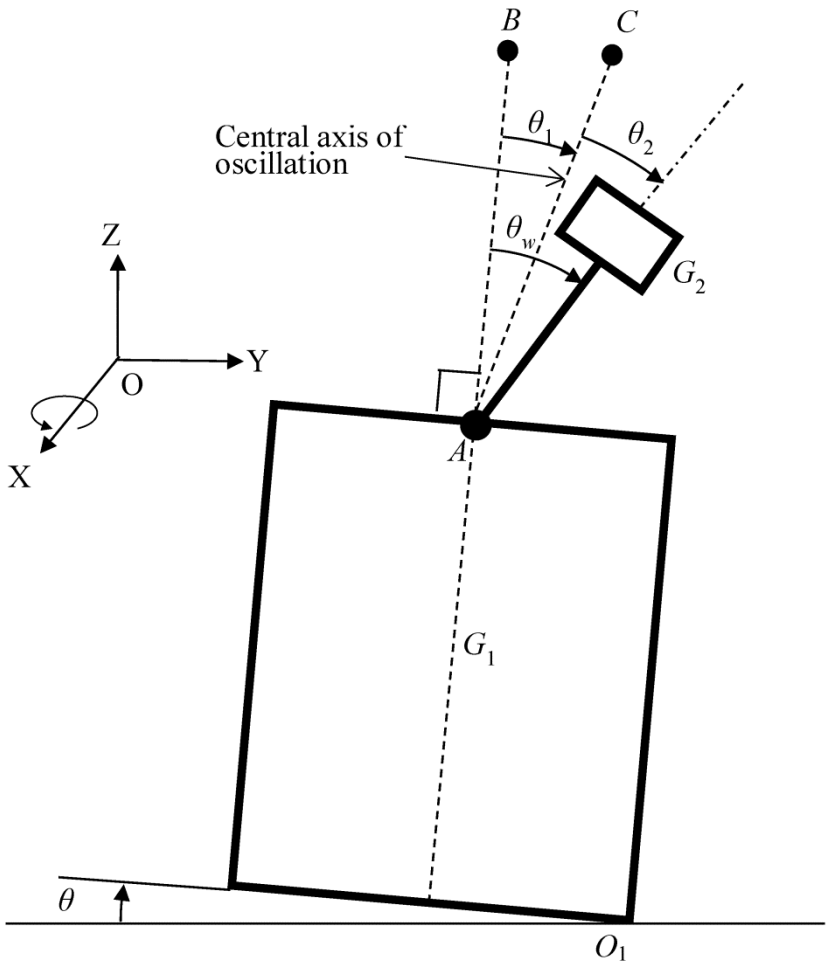

Fig. 2-11 Simplified model of lateral motion in turn control.

line segment *AC* is represented by θ_2.

The target trajectory of θ_w, θ_1 and θ_2 are represented by θ_{wt}, θ_{1t} and θ_{2t}, respectively. The target trajectory θ_{wt} is planned by θ_{1t} and θ_{2t}, because θ_{wt} is equal to $\theta_{1t}+\theta_{2t}$. The turning radius is controlled by θ_{1t}, and the gait of the quasi-passive walker is stabilized by periodic input of θ_{2t} determined based on the "stabilization control algorithm".

In the "stabilization control algorithm", the period of lateral motion T_L is controlled and always synchronized with the period of swing leg motion T_S by periodic oscillation of the mechanical oscillator. Following the method, in turn control θ_{2t} is also periodic and thus is planned by controlling its period, amplitude and phase, respectively, as shown in Fig.2-12.

The period and phase of θ_{2t} is determined by the "stabilization control algorithm". The amplitude β of the θ_{2t} is determined by a proportional algorithm based on the "stabilization control algorithm",

$$\beta = \alpha + K_p(T_S - T_L), \tag{2.9}$$

where K_P is the proportional gain, and α, which is a constant value determined by preliminary simulation, determines the initial value of β.

According to y, $\dot{y}$, β, and phase difference φ, the target trajectory θ_{2t} is determined as

$$\theta_{2t} = \beta\left(\frac{1}{c_1}\dot{y}\cos\varphi - \frac{1}{c_2}y\sin\varphi\right), \tag{2.10}$$

where c_1 and c_2 are the amplitudes of y and $\dot{y}$.

The target trajectory of θ_1 is represented by θ_{1t}, which is planned to control the turning direction and turning radius r. When θ_1 is positive, the quasi-passive walker turns right, and when θ_1 is negative, the quasi-passive walker turns left. In order to investigate the relationship between the turning radius r and θ_1, r is measured when θ_1 is set to a constant value in ODE simulation. The results are shown in Fig. 2-13. The vertical axis is r, and the horizontal axis is θ_1. The symmetric curve about the vertical axis is obtained. The minimum turning radius is 0.53 m when θ_1 is set to $-60°$ or $60°$.

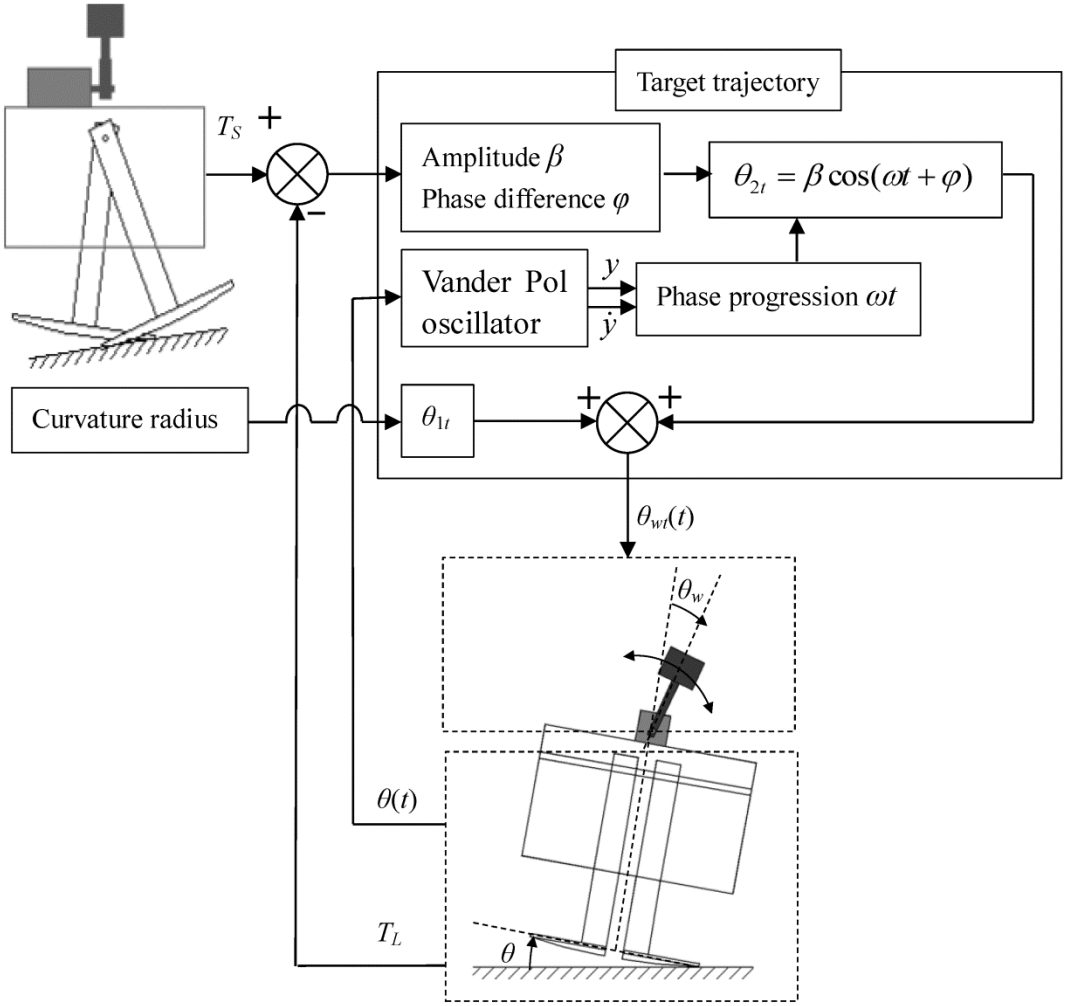

Fig. 2-12 Turn control algorithm.

If the absolute value of θ_1 is larger than 60°, the quasi-passive walker cannot turn stably in simulation, because the inclination of the central axis of oscillation changes the dynamics of lateral motion.

In order to control r, based on Fig. 2-13, the relationship between θ_1 and r_t is expressed by a function obtained by a curve fitting method based on least squares method, as

$$\sin(\theta_{1t}) = \frac{\pm 2.23}{(r_t + 1.935)} \quad (r_t > 0.53 \text{ [m]}) \tag{2.11}$$

The plus and minus signs "±" in Eq. (2.11) are used in left and right turn control, respectively.

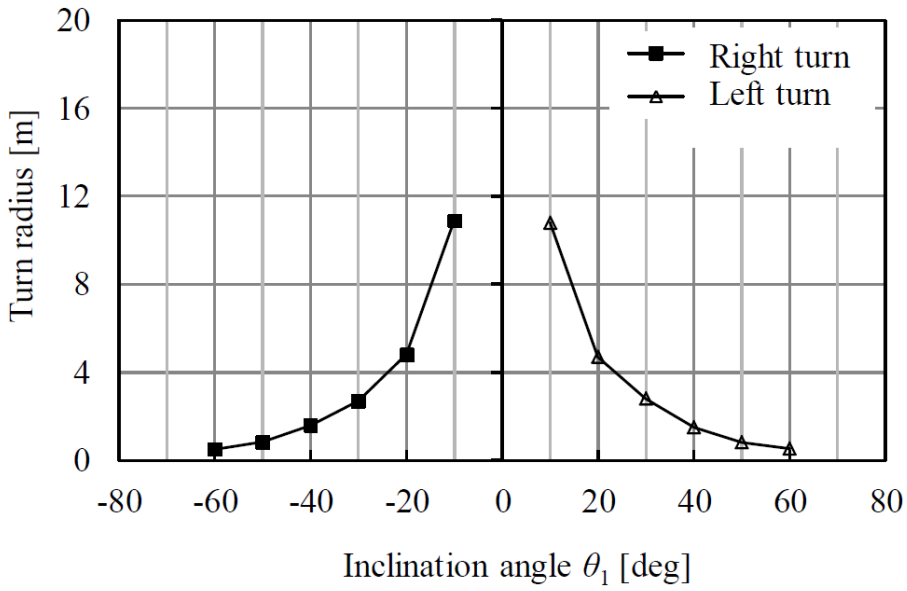

Fig. 2-13 Turn radiuses as a function of the inclination angle of the central axis of oscillation.

2.5.2 Simulation and experiment

The turn control is demonstrated in the ODE simulation. As shown in Fig. 2-14, the quasi-passive walker walks straight on a flat ground for 3 seconds to stabilize the walking gait, then θ_1 is set to -60° and the quasi-passive walker begins to turn right. The path of the center of mass of the quasi-passive walker in right turn, where the horizontal and vertical axis are X and Y axis of the global coordinate, respectively. The turning radius is about 0.53 m, and the path of the center of mass shows meandering shape because the quasi-passive walker rolls in the lateral plane and the center of mass of the quasi-passive walker moves between the left and right foot.

The period of right lateral motion T_{right} is defined as the period of twice the time while θ is positive (the quasi-passive walker inclines to right) in one walking cycle, and the period of left lateral motion T_{left} is defined as the period twice of the time while θ is minus (the quasi-passive walker inclines to left) in one walking cycle. In straight walking, T_{right} and T_{left} agree because of the symmetric left and right lateral motion.

However, T_{right} and T_{left} become different in turn control by the inclination of the central axis of oscillation θ_1. The relation between θ_1 and the period difference "$T_{right} - T_{left}$" is investigated in simulations and experiments, and the results are as shown in Fig. 2-15, where the vertical axis is the period difference "$T_{right} - T_{left}$" and the horizontal axis is the inclination angle θ_1. The period difference increases when θ_1 increases. The results of the simulation and experiments show that the method is effective to control the period difference "$T_{right} - T_{left}$". From Fig. 2-13 and Fig. 2-15, if $|T_{right} - T_{left}|$ is larger, the turn radius becomes smaller, because larger $|T_{right} - T_{left}|$ leads larger difference between strides of the left and right leg and makes the quasi-passive walker turn with smaller turn radius.

Turn is an important ability of the quasi-passive walker in variable environments, so the turn control method is examined with the experimental quasi-passive walker and simulation model walking on a path with different turn radiuses on flat ground. In the experiment, the path has two bends and the turn radiuses are 0.75 m and 2.0 m, as shown in Fig. 2-16 (a), so the quasi-passive walker has to switch its turn radius to

adapt to the changing environment. There are no external sensors on the quasi-passive walker to sense the changing environment, so θ_{1t} is calculated in advance according to the turn radiuses. When the turn radiuses are set to 0.75 m and 2.0 m, θ_{1t} is calculated by Eq. (2.11) and adjusted to -58° and 35°, respectively. The quasi-passive walker shows stable walking through the path in the experiments as shown in Fig. 2-16 (b), which shows that the turn control makes it possible for the quasi-passive walker to realize stable walking even under different conditions.

In the simulation, a more complicated path is examined, and the same as the experiment is applied. Here, θ_{1t} is also calculated in advance according to the turn radii. The quasi-passive walker shows stable walking through the path, as shown in Fig. 2-17, where the location of the quasi-passive walker is shown in the mini map of the path.

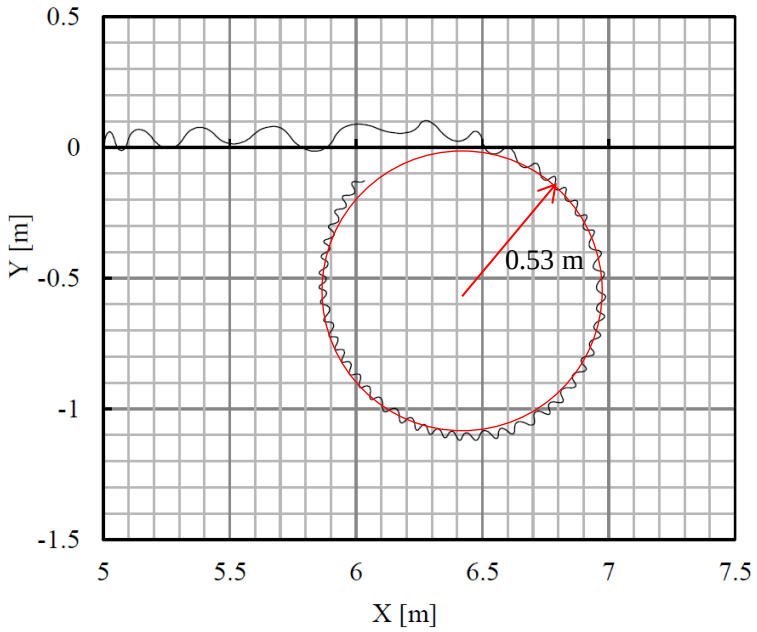

Fig. 2-14 Trajectory of the center of mass of the quasi-passive walker in right turn.

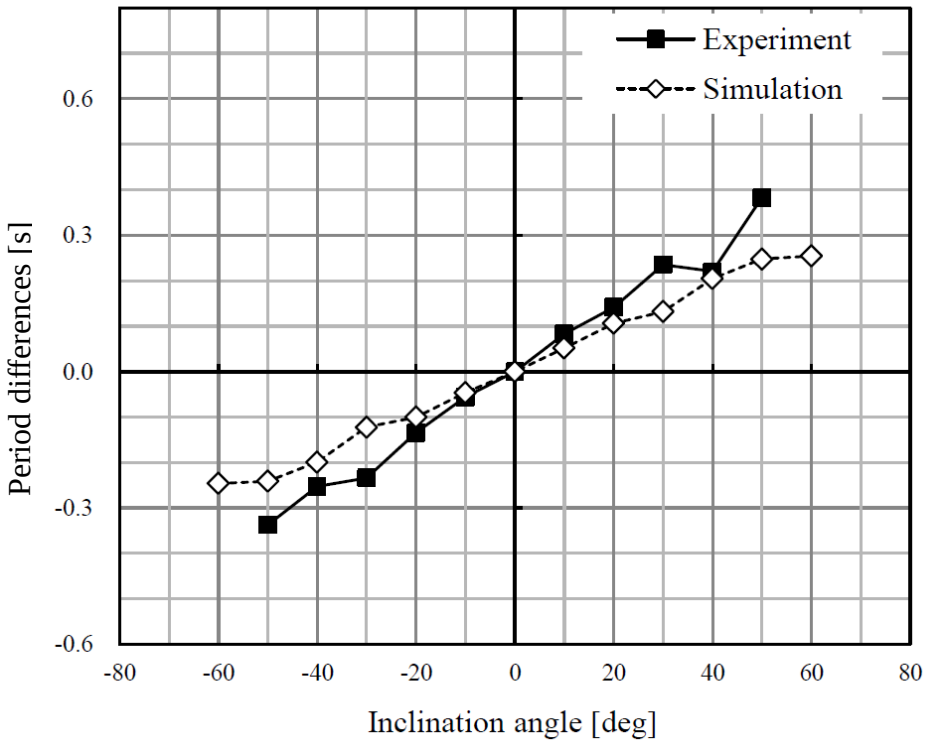

Fig. 2-15 Period differences between the right and left lateral motion versus the inclination angle of the central axis of oscillation.

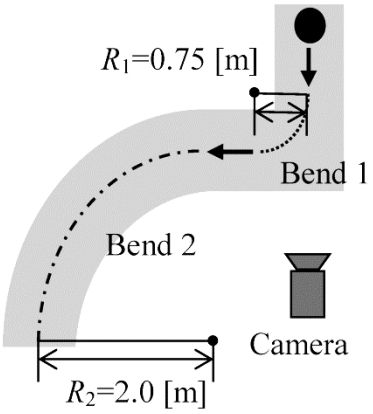

(a) The path with different turn radiuses.

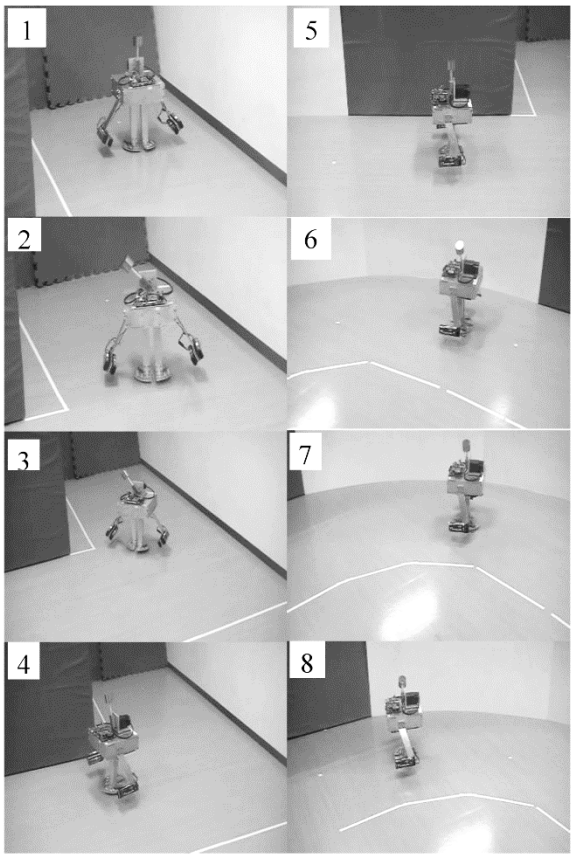

(b) Experiments.

Fig. 2-16 Experiments of turn control.

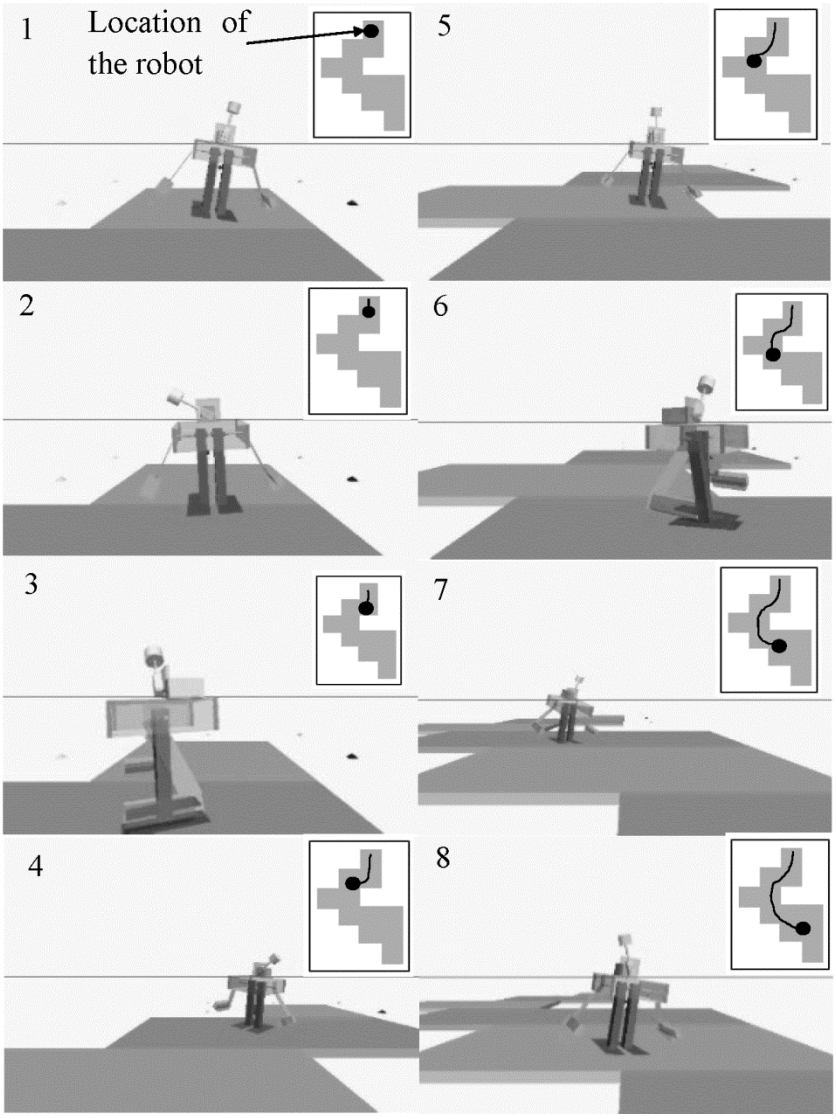

Fig. 2-17 Simulation of turn control.

2.5.3 Comparison of turn and straight walking

In order to investigate the gait of the quasi-passive walker in turn control, the pitch angles of the right and left legs in right turn are compared with that in straight walking by simulation as shown in Fig. 2-18. The vertical axis is the pitch angle, and the horizontal axis is time. In straight walking, the pitch angles of the two legs indicate similar curves with almost same periods, amplitudes and opposite phase, thus the time of left and right swing phase almost agrees as shown in Fig. 2-18(a). However, in right turn, the pitch angles of the two legs indicate different wave shape and phases, and the time of the left swing phase is larger than the time of the right swing phase as shown in Fig. 2-18(b).

The lateral motion of the quasi-passive walker in right turn is compared with straight walking by using phase plane trajectories, as shown in Fig. 2-19. The horizontal axis is the roll angle of the lateral motion θ, and the vertical axis is the angular velocity of the lateral motion, where the black dots indicate the initial state, and the black arrows indicate the end of phase plane trajectories. In straight walking, the phase plane trajectories are almost symmetric with respective to the left and right half plane as shown in Fig. 2-19(a). However, in right turn, the phase plane trajectory is asymmetric with respective to the left and right half plane as shown in Fig. 2-19(b), and the asymmetry comes from the inclination of the central axis of the mechanical oscillator movement generated by turn control. In right turn the roll angle of lateral motion in right stance phase is larger than left stance phase.

The asymmetric lateral motion of the quasi-passive walker can be understood from the viewpoint of mechanical work, so the positive and negative work performed by the motor on the quasi-passive walker in right turn are calculated and compared with that in straight walking in ODE simulation. The positive and negative works in right turn and straight walking are shown in Fig. 2-20. The positive and negative works are represented by W_p and W_n, respectively. The left vertical axis shows the work performed by the motor on the quasi-passive walker, and the right vertical axis shows the roll angle of the quasi-passive walker θ. From the roll angle θ, the right and left stance phase can be distinguished easily, because stance leg changes when θ is 0. In

the right stance phase under right turn control, the motor performs more positive work than negative work, thus the mechanical energy, the amplitude of lateral motion of the quasi-passive walker and the time of right stance phase increases as shown in Fig. 2-20(a). In the left stance phase, the motor performs more negative work than positive work, thus the mechanical energy, the amplitude of lateral motion of the quasi-passive walker and the period of right lateral motion decreases. Therefore, the period differences between the right and left lateral motion increase, as shown in Fig. 2-15. In the other hand, under the straight walking, the negative work W_n, is almost zero as shown in Fig. 2-20(b), so effective walking is achieved by proposed method.

Although the mechanical oscillator always accelerates and decelerates to periodically sway left and right in the frontal plane, positive work accounts for 91% of total mechanical work on average in both right and left stance phase. Therefore, the right and left lateral motions of the quasi-passive walker are symmetric, as shown in Fig. 2-20(b).

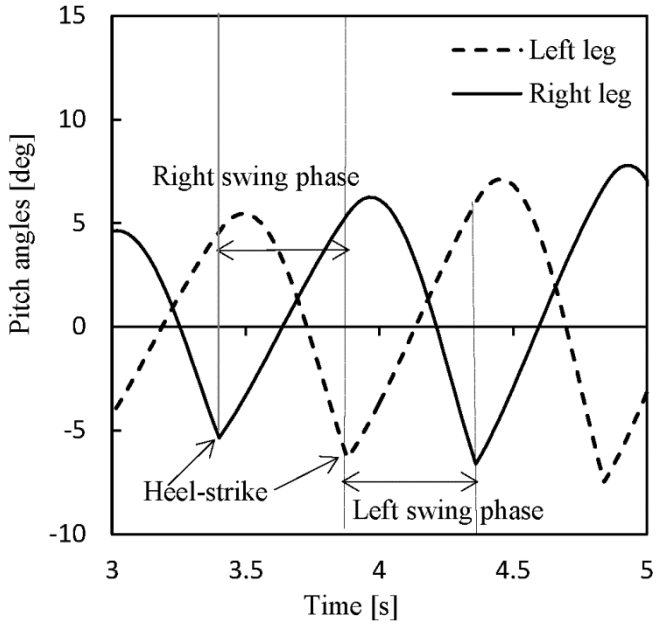

(a) Straight walking

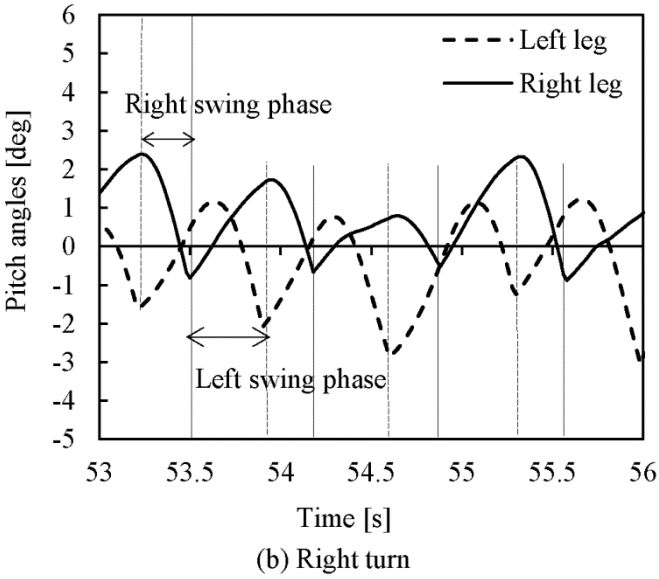

(b) Right turn

Fig. 2-18 Pitch angles of the legs in straight walking and right turn.

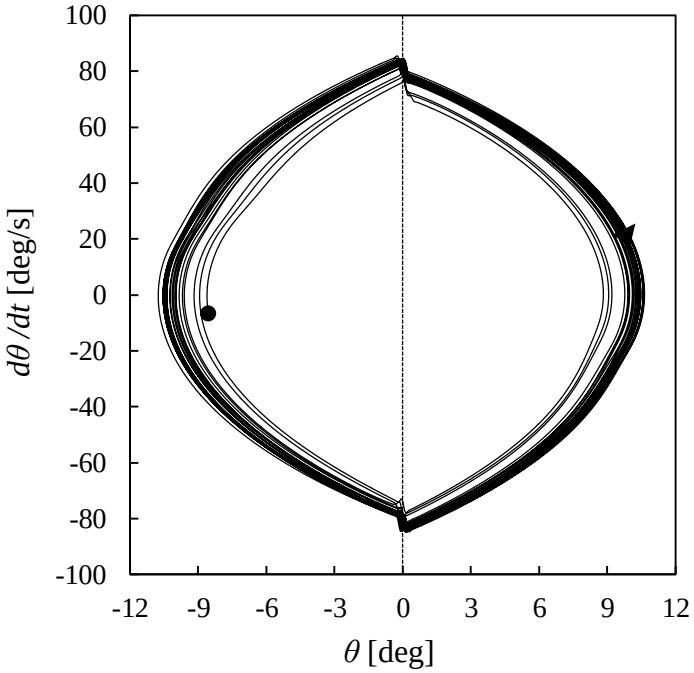

(a) Straight walking

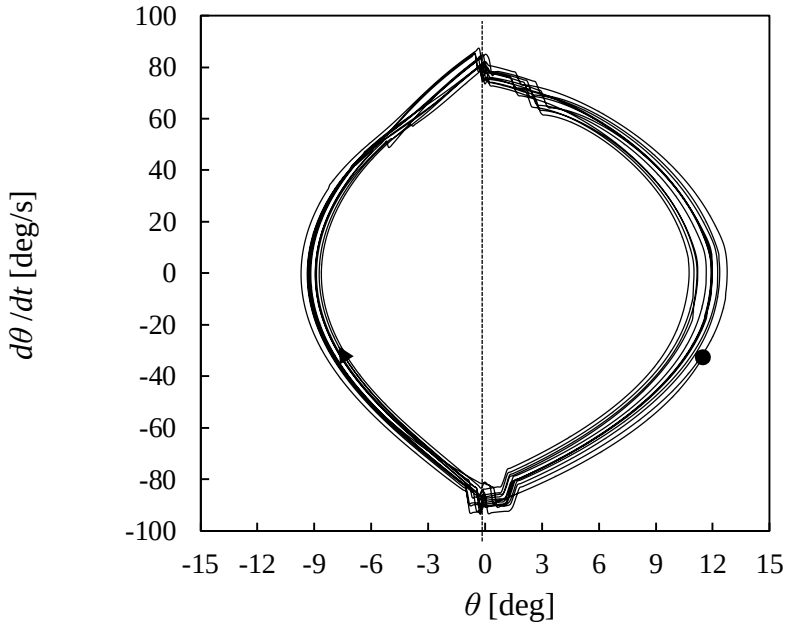

(b) Right turn

Fig. 2-19 Phase plane portraits of lateral motion of the quasi-passive walker in straight walking and right turn.

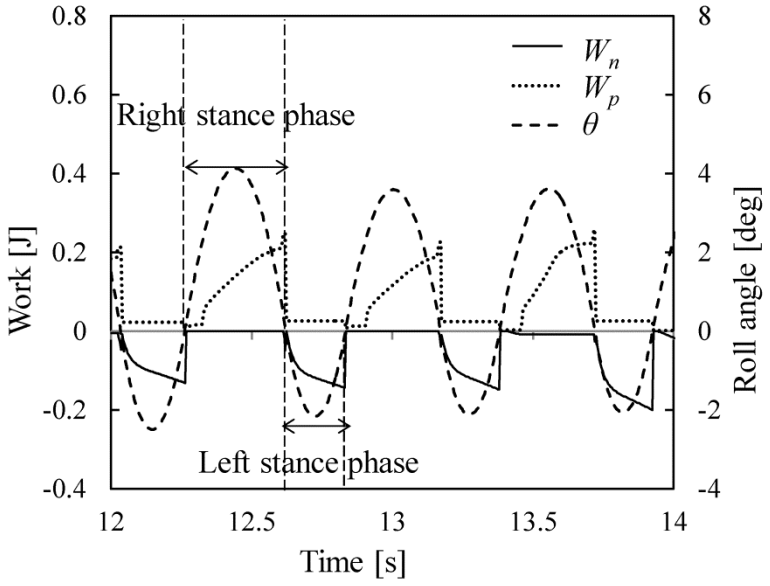

(a) Right turn

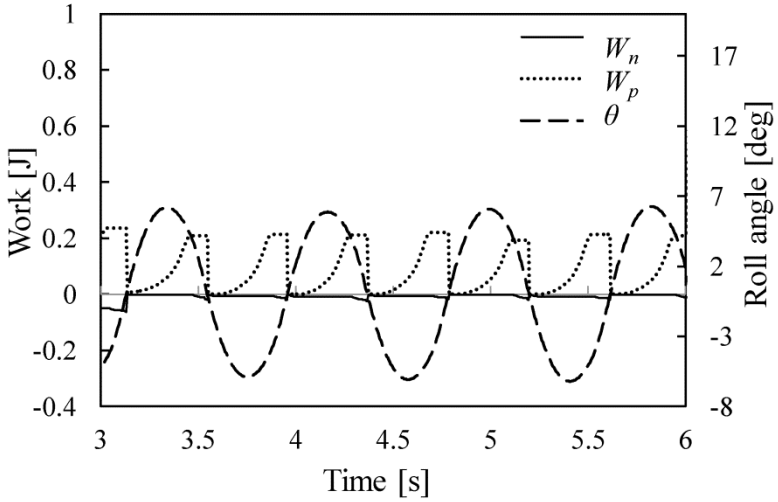

(b) Straight walking

Fig. 2-20 Positive and negative work in right turn and straight walking.

2.6 Conclusion

In this chapter the simulation model, experimental quasi-passive walker of a 3D quasi-passive walker and the “stabilization control algorithm” are introduced. In order to improve the environmental adaptability of the quasi-passive walker, the control method for turn, uphill and level walking are proposed based on the “stabilization control algorithm”, and are numerically and experimentally examined.

First, we achieved uphill and level walking of a 3D quasi-passive walker on a variable slope in ODE simulation by improving the determination method of the amplitude of the target path for the mechanical oscillator by PI algorithm. The control method based on forced entrainment was compared with two similar quasi passive walkers proposed by other researchers. The two quasi-passive walkers are controlled by the sine forced oscillation by applying the sine oscillation to our quasi-passive walker. The results show that the quasi-passive walker becomes sensitive to initial conditions, initial period, and phase of lateral motion of the quasi-passive walker, under the control based on the sine oscillation. Therefore the environmental adaptability of the method based on sine force oscillation is worse than that of the “stabilization control algorithm” in the model of our quasi-passive walker. However, the determination method of the amplitude of the mechanical oscillator based on “period stabilization condition” leads to excess or deficiency of input energy, and the problem will be reconsidered and solved in viewpoint of energy balance.

Second, in turn control, the turn radius of the quasi-passive walker can be controlled by the inclination angle of the central axis of oscillation of the mechanical oscillator. Based on the proposed turn control method, the quasi-passive walker successfully walks through a curved path with desired curvature radius, which indicates that it is possible for the quasi-passive walker to realize stable walking in variable environments. In addition, the gait and mechanical work of turn control are investigated and compared with that in straight walking. The negative work performed by the quasi-passive walker in turn control leads to the asymmetric left and right lateral motions, which enable the quasi-passive walker to turn.

3. Energy transfer, transformation and efficiency of walking

3.1 Introduction

The energy efficiency of passive or quasi-passive walkers can approach that of human, and is much higher than that of humanoid robots [12]. The high energy efficiency of passive or quasi-passive walking is because of passive dynamics and fewer actuators. In this chapter, the energy efficiency of passive walkers, quasi-passive walkers, humanoid robots, and human are investigated and compared with each other. The level and uphill waking of our quasi-passive walker are analyzed from the perspective of energy transformation and transfer, which can help us to further understand the energy efficiency of passive walking.

First, the energy efficiency of our quasi-passive walker is investigated and compared with human and other biped robots. Second, the walking of our quasi-passive walker is analyzed from the perspective of energy transformation and transfer to investigate energy balance. Third, the energy efficiencies of the quasi-passive walker under different control methods are compared based on ODE simulation.

3.2 Mechanical cost of transport in uphill and level walking

In level walking, to compare mechanical energy efficiencies of steady walking of different-sized robots and human, a useful measure of energy efficiency is the specific mechanical cost of transport [12][58][59] (c_{mt}): c_{mt} = (mechanical energy used) / (weight × distance traveled), where "mechanical energy used" is divided by "weight" because different-sized robots have different weights. In quasi-passive walking, some robots only perform positive work in level walking, such as a Cornell biped [24], and thus their "mechanical energy used" is equal to the positive work. However, for humans and most biped robots, both positive work and negative work are performed by actuators, and thus the "mechanical energy used" during one walking cycle is equal to "$W_p - W_n$", where W_p is positive work, and W_n is negative work during one walking cycle (W_n has negative value).

In uphill walking, a part of the mechanical work is not consumed but transformed into potential energy, so "Mechanical energy used" is equal to "$W_p - W_n - \Delta E_p$",

where ΔE_p represents the total change in potential energy during one walking cycle. Therefore, c_{mt} can be extended to measure the efficiency of uphill and level walking as follows:

$$c_{mt} = \frac{W_p - W_n - \Delta E_p}{\text{weight} \times \text{distance travelled}}. \tag{3.1}$$

Equation (3.1) can still be used for passive walkers and robots that perform only positive work. For passive walkers, "$W_p - W_n - \Delta E_p$" is equal to "$-\Delta E_p$", which is positive in passive walking and equal to the loss of potential energy. For quasi-passive walkers which perform only positive work in level walking, "$W_p - W_n - \Delta E_p$" is equal to W_p. Therefore, the energy efficiencies of uphill walking, level walking and downhill walking can be calculated and compared with each other by c_{mt} extended by the Eq. (3.1).

Average values of c_{mt} of our quasi-passive walker in level walking, uphill walking, and passive walking are shown in Table 3.1, which also shows c_{mt} of humans and several other biped walking robots investigated by Collins et al. [24]. In this table, c_{mt} of uphill walking was measured when our quasi-passive walker walked on an upward slope with inclination of 3 degree. In uphill walking, since both "mechanical energy used" and "distance travelled" decrease during one walking cycle, c_{mt} of uphill walking and the level walking are similar. The collision at the heel strike of our quasi-passive walker is set to inelastic collision in the ODE simulation, and the simulation model therefore consumes more mechanical energy than some other experimental quasi-passive walkers.

Some understanding of the energy efficiency of humans and robots can be obtained from the perspective of energy transformation. In level walking of humans, most of the mechanical energy is dissipated by humans themselves rather than by the external factor such as heel strike etc.. The positive work of muscles offsets most of the negative work of muscles, and small amount of mechanical energy is dissipated at heel strike in each walking cycle. For example, during a double support phase of human walking, most of the negative work is performed by the leading leg to redirect the velocity of the center of mass and to maintain steady walking [60]. Although

human walking is self-resistive, humans can walk much more efficiently than humanoid robots. Humanoid robots need to accelerate and decelerate their joints to trace a planned trajectory, and if the trajectory is planned inappropriately, much more negative work consumes its positive work. Although the walking of humanoid robots and walking of humans are both self-resistive, humans can utilize mechanical energy much more efficiently than can humanoid robots.

Energy transformations of passive and quasi-passive walking are different from that in human walking. Passive walkers perform no work but consume potential energy in walking on a downward slope, and their mechanical energy is dissipated at heel strike. Some quasi-passive walkers can perform only positive work in level walking, and their mechanical energy is also dissipated at heel strike. Although our quasi-passive walker performs both positive work and negative work in walking, the quasi-passive walker can still walk efficiently. Moreover, passive walkers utilize potential energy in downhill-walking, but our quasi-passive walker performs positive work against the pull of gravity in uphill and level walking. Investigation Energy transformation of our quasi-passive walker is necessary to understand the efficient uphill and level walking of the quasi-passive walker.

Table 3-1 Energy efficiencies of human and several biped robots

Human and robots	c_{mt}
Humans	0.05
ASIMO	1.60
Our quasi-passive walker	
(uphill walking)	0.108
(level walking)	0.095
(passive walking)	0.052
Delft's Denise	0.08
Cornell Biped	0.055
McGeer's Dynamite	0.04

3.3 Energy efficiency and energy transformation

The torque of the motor is a non-conservative force (generalized force), and the mechanical energy of the quasi-passive walker is therefore not conserved. According to the law of conservation of energy, the relationship between mechanical work and mechanical energy of the quasi-passive walker during some time can be expressed as

$$W_r - E_i = \Delta E_r, \tag{3.2}$$

where W_r is the total mechanical work performed by the motor on the quasi-passive walker, ΔE_r is the total change in mechanical energy of the quasi-passive walker, and E_i is total energy loss at heel strike during some time. The work of the motor changes the mechanical energy during a single support phase, and some of the energy is dissipated at heel strike. In a single support phase without heel strike, Eq. (3.2) can be simplified as

$$W_r = \Delta E_r, \tag{3.3}$$

which shows that the work performed by the motor only changes the mechanical energy during a single-support phase.

W_r, ΔE_r and E_i are calculated to investigate energy transformation in walking. The mechanical oscillator and the trunk roll in the frontal plane by actuation of the motor. Therefore, work performed on the mechanical oscillator W_o, work performed on the trunk W_b, and work performed on the quasi-passive walker W_r, which are performed by the motor only in the frontal plane, are obtained by

$$W_o = \int_0^t T(t)\omega_{x1}(t)dt \tag{3.4}$$

$$W_b = \int_0^t [-T(t)]\omega_{x2}(t)dt \tag{3.5}$$

$$W_r = W_o + W_b = \int_0^t T(t)(\omega_{x1}(t) - \omega_{x2}(t))dt, \tag{3.6}$$

where $T(t)$, ω_{x1}(t) and ω_{x2}(t) are the torque of the motor, angular velocity of the mechanical oscillator and angular velocity of the trunk around the shaft of the motor, respectively. In Eq. (3.5), the minus sign "−" in front of $T(t)$ indicates reaction torque of the motor. In Eq. (3.6), "ω_{x1}(t)−ω_{x2}(t)" is the rotational speed of the motor, or the relative angular velocity of the mechanical oscillator to the trunk.

Aforementioned ΔE_r during some time is the total change in mechanical energy E_r, which is the sum of potential energies, translational kinetic energies and rotational kinetic energies of the each segments of the quasi-passive walker. Translational kinetic energy is calculated from the masses of the segments and the translational velocities of the centers of masses of the segments, and the rotational kinetic energy is calculated from the angular velocities of the segments and moments of inertia about their body axes through the centers of the masses. Potential energy is calculated from the height of the centers of masses from the ground.

The energy loss E_{i_1s} at heel strike in one step is expressed as

$$E_{i\_1s} = E_r^{t1-} - E_r^{t1+}, \tag{3.7}$$

where E_r^{t1-} and E_r^{t1+} are both the mechanical energies of the quasi-passive walker, "t1-" represents the moment immediately before heel strike, and "t1+" represents the moment immediately after heel strike. E_i is the sum of E_{i_1s} during some time.

The work W_r obtained by Eq. (3.2), energy loss E_i obtained by Eq. (3.7) and the total change in mechanical energy ΔE_r in one uphill walking cycle are calculated by the ODE simulation, as shown in Fig. 3-1. The sampling period of the simulation is set to 0.01 s. The walking cycle begins immediately after heel strike at 5.97 s and ends immediately before heel strike at 6.71 s. The walking cycle includes a swing phase, a double support phase and a stance phase for each leg. The results show that E_r is decreased at heel strike and energy loss E_i is increased at 6.35 s, but E_r is restored by W_r in a single-support phase. The difference between W_r and (ΔE_r + E_i) can be caused by the first order semi-implicit integrator of the ODE, in which inaccuracy in implicit integrators damps the system energy, and inaccuracy in explicit integrators increases the system energy [56]. To minimize the error, the bounce parameter and constraint force mixing parameter (CFM) of the ODE, which are related with heel-strikes, are set to 0 and 0.0001, respectively.

In order to investigate the energy utilization rate of the motor, the energy utilization rate (r_{eu}) is defined to be "(W_p+W_n) / (W_p−W_n)", where "W_p+W_n" is equal to the increase in mechanical energy of the quasi-passive walker inputted by the motor, and

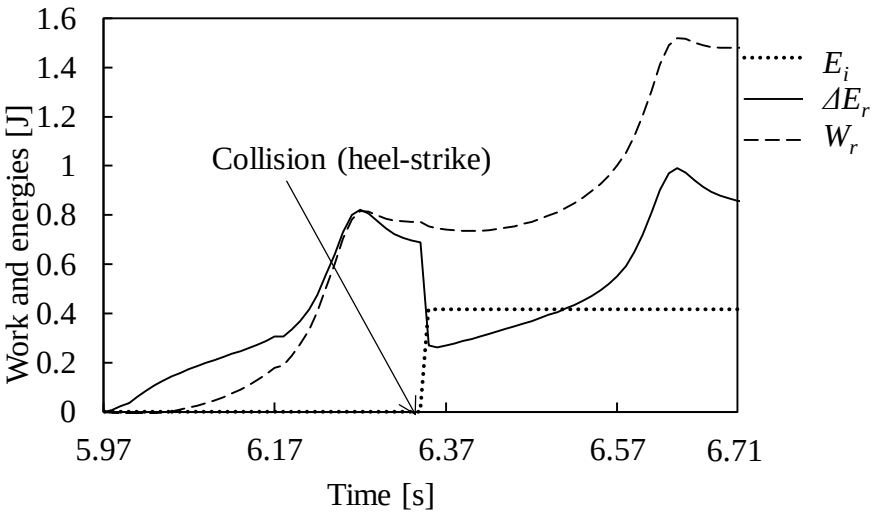

Fig. 3-1 Dissipated energy E_i, change in mechanical energy ΔE_r and work performed by the motor on the robot W_r

"$W_p - W_n$" is equal to the total work performed by the motor, because W_n always has negative value according to the definition in section 3.1. W_p accounts for approximately 88.65 % of "$W_p - W_n$" on average, and "$-W_n$" accounts for 11.35 % of "$W_p - W_n$" in level walking, so r_{eu} of our quasi-passive walker in level walking is 77.3 %. This means that 77.3 % of "$W_p - W_n$" is transformed into mechanical energy of the quasi-passive walker, and the remaining 22.7 % is consumed by the motor itself. Direct actuation methods can achieve higher r_{eu}, such as push-off in ankle joints of the Cornell biped [24], and the higher r_{eu} is one reason why the Cornell biped can walk more efficiently than our quasi-passive walker.

In order to optimize and improve the energy efficiency and energy utilization rate in uphill and level walking, the phase difference of the target trajectory of the mechanical oscillator, φ mentioned in Eq. (2.4), is set to 90°. The relationship of phase difference φ with the energy efficiency and energy utilization rate is shown in Fig. 3-2. The horizontal axis is phase difference, and the vertical axis is c_{mt} and r_{eu}, respectively.

When φ is set to 90°, c_{mt} is 0.095 in level walking and 0.108 in uphill walking on average, and r_{eu} is 77.3 % in level walking and 74.9 % in uphill walking. When φ becomes larger or smaller than 90°, r_{eu} decreases and c_{mt} increases, because more energy is consumed by the motor itself.

The total mechanical energy of the quasi-passive walker E_r consists of kinetic energy E_k and potential energy E_p as shown in Fig. 3-3. The height of the center of mass of the quasi-passive walker changes because of the roll and pitch motion of the stance leg, and mechanical energy is transformed between E_p and E_k. Fig. 3-3 shows that the kinetic energy of the walker changes periodically when the energy balance is satisfied in stable walking. In addition, 18.7 % of E_k in uphill walking and 23.3 % of E_k in level walking are dissipated at heel strike on average.

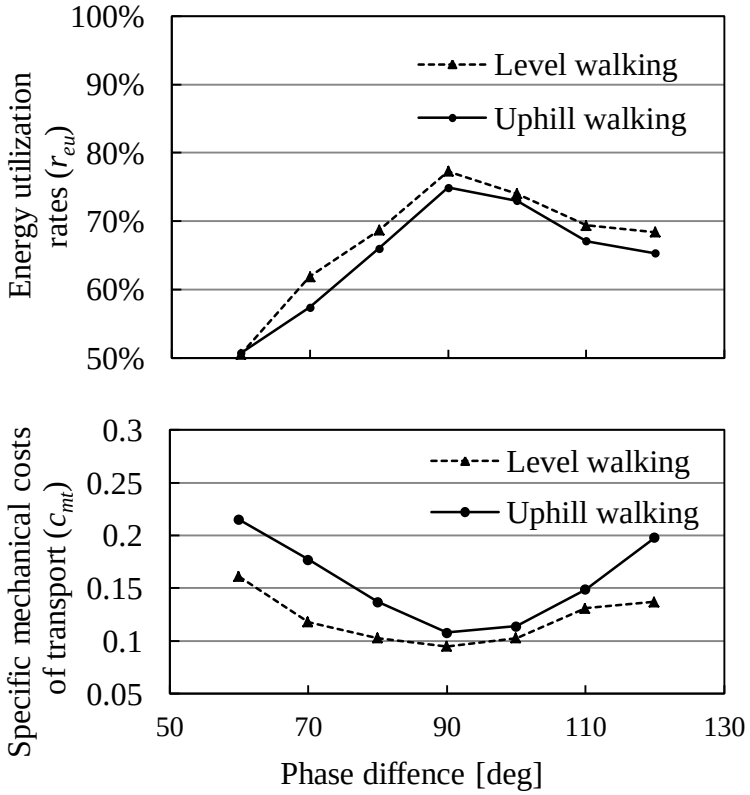

Fig. 3-2 Energy utilization rate and c_{mt} versus phase difference φ

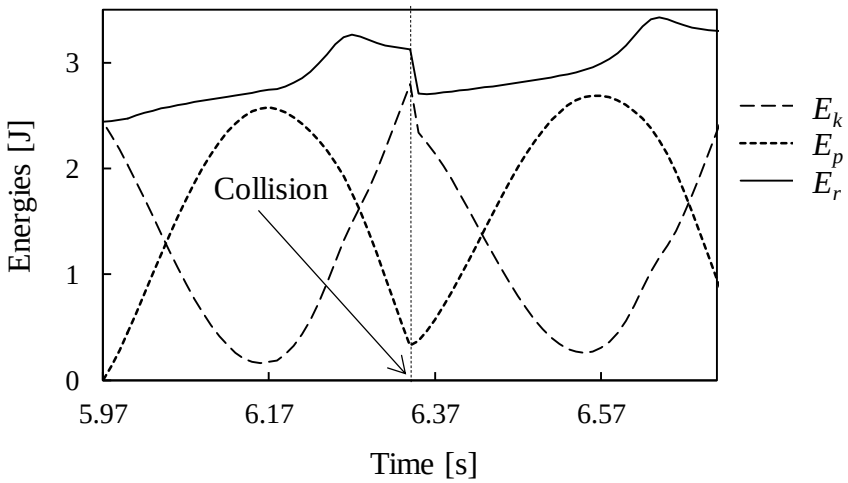

Fig. 3-3 Energy transformation between kinetic energy and potential energy in a walking cycle

3.4 Comparison of energy efficiency under different control methods

In order to investigate the energy efficiency of a similar control method used in a quasi-passive walker "Toddler" [25], which is mentioned in section 2.4.3, the sine oscillator used by "Toddler", $d(t)=A\sin(2\pi t/T_{sf})$, is applied to our quasi-passive walker to determine the target trajectory of the mechanical oscillator. In the sine function, A is the amplitude, and T_{sf} is the period. Under the control method based on sine oscillator, the phase difference, between the lateral motions of the mechanical oscillator and the quasi-passive walker, automatically changes with the change of T_{sf} (the period of sine function). It is an interesting phenomenon that has never been found in the simulation or experiments.

The next question is that how T_{sf} affects the energy efficiency under the control method. The amplitude of the sine function A is set to 0.3 rad to compare the method based on sine oscillator in the same amplitude condition with the method proposed by this study. When the period of the sine oscillator T_{sf} is changed from 0.4 s to 0.75 s the quasi-passive walker can walk stably. When a longer or shorter period is given, the gait becomes unstable. The relationship of the period of the sine function T_{sf} with c_{mt} and r_{eu} in stable level walking is shown in Fig. 3-4. The horizontal axis is period of the sine function T_{sf}, and the vertical axes are c_{mt} and r_{eu}. When T_{sf} is set to the value between 0.4 and 0.55, r_{eu} increases and c_{mt} decreases with the increase of T_{sf}, which means that the energy efficiency of walking becomes higher as the T_{sf} increases. When T_{sf} is set to the value between 0.55 and 0.75, r_{eu} and c_{mt} do not change obviously, and the energy efficiency of walking keeps high value. In this case, r_{eu} is larger than 95% and c_{mt} is between 0.06 and 0. 07. The maximum of r_{eu} is 97.8%, and the minimum of c_{mt} is 0.061.

In comparison with the control method proposed by this thesis, the control method based on sine oscillator is more energy efficient. One reason is that θ_w generated by proposed control method, which uses forced Van der Pol oscillator, is not harmonic wave. In section 2.4.2 and 2.4.3, Fig. 2-8 shows the motion of the quasi-passive walker under the control method based on forced Van der Pol oscillator, and Fig. 2-10 (c) shows the motion of the quasi-passive walker under the control method based on

sine oscillator. By comparing Fig. 2-8 with Fig. 2-10 (c), it is easily seen that the amplitude, period and phase of θ and θ_w are almost same. However, the level walking shown in Fig. 2-8 shows lower energy efficiency because non-harmonic oscillation can cause deterioration of energy efficiency.

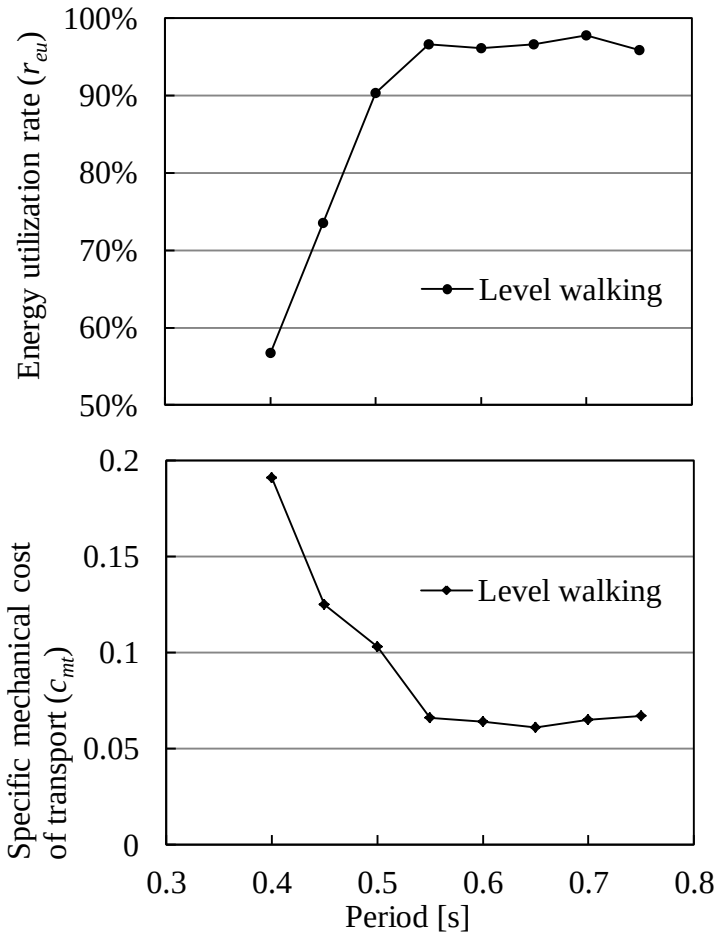

Fig. 3-4 Energy utilization rate and c_{mt} as a function of the period of the sine function T_{sf}

3.5 Mechanical energy transfer and transformation

Muscles generate and dissipate mechanical energy to actuate segments in human walking. Segments of passive walkers are actuated by gravity in passive walking. Our quasi-passive walker has only a motor that directly performs work on the mechanical oscillator and the trunk, and there are no actuators in other passive joints. Although the motor does not directly perform work on the legs, the work performed by the motor is transferred to the legs so that the quasi-passive walker can still walk on level ground and upward slopes. In order to investigate the energy transfer between the each segments of the quasi-passive walker, the relationships between work and energy for the mechanical oscillator, trunk and legs in a single-support phase are expressed as

$$W_o + W_{co} = \Delta E_o, \tag{3.8}$$

$$W_b + W_{cb} = \Delta E_b, \tag{3.9}$$

$$W_{cL} = \Delta E_L, \tag{3.10}$$

$$W_{cR} = \Delta E_R, \tag{3.11}$$

respectively. With respect to the mechanical oscillator, W_o, W_{co} and ΔE_o in Eq. (3.8) are the total work performed by the motor on the oscillator, the total work performed by constraint forces of the joint on the oscillator, and total change in mechanical energy of the oscillator, respectively. The rolling motion of the mechanical oscillator is controlled by the motor, but its pitching and yawing motions are constrained by its joint, as shown in Fig. 2-1. And the constraint forces of the joints perform work on the oscillator. With respect to the trunk, W_b, W_{cb}, and ΔE_b in Eq. (3.9) are the total work performed by the motor on the trunk, the total work performed by the constraint forces of the joint on the trunk, and total change in mechanical energy of the trunk, respectively. With respect to the left leg, W_{cL} and ΔE_L in Eq. (3.10) are the total work performed by constraint forces of the joint on the left leg and total change in mechanical energy of the left leg, respectively. With respect to the right leg, W_{cR} and ΔE_R in Eq. (3.11) are the total work performed by the constraint forces of joint on the right leg and total change in mechanical energy of the right leg, respectively. The

constraint forces of the joints perform work on each segment, but these constraint forces do not change the total mechanical energy of the whole system by assuming ideal constraints. Thus, following equation

$$W_{co} + W_{cb} + W_{cL} + W_{cR} = 0. \tag{3.12}$$

is satisfied because of the assumption of ideal constraints.

The work performed by the motor and mechanical energy of the quasi-passive walker can be directly calculated in numerical simulation, and then the works performed by constraint forces (W_{co}, W_{cb}, W_{cL}, W_{cR}) can be calculated by using equations (3.8), (3.9), (3.10) and (3.11).

According to Eq. (3.8), the work performed by the motor W_o, the constraint forces on the mechanical oscillator W_{co} and the change in mechanical energy ΔE_o in two steps are shown in Fig. 3-5(a). According to Eq. (3.9), the work performed by the motor W_b, the constraint forces on the trunk W_{cb} and the change in mechanical energy ΔE_b in two steps are shown in Fig. 3-5(b). The constraint forces perform more negative work than positive work on the mechanical oscillator and trunk (W_{co} in Fig. 3-5(a) and W_{cb} in Fig. 3-5(b)). According to Eq. (3.12), if W_{co} and W_{ct} are negative, "W_{cL} + W_{cR}" are positive. Some of the mechanical energy is transferred to the legs by the constraint forces. As shown in Fig. 3-5(c), W_{cL} and W_{cR} are calculated by equations (3.10) and (3.11), and E_{i_L} and E_{i_R} are the dissipation energy of the left and right legs in the collision. The swing leg acquires more mechanical energy than the stance leg does in a single-support phase. In the process of energy transfer, constraint forces neither change the total mechanical energy nor consume additional energy, and there is therefore no energy loss in the process.

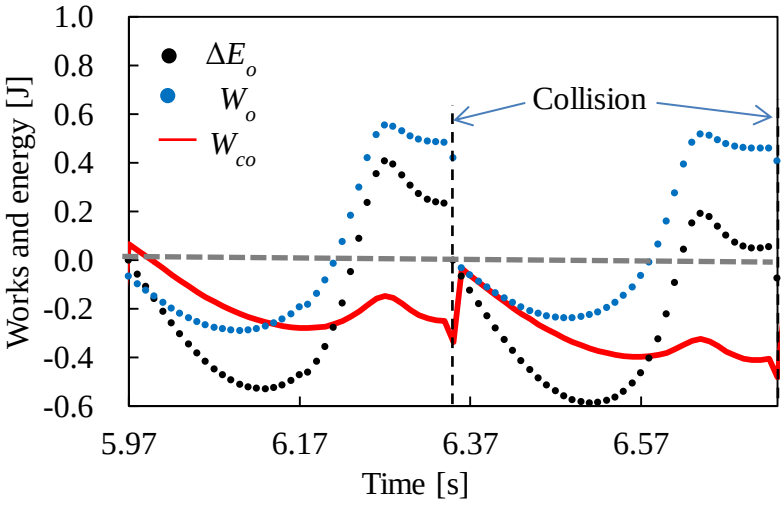

(a) Mechanical oscillator

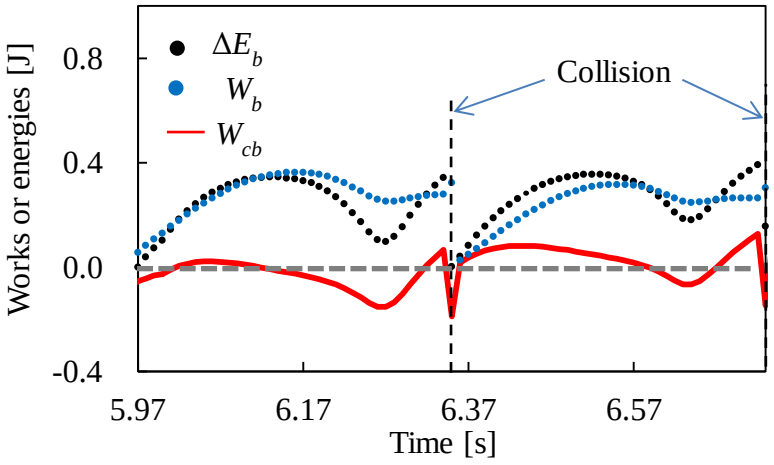

(b) Trunk

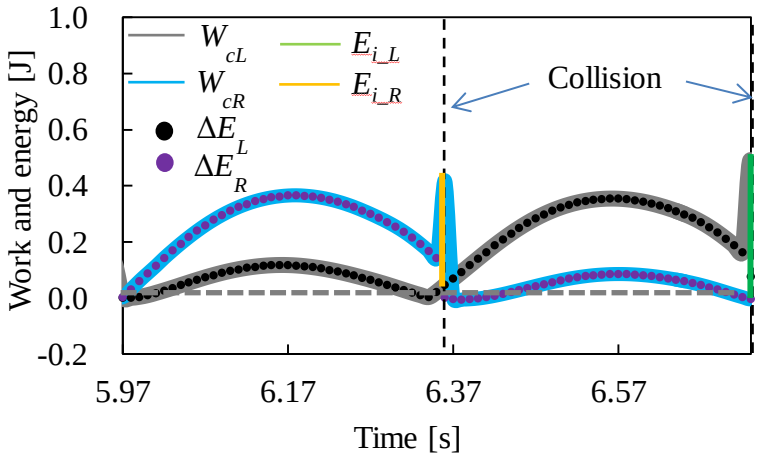

(c) Legs

Fig. 3-5 Energy transfer between the segments of the robot in two steps

3.6 Conclusion

There are several findings or conclusions in this chapter. First, the energy efficiency of the quasi-passive walker was investigated and analyzed from the viewpoint of energy transformation. The results show that high energy utilization rate of the motor helps to increase the energy efficiency in walking. In a future work, in order to further improve energy efficiency of the quasi-passive walker, we will focus on improving the trajectory of the mechanical oscillator and on reducing the energy loss at heel strike by improvement in the design or by additional control. Besides, the quasi-passive walker can walk efficiently even though the target trajectory of the mechanical oscillator is generated online.

Second, the energy efficiency of the quasi-passive walker under different control methods is compared based on ODE simulation. The results show that the control method based on sine oscillator shows higher energy efficiency than our method based on forced Van der Pol oscillator, but our control method is more robust.

Third, energy transfer and transformation from the trunk to the legs were analyzed qualitatively based on mechanical energy. The constraint forces of joints transfer mechanical energy to the legs, and potential energy is transformed to kinetic energy of the legs, and thus the legs can move forward without active hip joints. By the energy transformation of the quasi-passive walker, the change in kinetic energy of the quasi-passive walker is periodic in stable walking when energy balance is satisfied. The next chapter indicates that it is possible to stabilize the quasi-passive walker even under uncertain ground condition by recovering the kinetic energy loss in walking.

4. Stabilization method based on energy balance

4.1 Introduction

In section 2.3, the “stabilization control algorithm” is introduced. According to the control algorithm, the motion of the mechanical oscillator is always entrained into the lateral motion of the quasi-passive walker based on forced entrainment, and thus the motor of the walker can efficiently change the period of the lateral motion T_L and input mechanical energy into the quasi-passive walker. Further, based on the “period stabilization condition”, the amplitude of the mechanical oscillator is determined by the period difference of the lateral motion and swing leg motion by multiplying proportional gain to synchronize the two motions and to stabilize the gait of the walker.

However, the determination method of the amplitude leads to deficiency of input energy in uphill walking. In section 2.4, the determination method of the amplitude of the mechanical oscillator based on the “period stabilization condition” is improved by PI components, and uphill walking is realized. However, the method improved by PI components leads to excess of input energy in downhill walking. The “period stabilization condition” is only the necessary but not sufficient condition for stable walking. The determination method of the amplitude of the mechanical oscillator based on “period stabilization condition” cannot provide appropriate input energy for stable walking under more complex ground conditions, such as a path with both of upward and downward slopes.

In this chapter, a stabilization method based on energy balance is proposed to improve the environmental adaptability of the quasi-passive walker even under uncertain ground condition. The proposed method is a development of the “stabilization control algorithm”, and the method combines energy balance and the merits of “stabilization control algorithm”. According to the proposed method, the target path of the mechanical oscillator is determined by period, phase and amplitude, respectively. The determination method of period and phase of the mechanical oscillator are the same as “stabilization control algorithm”. In order to provide appropriate input energy for stable walking, the amplitude of the mechanical oscillator

β is determined by the required input energy E_{N_1s} in one step based on energy balance.

First, in order to calculate β by E_{N_1s}, the relationship between β and mechanical work performed by the quasi-passive walker W_{r_1s} (=E_{N_1s} in stable walking) is investigated based on the dynamics of the quasi-passive walker. Second, energy balance in stable walking is defined from the viewpoint of energy transformation, and the energy balance equation for stable walking is proposed. Third, a direct method for the determination of β based on the energy balance equation is proposed in section 4.4. Fourth, an indirect method based on a transformation of energy balance equation is proposed for the experimental quasi-passive walker. In ODE simulation, the accurate value of the required motion information used for the direct method can be acquired. However, it is difficult to acquire the accurate value of the required motion information of the experimental quasi-passive walker, the reason of which is analyzed in section 4.5. Therefore, an indirect method is proposed to solve the problem.

4.2 Relationship between the amplitude of the mechanical oscillator and the work performed by the quasi-passive walker

First, the dynamics of a simplified model of the quasi-passive walker and the simplified model of the switching of stance leg are presented. Second, the relationship between the amplitude of the mechanical oscillator β and the mechanical work performed by the motor W_{r_1s} is investigated based on the dynamics of the simplified model.

4.2.1 Dynamics of lateral motion of the quasi-passive walker with spherical foot sole

Since the mechanical oscillator is actuated by the motor in the frontal plane, the input energy is generated in the lateral motion of the walker in the frontal plane. Therefore, a simplified model of the lateral motion of the quasi-passive walker is used to investigate the relationship between β and W_{r_1s}. The simplified model of the quasi-passive walker is shown in Fig. 4-1, where θ and θ_w represent the absolute

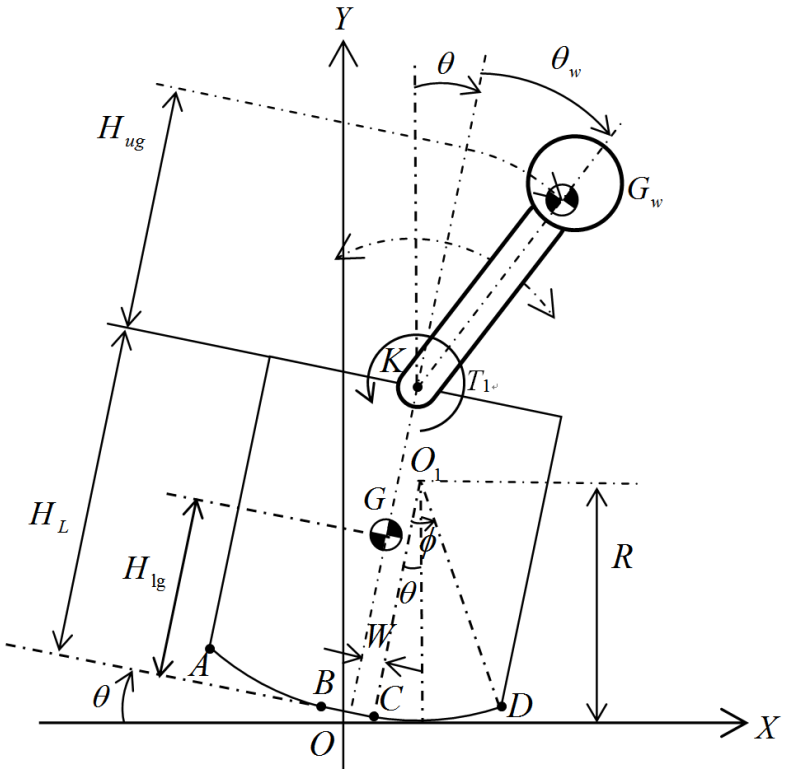

Fig. 4-1 A simplified model of the lateral motion of the quasi-passive walker

rotational angle of the trunk and the rotational angle of the mechanical oscillator relative to the trunk. The model retains one important motion features of the lateral motion of the walker. The feature is the pure roll motion of the spherical foot sole on the ground during walking. The trunk and legs of the experimental quasi-passive walker, which is shown in Fig. 2-5, are simplified to a block with curved bottom, which represents the spherical foot sole of the quasi-passive walker. The spherical foot sole is important for stability of gait and the energy transformation between kinetic energy and potential energy during walking.

It is supposed that the stance leg rolls on the ground without slip, and the friction of joints is negligible. The torque of the motor is the only non-conservative force (generalized force). The parameters of the model are shown as follows:

W: Half length of the clearance between the left and right feet [m]

G: The center of mass of the block

G_w: The center of mass of the mechanical oscillator

H_{lg}: Vertical distance of the center of mass of the block from the bottom of the block [m]

H_{ug}: Vertical distance of the center of mass of the mechanical oscillator from the top of the block [m]

H_L: Vertical distance of the block [m]

O_1: The center of the circle of the curved foot

R: The radius of foot sole [m]

θ: Roll angle of the quasi-passive walker [rad]

θ_w: Roll angle of the oscillator relative to the block [rad]

m_b : Mass of the block which models the trunk and the feet of the quasi-passive walker [kg]

m_w: Mass of the mechanical oscillator [kg]

I_b: Moment of inertia of the block around the axis passing through the center of mass of the block [kg·m^2]

I_w: Moment of inertia of the mechanical oscillator around the axis passing through

the center of mass of the mechanical oscillator [kg·m^2]

T_1: Torque of the motor [N·m]

The value of the parameters, which are used in the calculation of $W_{r\_1s}(\beta)$, are shown in Table 4-1.

Table. 4-1 Parameters of the simplified model

W [m]	H_L [m]	H_{ug} [m]	I_w [kg·m^2]	m_w [kg]	R [m]
0.015	0.349	0.149	0.0031	1.241	0.8

By using Lagrange Equation, the equations of dynamics for the model shown in Fig. 4-1 are

$$J_1\ddot{\theta}(t) + J_2\ddot{\theta}_w(t) + 2J_3\dot{\theta}(t)\dot{\theta}_w(t) + J_4\dot{\theta}(t)^2 + J_5\dot{\theta}_w(t)^2 + J_6 = 0\,, \tag{4.1}$$

$$J_7\ddot{\theta}(t) + J_8\ddot{\theta}_w(t) + J_9\dot{\theta}(t)^2 + J_{10} = T_1\,, \tag{4.2}$$

where the parameters J_1~J_{10} are shown as follows.

$$\begin{aligned} J_1 = {} & I_b + I_w + m_b H_{\lg}^2 + 2\left(m_b H_{\lg} + m_w H_L\right)R\cos\theta(t) + 2\left(m_b + m_w\right)RW\sin\theta(t) \\ & + 2m_w\left\{W\sin\theta(t) + \cos\theta(t)H_L + R\left(1-\cos\theta(t)\right)\right\}H_{ug}\cos\left(\theta(t)+\theta_w(t)\right) \\ & + 2m_w\left(H_L\sin\theta(t) - R\sin\theta(t) - WH_{ug}\cos\theta(t)\sin\left(\theta(t)+\theta_w(t)\right)\right. \\ & + 2m_w\left(H_L\sin\theta(t) - R\sin\theta(t) - W\cos\theta(t)\right)H_{ug}\sin\left(\theta(t)+\theta_w(t)\right) \\ & + m_w\left\{H_{ug}^2 + 2R^2\left(1-\cos\theta(t)\right) + W^2 + H_L^2 - 2RH_L\right\} \\ & + m_b\left\{W^2 + 2R^2\left(1-\cos\theta(t)\right) - 2RH_{\lg}\right\} \end{aligned}$$

$$\begin{aligned} J_2 = {} & I_w + m_w H_{ug}\cos\left(\theta(t)+\theta_w(t)\right)\left\{R\left(1-\cos\theta(t)\right) + W\sin\theta(t) + H_L\cos\theta(t)\right\} \\ & + m_w H_{ug}\sin\left(\theta(t)+\theta_w(t)\right)\left(H_L\sin\theta(t) - R\sin\theta(t) - W\cos\theta(t)\right) + m_w H_{ug}^2 \end{aligned}$$

$$J_3 = m_w H_{ug}\left[\cos\left(\theta(t)+\theta_w(t)\right)\left\{H_L\sin\theta(t) - R\sin\theta(t) - W\cos\theta(t)\right\}\right.$$

$$+\sin(\theta(t)+\theta_w(t))\{R(\cos\theta(t)-1)-W\sin\theta(t)-H_L\cos\theta(t)\}]$$

$$J_4 = R\{(m_b+m_w)(R\sin\theta(t)+W\cos\theta(t))-m_bH_{\lg}\sin\theta(t)$$
$$-m_wH_L\sin\theta(t)-m_wH_{ug}\sin(\theta(t)+\theta_w(t))\}$$

$$J_5 = m_wH_{ug}[\sin(\theta(t)+\theta_w(t))\{R(\cos\theta(t)-1)-W\sin\theta(t)-H_L\cos\theta(t)\}$$
$$+\cos(\theta(t)+\theta_w(t))(H_L\sin\theta(t)-R\sin\theta(t)-W\cos\theta(t))]$$

$$J_6 = m_bg(R\sin\theta(t)-H_{\lg}\sin\theta(t)+W\cos\theta(t))$$
$$+m_wg\{R\sin\theta(t)+W\cos\theta(t)-H_L\sin\theta(t)-H_{ug}\sin(\theta(t)+\theta_w(t))\}$$

$$J_7 = m_wH_{ug}\sin(\theta(t)+\theta_w(t))(H_L\sin\theta(t)-R\sin\theta(t)-W\cos\theta(t))$$
$$+m_wH_{ug}\cos(\theta(t)+\theta_w(t))\{W\sin\theta(t)+R(1-\cos\theta(t))+H_L\cos\theta(t)\}+m_wH_{ug}^2+I_w$$

$$J_8 = m_wH_{ug}^2+I_w$$

$$J_9 = m_wH_{ug}\sin(\theta(t)+\theta_w(t))(H_L\cos\theta(t)+W\sin\theta(t)-R\cos\theta(t))$$
$$+m_wH_{ug}\cos(\theta(t)+\theta_w(t))(W\cos\theta(t)-H_L\sin\theta(t)+R\sin\theta(t))$$

$$J_{10} = -m_wgH_{ug}\sin(\theta(t)+\theta_w(t))$$

Equation (4.1) describes the lateral motion of the block and Eq. (4.2) describes the lateral motion of the mechanical oscillator.

4.2.2 Simplified model of switching of stance leg

The switching of stance leg in walking is a discrete event, and leads to the state jump and energy loss because of the collision (heel strike) of the swing leg with

ground. The collision occurs in double support when both of the points *B* and *C* in Fig. 4-1 simultaneously contact with ground.

The collision model of the quasi-passive walker can be simplified to a model of a rocking block, as shown in Fig. 4-2. The points *B* and *C* represent the inside edge of left and right feet. In Fig. 4-2, point C is the support point, and point B collides with ground. The center of mass of the quasi-passive walker is represented by G_r, which exists at left or right side of the geometrical central line of the quasi-passive walker in double support, because the center of mass of the mechanical oscillator exists at the left or right side of the trunk. Other parameters and variables are shown as follows:

m_r: Mass of the quasi-passive walker [kg]

θ: Roll angle of the quasi-passive walker [rad]

$\dot{\theta}^-$: Angular velocity of the quasi-passive walker immediately before collision [rad/s]

$\dot{\theta}^+$: Angular velocity of the quasi-passive walker immediately after collision [rad/s]

H_g: Vertical distance of center of mass of the quasi-passive walker [m]

W_L: Horizontal distance between G_r and inside edge of left foot [m]

W_R: Horizontal distance between G_r and inside edge of right foot [m]

I_g: The moment of inertia of the quasi-passive walker around the axis passing through G_r [kg·m^2]

The collision is supposed to be inelastic, and slip of support points *B* and *C* are ignore at the moment of collision. The angular momentum of the quasi-passive walker around the axis passing through point *B* immediately before the collision is expressed as

$$L_1 = m_r\sqrt{(H_g^2 + W_L^2)(H_g^2 + W_R^2)}\dot{\theta}^- \cos\phi_1 + I_g\dot{\theta}^-, \tag{4.3}$$

where $\cos\phi_1$ is

$$\cos\phi_1 = \frac{H_g^2 - W_L W_R}{\sqrt{(H_g^2 + W_L^2)(H_g^2 + W_R^2)}}$$

given from geometrical relationship.

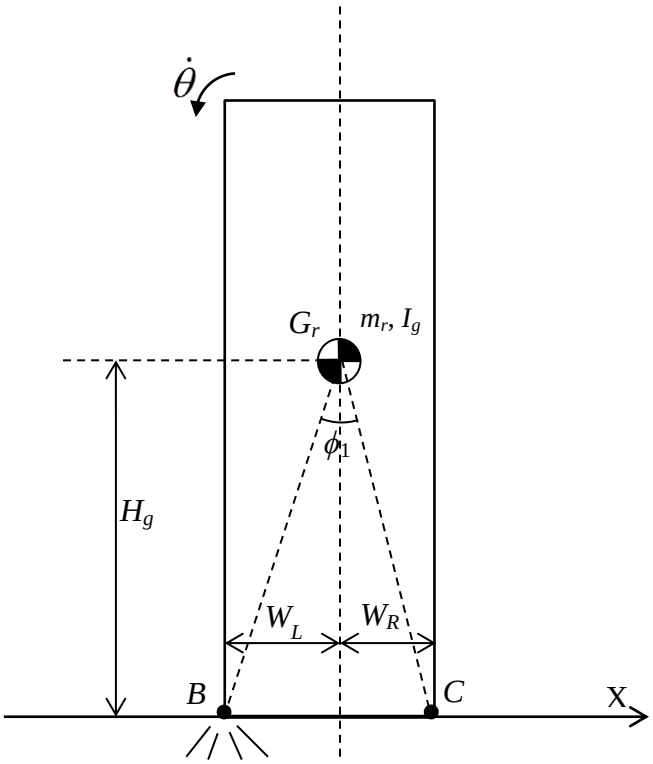

Fig. 4-2 A simplified collision model of lateral motion of the quasi-passive walker

The angular momentum of the quasi-passive walker around the axis passing through the point *B* immediately after collision is expressed as

$$L_2 = m_r(H_g^2 + W_L^2)\dot{\theta}^+ + I_g\dot{\theta}^+ . \tag{4.4}$$

The angular momentum of the quasi-passive walker around the axis passing through the point *B* is conserved at collision. Therefore, conservation law of angular momentum,

$$L_1 = L_2,$$

is satisfied.

From Eq. (4.3) and Eq. (4.4), the angular velocity of the quasi-passive walker immediately after collision can be derived as

$$\dot{\theta}^+ = \frac{m_r(H_g^2 - W_L W_R) + I_g}{m_r(H_g^2 + W_L^2) + I_g}\dot{\theta}^-$$

$$= \lambda\dot{\theta}^- . \tag{4.5}$$

From Eq. (4.5), $0 < \lambda < 1$ is satisfied, because $W_L \neq 0$ and $W_L^2 > -W_L W_R$ in double support. Besides, Eq. (4.5) can be utilized to optimize the parameters of the quasi-passive walker to decrease the energy consumption at collision.

4.2.3 Relationship between the amplitude and the work

The relationship between the amplitude of the mechanical oscillator β and the work performed by quasi-passive walker W_{r_1s} in one step is analytically investigated based on dynamics of the simplified model, in order to determine β by the required input energy E_{N_1s} in one step. W_{r_1s} can be defined as shown in Eq. (4.6) in one walking cycle, in which the roll angle of the mechanical oscillator θ_w changes from 0 degree to β and then returns to 0 degree.

$$W_{r\_1s}(\beta) = \int_0^{\beta} T_1(\theta_w)d\theta_w + \int_{\beta}^{0} T_1'(\theta_w)d\theta_w , \tag{4.6}$$

where $T'_1(\theta_w)$ is the torque of the motor when θ_w changes from β to 0 degree. Equation (4.6) is a general definition of $W_{r\_1s}(\beta)$. If the analytical solutions of Eq. (4.1) and Eq. (4.2) can be obtained, $T_1(\theta_w)$ can be calculated from Eq. (4.2). However, it is

very difficult to find the analytical solutions of Eq. (4.1) and Eq. (4.2), so the $T_1(\theta_w)$ cannot be calculated and $W_{r\_1s}(\beta)$ cannot be obtained from Eq. (4.6).

If the integrating range of the Eq. (4.6) can be transformed from angle to time, $W_{r\_1s}(\beta)$ can be calculated by using $T_1(t)$ based on Eq. (4.2). Based on the assumption of θ_w and θ in the "stabilization control algorithm" proposed by reference [50], θ_w and θ are shown as Eq. (4.7) and Eq. (4.8).

$$\theta_w = \beta\cos(\omega t + \varphi), \tag{4.7}$$

$$\theta = k_\beta \beta\cos(\omega t), \tag{4.8}$$

where k_β is the proportionality factor of the amplitude. The value of k_β depends on the conditions and parameters of environment, such as the coefficient of restitution and the inclination angle of slope. And k_β is a constant value in stable periodic walking. Here, the phase difference φ is set to $\pi/2$, because in level and uphill walking φ is automatically selected to $\pi/2$ when β is positive. Therefore, from Eq. (4.7), $d\theta_w$ can be expressed by

$$d\theta_w = -\omega\beta\cos(\omega t)dt. \tag{4.9}$$

Besides, when φ is equal to $-\pi/2$, the problem can be investigated in the same manner.

The integration ranges of θ_w in Eq. (4.6) is [0, β) and [β, 0) in one walking cycle. When θ_w becomes to 0 rad,

$$\theta_w = -\beta\sin(\omega t) = 0 \Rightarrow t = \frac{n\pi}{\omega}, \tag{4.10}$$

where n means n step. Therefore the integrating range [0, β) and [β, 0) of the Eq. (4.6) can be transformed to the integrating range [$n\pi/\omega$, $(n+1)\pi/\omega$) given by time, which is one walking cycle. Based on equations (4.6) ~ (4.10), W_r can be obtained by

$$W_{r\_1s}(\beta) = \int_{\frac{n\pi}{\omega}}^{\frac{(n+1)\pi}{\omega}} -T_1(t)\omega\beta\cos(\omega t)dt, \tag{4.11}$$

where $T_1(t)$ is expressed by Eq. (4.1). However, some terms in Eq. (4.1) cannot be integrated because of nonlinear terms, such as $\sin(\theta_w+\theta)$, $\sin(\theta)$ and $\cos(\theta)$. To solve the problem, the non-integrable terms are approximately simplified to

$$\sin(\theta+\theta_w)\approx\theta+\theta_w,$$

$$\cos(\theta+\theta_w)\approx 1,$$

$$\sin(\theta)\approx\theta,$$

$$\cos(\theta)\approx 1,$$

by assuming that θ_w and θ changes near 0 rad. Based on the above approximation, $W_{r\_1s}(\beta)$ can be calculated from Eq. (4.11) as follows:

$$W_{r\_1s}(\beta)=\frac{1}{15}k_\beta\left(10m_wH_{ug}\omega^2Wk_\beta^2\cos^3(n\pi)-6m_wH_{ug}\omega^2Wk_\beta^2\cos^5(n\pi)\right)\beta^5 \tag{4.12}$$

$$+\frac{3}{8}k_\beta\left(m_w\pi H_{ug}^2\omega^2-m_wH_{ug}\omega^2k_\beta^2R\pi+m_wH_{ug}\omega^2k_\beta^2H_L\pi+m_wH_{ug}^2\omega^2k_\beta^2\pi\right)\beta^4$$

$$+\frac{2}{3}k_\beta\left(m_wH_{ug}\omega_1^2W\cos^3(n\pi)\right)\beta^3$$

$$+\frac{1}{2}k_\beta\left(m_wgH_{ug}\pi+m_w\pi H_{ug}^2\omega^2+\pi\omega^2J_w+m_w\pi H_LH_{ug}\omega^2\right)\beta^2$$

The parameters of Eq. (4.9) are shown in table 4-1, and the angular frequency ω of θ is set to an average value of $20\pi/7$ rad/s. Because of the error caused by approximation, there are two results of $W_{r\_1s}(\beta)$ when n is an odd or even number. When n is odd number, $W_{r\_1s}(\beta)$ is shown as Eq. (4.13).

$$\begin{aligned}W_{r\_1s}(\beta)&=-0.059531k_\beta^3\beta^5-5.295041k_\beta^3\beta^4+2.61245k_\beta\beta^4\\&\quad-0.148826k_\beta\beta^3+9.187551k_\beta\beta^2\\&=-0.059531\theta_{\max}^3\beta^2-5.295041\theta_{\max}^3\beta+2.61245\theta_{\max}\beta^3\\&\quad-0.148826\theta_{\max}\beta^2+9.187551\theta_{\max}\beta,\end{aligned} \tag{4.13}$$

Where θ_{max} is the amplitude of lateral motion of the robot and is equal to $k_\beta\beta$. The 3D function of Eq. (4.13) is shown in Fig. 4-3.

When n is an even number, $W_{r\_1s}(\beta)$ is shown as Eq. (4.14).

$$\begin{aligned}W_{r\_1s}(\beta)&=0.059531k_\beta^3\beta^5-5.295041k_\beta^3\beta^4+2.61245k_\beta\beta^4\\&\quad+0.148826k_\beta\beta^3+9.187551k_\beta\beta^2\end{aligned} \tag{4.14}$$

$$= 0.059531\theta_{\max}^3\beta^2 - 5.295041\theta_{\max}^3\beta + 2.61245\theta_{\max}\beta^3$$

$$+0.148826\theta_{\max}\beta^2 + 9.187551\theta_{\max}\beta,$$

where the sign of the first and fourth terms are opposite to Eq. (4.13). The 3D function of Eq. (4.14) is shown in Fig. 4-4. The surfaces shown in Fig. 4-3 and Fig. 4-4 almost agrees with each other because the coefficients of the different terms in Eq. (4.13) and Eq. (4.14) are very small. When θ_{max} is fixed, there is an approximate linear relationship between $W_{r\_1s}(\beta)$ and β.

The values of the first four terms are much smaller than the value of the last term in both of Eq. (4.13) and Eq. (4.14). Therefore, the relationship between $W_{r\_1s}(\beta)$ and β can be approximately simplified as

$$W_{r\_1s}(\beta) = 9.187551k_\beta\beta^2 = 9.187551\theta_{\max}\beta \tag{4.15}$$

Because the change of θ_{max} in continuous two steps is small in steady walking, the relationship between $W_{r\_1s}(\beta)$ and β can be approximated as linear relationship for simplicity of control algorithm.

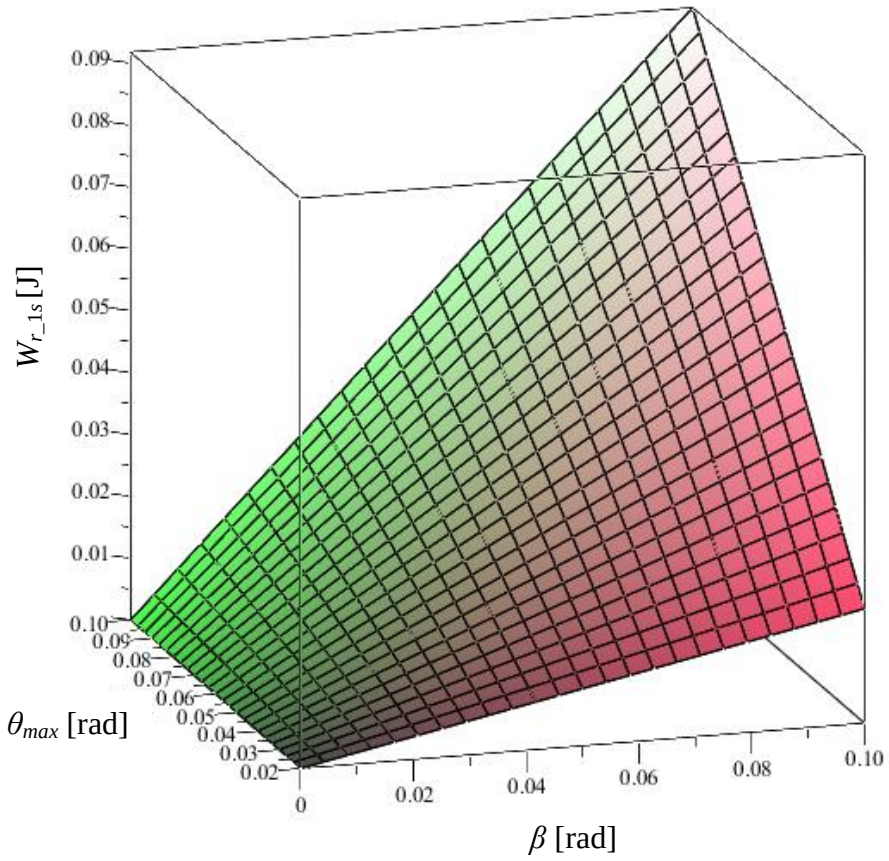

Fig. 4-3 Mechanical work W_{r_1s} as a function of amplitude θ_{max} and k_β when n is an odd number.

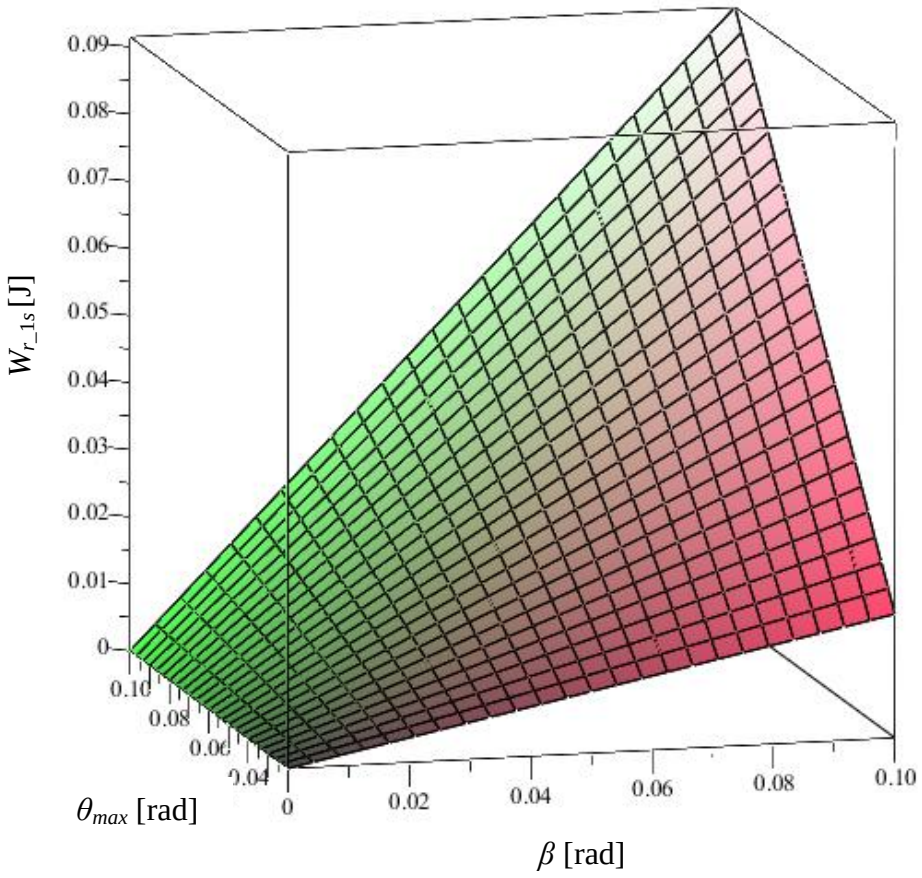

Fig. 4-4 Mechanical work W_{r_1s} as a function of amplitude θ_{max} and k_β when n is an even number.

4.3 Energy balance in stable walking

Energy transformation of the quasi-passive walker is mentioned in section 3.3, and the energy transformation of the quasi-passive walker in one step can be expressed by

$$W_{r\_1s} = \Delta E_{K\_1s} + \Delta E_{P\_1s} + E_{D\_1s}, \tag{4.16}$$

where W_{r_1s} is the work performed by the quasi-passive walker in one step, ΔE_{K_1s} is the change of the kinetic energy of the quasi-passive walker in one step, ΔE_{P_1s} is the change of potential energy in one step, and E_{D_1s} is the dissipation energy in one step. In ODE simulation, E_{D_1s} is equal to the energy loss at heel-strike E_i in one step, which is defined in Eq. (3.2), because the friction of the joints of the quasi-passive walker is set to 0. However, E_{D_1s} includes both E_i and energy loss from friction. Moreover, one step has the same meaning as one walking cycle in this study, but the initial and final states of one step have different definition in direct and indirect methods. In direct method, initial state of one step is the moment immediately after heel-strike, and final state of one step is the moment immediately before the next heel-strike.

Because the movement of the quasi-passive walker is periodic under steady-state walking, the kinetic energy of the quasi-passive walker varies periodically under constant ground condition. In the condition, the kinetic energies at the initial state agree with that of the final state in one step, and thus the change of kinetic energy ΔE_{K_1s} is equal to 0. Therefore, Eq. (4.16) can be simplified as

$$W_{r\_1s} = \Delta E_{P\_1s} + E_{D\_1s}. \tag{4.17}$$

Therefore, the energy balance equation is defined as

$$E_{N\_1s} = \Delta E_{P\_1s} + E_{D\_1s}, \tag{4.18}$$

which shows that input energy E_{N_1s} in one step is transformed into potential energy and dissipation energy in stable walking. According to Eq. (4.18), if the input energy E_{N_1s} in one step is equal to "ΔE_{P_1s} +E_{D_1s}", the quasi-passive walker can be stabilized even under uncertain ground condition. Based on the idea, a stabilization method based on energy balance is proposed in section 4.4.

4.4 Direct method for the determination of the amplitude of the mechanical oscillator

The direct method keeps the energy balance of the quasi-passive walker to stabilize the quasi-passive walker. The input energy E_{N_1s} is determined by the sum of E_{D_1s} and ΔE_{P_1s} according to Eq. (4.18). The amplitude β is determined based on E_{N_1s}. The calculation methods of the dissipation energy E_{D_1s}, the change in potential energy ΔE_{P_1s} and the amplitude of the mechanical oscillator β are introduced in this section.

4.4.1 Dissipation energy

The dissipation energy E_{D_1s} of the quasi-passive walker is mainly caused by the heel strike of the swing leg with ground. In the ODE simulation, assuming that the deformation of body and the friction of joints can be ignored, the dissipation energy E_{D_1s} at heel strike is expressed as

$$E_{D\_1s} = E_r^{t1-} - E_r^{t1+}, \tag{4.19}$$

where E_r^{t1-} and E_r^{t1+} are both the mechanical energies of the quasi-passive walker, "t1-" represents the moment immediately before heel strike, and "t1+" represents the moment immediately after heel strike.

The mechanical energy of the quasi-passive walker E_r is the sum of potential energy E_P, translational kinetic energy E_{TK} and rotational kinetic energy E_{RK} as follows

$$E_r = E_P + E_{TK} + E_{RK}. \tag{4.20}$$

The translational and rotational kinetic energy of the segments are calculated separately in this study. The mass and moment of inertia of each segment, around body axes passing through the center of mass, are shown in Table 2-1 and Table 2-2. Translational kinetic energy E_{TK} and rotational kinetic energy E_{RK} can be calculated as

$$E_{TK} = \frac{1}{2}(m_T V_T^2 + m_{LR} V_{LR}^2 + m_{LL} V_{LL}^2 + m_o V_o^2), \tag{4.21}$$

and

$$E_{RK} = E_{RT} + E_{RLR} + E_{RLL} + E_{RO}, \tag{4.22}$$

where m_T, m_{LR}, m_{LL} and m_o are the masses of the trunk, right leg, left leg and mechanical oscillator; V_T, V_{LR}, V_{LL}, V_o are the translational velocities of the trunk, right leg, left leg and mechanical oscillator; E_{RT}, E_{RLR}, E_{RLL} and E_{RO} are the rotational kinetic energies of the trunk, right leg, left leg and mechanical oscillator. And E_{RT} can be expressed as

$$E_{RT} = \frac{1}{2}(I_{TX}\omega_{TX}^2 + I_{TY}\omega_{TY}^2 + I_{TZ}\omega_{TZ}^2), \tag{4.23}$$

where I_{TX}, I_{TY} and I_{TZ} are the moments of inertial of the trunk around the body axes of the trunk, and ω_{TX}, ω_{TY} and ω_{TZ} are the rotational angular velocity of the trunk around the same body axes. E_{RLR}, E_{RLL} and E_{RO} can be calculated in the same manner with Eq. (4.23).

4.4.2 Potential energy

The change in potential energy in one walking cycle can be calculated from the geometrical relationship of foot sole with ground, as shown in Fig. 4-5. The double support phase of the quasi-passive walker is instantaneous because of the geometrical constrain of the quasi-passive walker, so “double support phase” is called “double support” for simplicity in this study. The attitudes of the quasi-passive walker in double support are indicated by the broken line model and the solid line model. The broken line model represents the attitude of the initial state of one walking cycle, and the solid line model represents the attitude final state of one walking cycle. Point *A′*, *B* and *C* are the tangency points of spherical foot sole with ground, point *O′* and *O* are the hip joint of the quasi-passive walker, point *D*, *E* are the center of the spherical foot sole, and point *F* is the center of the segment *DE*. The radius of the foot sole is R, and the length of the leg is *L* (<R). In double support the quasi-passive walker is always symmetrical about the central axis *OF* because of the geometric constrain.

The change of potential energy can be calculated by the change of vertical height of *O′O*. The length of the segment *O′O* is indicated by *X*. In stable periodic waking, *O′O* is parallel to the ground, and *X* agrees with the translational distance of one step. The right foot sole of the dotted line model is not showed for simplicity, because it does

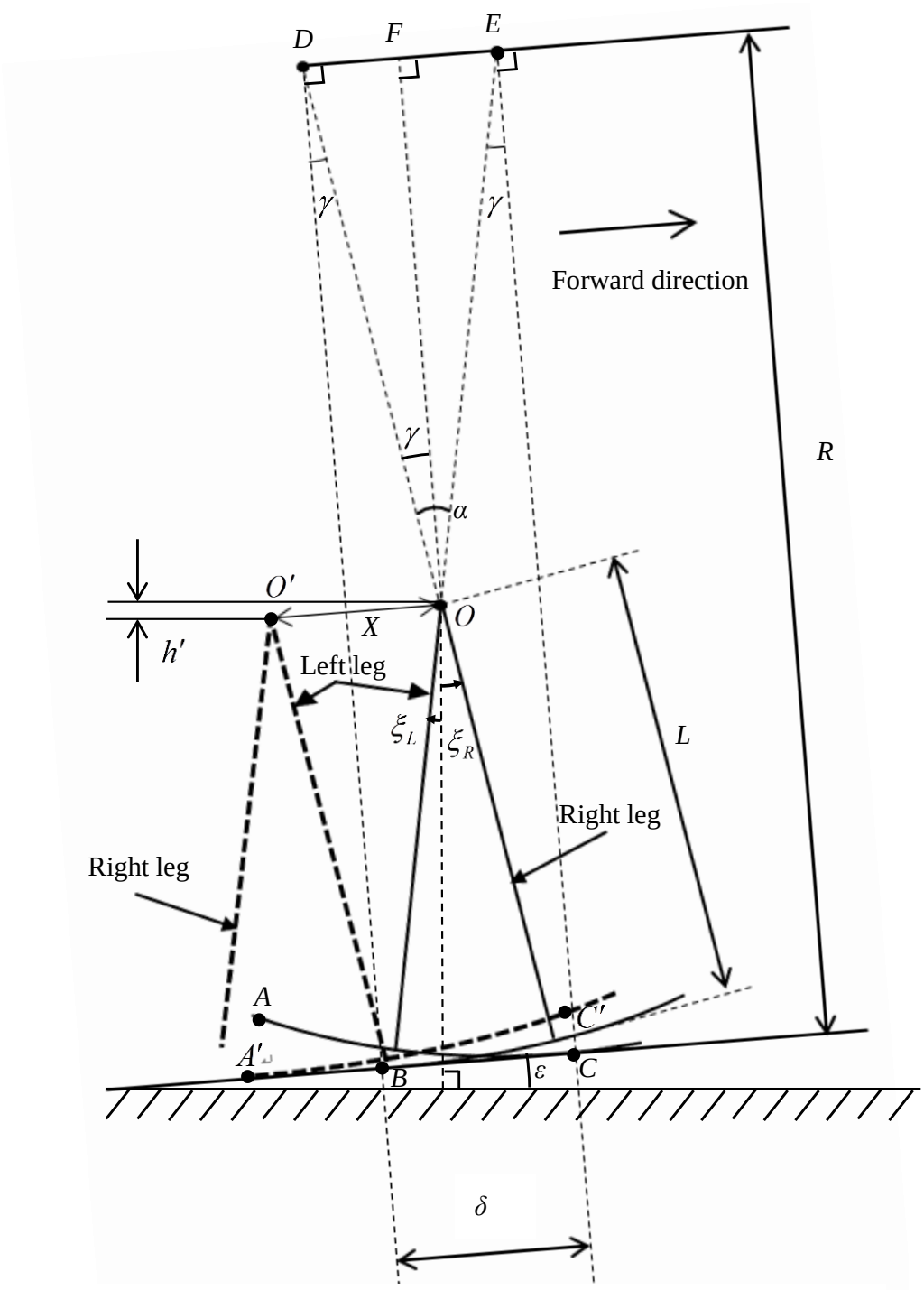

Fig. 4-5 Geometrical relationship of foot sole with ground in the sagittal plan in one walking cycle.

not affect the calculation of potential energy. The change of the potential energy can be expressed as

$$\Delta E_{P\_1s} = m_R g h', \tag{4.24}$$

where h' can be expressed as

$$h' = X \sin\varepsilon . \tag{4.25}$$

Here, h' and ε represent the change of the vertical position of the gravity center of the quasi-passive walker and the inclination angle of the slope. And from the geometrical relationship,

$$X=O'O=A'B=A'C-BC, \tag{4.26}$$

$$A'C=\widehat{AC}=\alpha \cdot R=(\xi_R-\xi_L)R, \tag{4.27}$$

$$BC=\delta=2(R\text{-}L)\sin\gamma = 2(R-L)\sin(\tfrac{\xi_R-\xi_L}{2}), \tag{4.28}$$

$$\varepsilon = \tfrac{\xi_R+\xi_L}{2}, \tag{4.29}$$

are obtained. In Equations (4.24) ~ (4.29), α represents the angle between the legs, ζ_R and ζ_L represent the angle of right and left leg relative to vertical line of horizontal plane, and γ represents the angle of right and left leg relative to vertical line of the slope. Based on the Equations (4.24) ~ (4.29), the change of the potential energy can be expressed as

$$\Delta E_{P\_1s} = m_R g\left[(\xi_R-\xi_L)R-2(R-L)\sin\frac{\xi_R-\xi_L}{2}\right]\sin\frac{(\xi_R+\xi_L)}{2} \tag{4.30}$$

4.4.3 Determination of the amplitude based on input energy

The relationship between amplitude of the mechanical oscillator and mechanical work W'_{r_1s} can be obtained by

$$W'_{r\_1s} = \int_0^{\beta'} T(\theta_w)d\theta_w + \int_{\beta'}^{0} T'(\theta_w)d\theta_w , \tag{4.31}$$

where β' is the amplitude of the mechanical oscillator and W'_{r_1s} is the mechanical work performed by the quasi-passive walker in the last walking cycle. W'_{r_1s} is equal to the integral of the torque of motor $T(\theta_w)$ and $T'(\theta_w)$ over the roll angle of the mechanical oscillator θ_w, where $T(\theta_w)$ represents the motor torque when θ_w changes

from 0 to β', and $T'(\theta_w)$ represents the motor torque when θ_w changes from β' to 0. Assuming that θ_w and θ have sufficiently close value to 0, the approximate linear relationship between amplitude β and mechanical work W_r can be expressed by

$$\frac{\beta}{\beta'} = \frac{W_{r\_1s}}{W'_{r\_1s}} = \frac{E_{N\_1s}}{W'_{r\_1s}}. \tag{4.32}$$

Therefore, β_1, which is the amplitude of the mechanical oscillator determined by energy balance, can be calculated from Eq. (4.18) and Eq. (4.32), as follows

$$\beta_1 = \frac{E_{N\_1s}}{W'_{r\_1s}}\beta' = \frac{\Delta E_{P\_1s} + E_{D\_1s}}{W'_{r\_1s}}\beta'. \tag{4.33}$$

In Eq. (4.30), ΔE_{P_1s} is calculated in double support in the sagittal plane by assuming that the roll and yaw angles of the quasi-passive walker are 0. Note that the roll and yaw angles of the quasi-passive walker change even in straight walking and slight yaw motion occurs in double support, which leads to the error in the calculation of ΔE_{P_1s}. Besides, β_1 is calculated by using the approximate linear relationship of mechanical work and amplitude given by Eq. (4.32), which leads to the error in the calculation of the amplitude β_1.

The errors make it difficult to stabilize the quasi-passive walker under uncertain ground condition only by only the control method. If the amplitude is determined only by β_1, the input energy is not enough to recover the kinetic energy for keeping stable walking. Lack of the input energy, the stride of the quasi-passive walker decreases gradually, and ΔE_{P_1s} and E_{D_1s} decreases.

To solve the problem, the integral of the change of the period of swing leg motion T_{int} given by

$$T_{int} = \sum_{i=1}^{n} (T_{si-1} - T_{si}), \tag{4.34}$$

which is utilized to determine the assistant component of the amplitude beside β_1. In Eq. (4.34), T_{si} is the current period of the swing leg motion and $T_{si\text{-}1}$ is the period of the swing leg motion of the last walking cycle. By multiplying integral gain K_S to T_{int}, the assistant component β_2 of the amplitude is given as

$$\beta_2 = K_S T_{int}. \tag{4.35}$$

From Eq. (4.34) and Eq. (4.35), the amplitude of the mechanical oscillator β is obtained by

$$\beta = \beta_1 + \beta_2 . \tag{4.36}$$

From Eq. (4.36), if T_s is constant during stable walking, β is mainly determined by β_1 based on energy balance. In the other hand, if the T_s changes, β_2 can slow down the change of T_s. For example, if T_s gradually decreased, β_2 increases and enlarge the input energy to recover the kinetic energy for stable walking.

4.4.4 Simulation in the condition of a flat ground

The direct method is examined by ODE simulation in the condition of a flat ground in this section. The version 1 of the simulation model shown in Fig. 2-1 is used for the ODE simulation. The center of masses of the feet is adjusted backward for 0.01 m to generate a rotation moment around hip axis (as shown in Fig. 2-3), so as to enable the swing leg to naturally swing forward even on a flat slope.

The gait of the quasi-passive walker is stabilized for 3 seconds by "stabilization control algorithm" introduced in the section 2.3 at the beginning of the simulation, and then the "stabilization control algorithm" is switched to the direct method based on energy balance, because the proposed method can keep steady walking in the condition that the initial state of the gait of the quasi-passive walker is stable. The gain for β_2 in Eq. (4.35) K_S is set to 0.8, and the maximum amplitude β_{max} is set to 30 degree.

The gait of the quasi-passive walker is stabilized on a flat ground in the ODE simulation with the proposed method given by section 4.6. The sampling period of the simulation is set to 0.01 s. The change in the period of lateral motion T_L and the period of swing leg motion T_S in level walking are shown in Fig. 4-6. The horizontal axis is time, and the vertical axis is period. The dash line shows the time when the proposed method is switched from the "stabilization control algorithm" introduced in section 2.3. The level waking is stabilized and T_L is synchronized with T_S from Fig.

4-6.

The input energy and mechanical work performed by quasi-passive walker in one step are indicated by E_{N_1s} and W_{r_1s}, respectively. In the stable level walking, E_{N_1s} and W_{r_1s} are shown in Fig. 4-7. The horizontal axis is time, and the vertical axis is energy and work. When the quasi-passive walker is stabilized in level walking W_{r_1s} is a little larger than E_{N_1s}, because the minor component β_2 of β increases the value of W_{r_1s}.

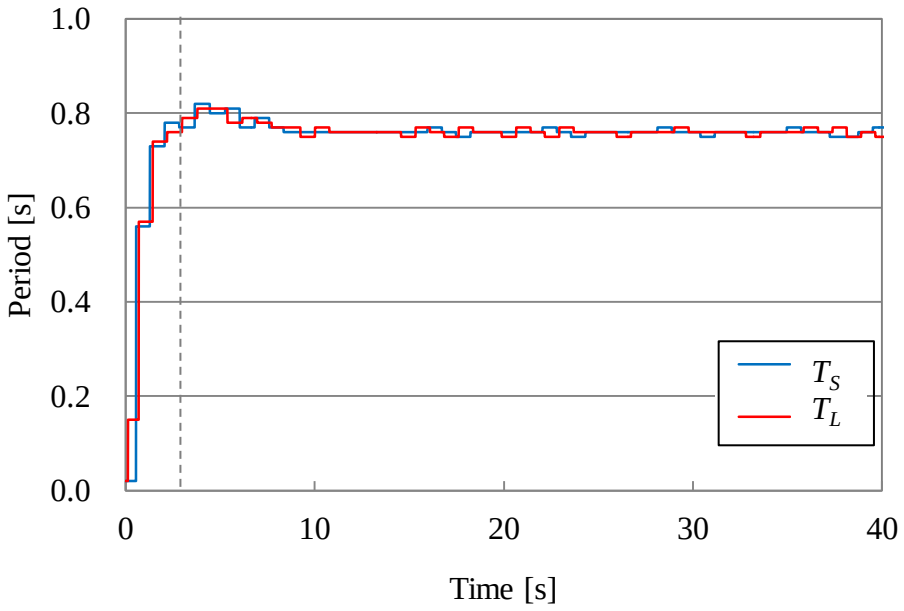

Fig. 4-6 The period of lateral motion T_L and the period of swing leg motion T_S in level walking

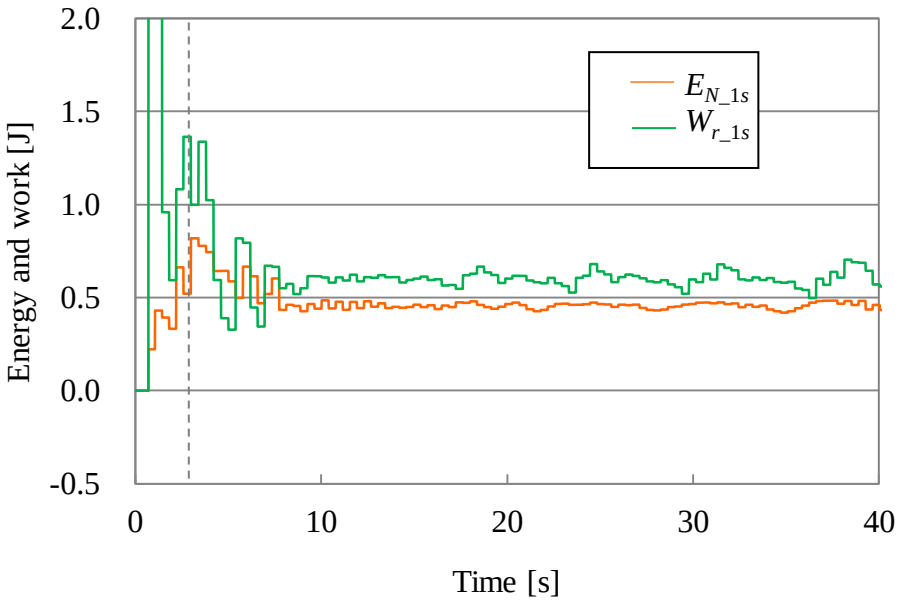

Fig. 4-7 The Input energy E_{N_1s} and the mechanical work performed by quasi-passive walker W_{r_1s} in one step of level walking

4.5 Indirect method for the determination of the amplitude of the mechanical oscillator

In section 4.4, the direct method based on the energy balance is proposed to calculate the input energy E_{N_1s} for the simulation model. And the change in potential energy ΔE_{P_1s} and dissipation energy E_{D_1s} in the energy balance equation can be directly calculated based on the gait information from the ODE simulation.

However, it is difficult to directly calculate ΔE_{P_1s} and E_{D_1s} for the experimental quasi-passive walker. First, ΔE_{P_1s} is calculated by estimating the slope angle of ground based on the gait information in the direct method, and the estimation method relies on the accuracy of the pitch angles of the two legs. The accurate value of the pitch angles of the two legs can be acquired in simulation. However, the accuracy of the pitch angles of the two legs significantly decreases in experiments because of the unsmooth rotation of the gears, which connect the hip axis and the rotary encoders, as shown in Fig. 2-5(b). Moreover, the pitch angle of one leg is calculated by the sum of pitch angle of the trunk and the rotational angle of the leg relative to the trunk. The rotational angles of the two legs can be acquired from the rotary encoders, and the initial values of the rotational angles are set to 0 in experiment. However, it is difficult to adjust the initial rotational angles of the legs to 0 degree, so the initial errors exist and cause low accuracy of the estimation of slope angles.

Second, E_{D_1s} of the experimental quasi-passive walker consists of the dissipation energies caused by friction, deformation of ground and heel-strike. It is difficult to estimate or calculate the dissipation energies caused by friction and deformation of ground in experiments, so E_{D_1s} cannot be calculated.

In this section, an indirect method is proposed to calculate E_{N_1s} based on a transformation of energy balance equation and to stabilize the gait of the experimental quasi-passive walker. According to the indirect method, the calculation of the change in potential energy is performed by utilizing the data of energy transformation during the last step, and does not rely on the estimation of slope angles and E_{D_1s}.

First, the transformation of the energy balance equation is presented in the section 4.5.1. Second, the calculation methods of the potential energy and the kinetic energy

are introduced in the sections 4.5.2 and 4.5.3. Third, a calculation method for the mechanical work W_{r_1s} performed by the experimental quasi-passive walker in one step is proposed in the section 4.5.4. Fourth, the determination method of the amplitude of the mechanical oscillator β is introduced in the section 4.5.5.

4.5.1 Transformation of the energy balance equation

In this section, the initial and final states during one step are redefined, and the energy balance equation given by Eq. (4.18) is transformed under the definition of one step. The initial and final states of one step are defined as the state when the roll angel of the quasi-passive walker becomes to the left and right maximum, as shown in Fig. 4-8. The trunk and legs are simplified to a block with curved bottom, which represents the spherical foot sole of the quasi-passive walker. One step is defined as the phase from the state A to the state B or the phase from the state B to the state A, because the left and right lateral motions of the quasi-passive walker alternately occur. The mechanical oscillator is always at the central line of the quasi-passive walker in the state A and B, because the phase difference between the mechanical oscillator and the quasi-passive walker is $\pi/2$ or $-\pi/2$. The parameters in Fig. 4-8 are shown as follows:

G_R: The center of mass of the quasi-passive walker

H_R: Vertical distance of the center of mass of the quasi-passive walker G_R from the bottom of the block [m]

H_G: Vertical distance of the center of mass of the quasi-passive walker G_R from the ground [m]

R: The radius of foot sole [m]

W: Half length of the clearance between the left and right feet [m]

θ: Roll angle of the quasi-passive walker [rad]

In one step, the change in potential energy ΔE_{P_1s} is determined by the slope angel and the change of the roll angel of the quasi-passive walker. Therefore, the energy balance equation can be expressed as

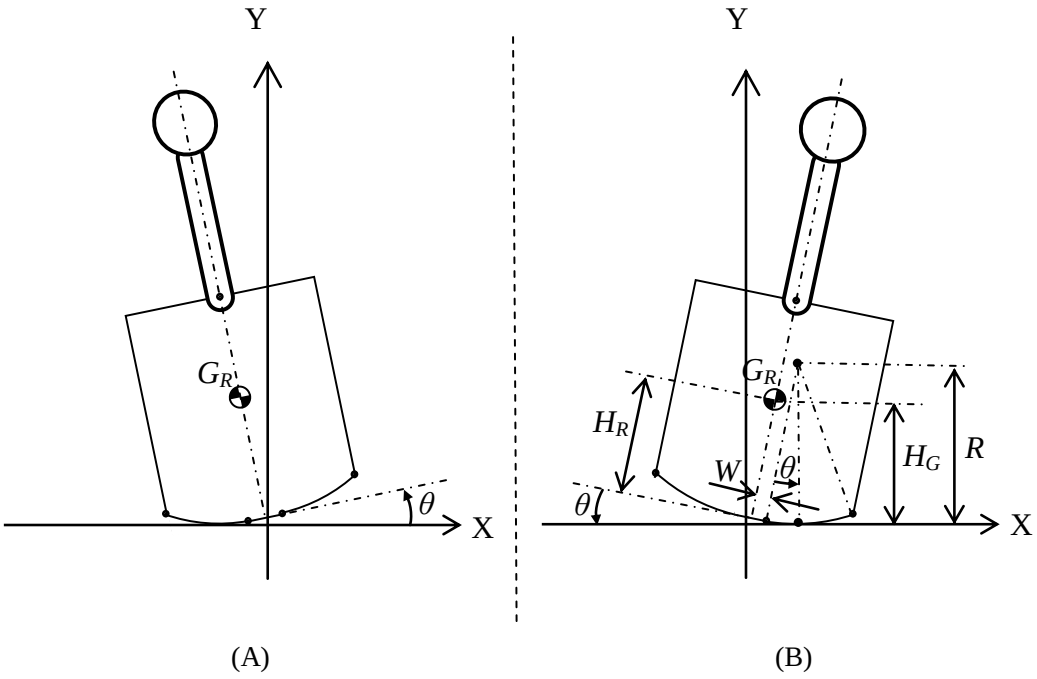

Fig. 4-8 The initial and final states with the maximum of roll angle during one step

$$E_{N\_1s} = \Delta E_{P\_1s} + E_{D\_1s} = \Delta E_{P\_slope\_1s} + \Delta E_{P\_roll\_1s} + E_{D\_1s}, \quad (4.37)$$

where $\Delta E_{P\_slope\_1s}$ is the change in potential energy determined by the slope angle, and $\Delta E_{P\_roll\_1s}$ is the change in potential energy determined by change of the roll angel of the quasi-passive walker during one step. In steady walking the left and right lateral motions are symmetric, and thus $\Delta E_{P\_roll\_1s}$ is equal to 0. Therefore, in steady walking the Eq. (4.37) can be simplified to

$$E_{N\_1s} = \Delta E_{P\_slope\_1s} + E_{D\_1s}. \quad (4.38)$$

If the initial state of one step is the state A in Fig. 4-8 and the final state is the state B in Fig. 4-8, the relationship between mechanical work and mechanical energy of the quasi-passive walker during the last one step is expressed as

$$W'_{r\_1s} = \Delta E'_{P\_slope\_1s} + \Delta E'_{P\_roll\_1s} + \Delta E'_{K\_1s} + E'_{D\_1s}, \quad (4.39)$$

where W'_{r_1s}, $\Delta E'_{P\_slope\_1s}$, $\Delta E'_{P\_roll\_1s}$, $\Delta E'_{K\_1s}$ and E'_{D_1s} are the mechanical work performed by the quasi-passive walker, the change in potential energy determined by the slope angle, the change in potential energy determined by change of the roll angel of the quasi-passive walker, the change in kinetic energy of the quasi-passive walker and the dissipation energy during the last one step, respectively.

If it is assumed that $\Delta E_{P\_slope\_1s} \approx \Delta E'_{P\_roll\_1s}$ and $E_{D\_1s} \approx E'_{D\_1s}$ in continuous two steps in steady walking, energy balance equation can be transformed into

$$E_{N\_1s} = W'_{r\_1s} - \Delta E'_{P\_roll\_1s} - \Delta E'_{K\_1s}, \quad (4.40)$$

from the Eq. (4.38) and Eq. (4.39). The calculation method of $\Delta E'_{P\_roll\_1s}$, $\Delta E'_{K\_1s}$ and W'_{r_1s} are introduced in the following sections to calculate E_{N_1s}.

4.5.2 Potential energy

The change in potential energy $\Delta E'_{P\_roll\_1s}$ caused by the lateral motion during one step is expressed by

$$\Delta E'_{P\_roll\_1s} = m_R g \Delta H_G, \quad (4.41)$$

where m_R is the mass of the quasi-passive walker, and ΔH_G is the change in the height of the center of the mass of the quasi-passive walker in states A and B. From the

geometrical relation of the quasi-passive walker in Fig. 4-8, H_G can be expressed by

$$H_G = R - (R - H_R)\cos\theta + W\sin|\theta|, \tag{4.42}$$

where the definition of the parameters are introduced in the section 4.8.1. The roll angle of the quasi-passive walker θ can be measured by the 6-axis (3-axis Gyro and 3-axis Accelerometer) motion-tracking sensor on the experimental quasi-passive walker. The change in potential energy $\Delta E_{P\_roll\_1s}$ caused by the lateral motion during one step can be calculated from Eq. (4.41) and Eq. (4.42).

4.5.3 Kinetic energy

The general calculation method of the kinetic energy is introduced in the section 4.6.1, where the translational and rotational kinetic energy of the segments of the quasi-passive walker can be calculated separately in simulation. However, it is difficult to use the method for the experimental quasi-passive walker, because the translational velocities of the all segments of the quasi-passive walker cannot be measured by the sensors of the quasi-passive walker.

When the quasi-passive walker is in the state A or B as shown in the Fig. 4-8, the angular velocity in the roll direction and the translational velocities of the trunk and legs in the frontal plane are equal to 0, and thus the kinetic energy of the lateral motion of the trunk and the legs is equal to 0. Moreover, the kinetic energy of the mechanical oscillator in the frontal plane is equal to the rotational kinetic energy of the mechanical oscillator around the motor axis in the state A or B. Therefore, the kinetic energy of lateral motion of the quasi-passive walker can be calculated without the information of translational velocity in the state A or B. Besides, the yaw motion of the quasi-passive walker is very small in the states A and B, and thus the yaw motion can be ignored in the calculation of the kinetic energy for simplicity.

In order to improve the calculation accuracy of the kinetic energy of the quasi-passive walker motion in the sagittal plane in the states A and B, the rotational kinetic energy of the legs is calculated based on the moment of inertia of the legs around the hip axis, because the translational velocity of the legs cannot be directly

measured in experiments. Therefore, in the state A or B, the kinetic energy of the quasi-passive walker can be expressed as

$$E_K = \frac{1}{2}(I_{R\_pitch}\omega_{R\_pitch}^2 + I_{L\_pitch}\omega_{L\_pitch}^2 + I_{(T+O)\_pitch}\omega_{T\_pitch}^2 + I_{O\_roll}\omega_{O\_roll}^2) + E'_{TK}\text{ , (4.43)}$$

where I_{R_pitch} and I_{L_pitch} are the moment of inertia of the right and left legs around the hip axis, respectively; I_{O_roll} is the moment of inertia of the mechanical oscillator around the motor axis, and $I_{(T+O)\_pitch}$ is the moment of inertia of the trunk and mechanical oscillator around the axis passing through the center of mass of them. In Eq. (4.43), ω_{R_pitch}, ω_{L_pitch} and ω_{T_pitch} are the angular velocities of the right leg in the pitch direction, left leg and the trunk, respectively. And ω_{O_roll} is the angular velocity of the mechanical oscillator around the motor axis. And E'_{TK} is the kinetic energy of the quasi-passive walker motion in the sagittal plane in the states A or B, and includes a part of the translational kinetic energy of the quasi-passive walker motion in the sagittal plane.

Angular velocity of the trunk in the pitch direction ω_{T_pitch} can be measured by the 6-axis motion-tracking sensor. Angular velocity of the right leg in the pitch direction ω_{R_pitch} is equal to the sum of ω_{T_pitch} and the angular velocity of the right leg relative to the trunk ω_{R_T}. The experimental quasi-passive walker can measure the angle of the right leg relative to the trunk by the rotary encoder fixed at the hip joint, and the differential of the relative angle is equal to ω_{R_T}. In the same manner, ω_{L_pitch} can be calculated. And ω_{O_roll} is the differential of the roll angle of the mechanical oscillator with respect to time, and is equal to the target path θ_{wt} because the mechanical oscillator is driven by the stepping motor which realizes accurate tracking to the target path. The moment of inertia of the segments is shown in the Table 4-2.

The change in the kinetic energy $\Delta E'_{K\_1s}$ is the difference of the kinetic energy of the final and initial state during one step. Since the kinetic energy E'_{TK} in the states A or B does not change significantly in steady walking, E'_{TK} is deleted in the calculation of the ΔE_{K_1s} for the experimental quasi-passive walker. Therefore, $\Delta E'_{K\_1s}$ is expressed by

$$\Delta E'_{K\_1s} = \frac{1}{2}[I_{R\_pitch}(\omega^2_{R\_pitch} - \omega'^2_{R\_pitch}) + I_{L\_pitch}(\omega^2_{L\_pitch} - \omega'^2_{L\_pitch}) + \tag{4.44}$$

$$I_{(T+O)\_pitch}(\omega^2_{T\_pitch} - \omega'^2_{T\_pitch}) + I_{O\_roll}(\omega^2_{O\_roll} - \omega'^2_{O\_roll})],$$

where ω'_{R_pitch}, ω'_{L_pitch} and ω'_{T_pitch} are the angular velocities of the right leg, left leg and the trunk in the pitch direction at the initial state of one step, respectively. And ω'_{O_roll} is the angular velocity of the mechanical oscillator around the motor axis at the initial state of one step.

Table 4-2 Parameters of the model shown in Fig. 4-8

R [m]: The radius of foot sole	0.8
H_R [m]: Vertical distance of the center of mass of the quasi-passive walker G_R from the bottom of the block	0.237
W [m]: Half length of the clearance between the left and right feet	0.015
I_{R_pitch} [kg·m^2]: The moment of inertia of the right leg around the hip axis	0.0115
I_{L_pitch} [kg·m^2]: The moment of inertia of the left leg around the hip axis	0.0115
$I_{(B+O)\_pitch}$ [kg·m^2]: The moment of inertia of the trunk and mechanical oscillator around the axis passing through their center of mass	0.181
I_{O_roll} [kg·m^2]: The moment of inertia of the mechanical oscillator around the motor axis	0.0246

4.5.4 Mechanical work performed by the quasi-passive walker

The work of the experimental quasi-passive walker W_{r_1s} in one step is performed by the stepping motor, the torque of which can be measured by sensors, such as a torque meter. However, no sensors for measuring torque are used for the simplicity of the structure of the experimental quasi-passive walker. In this study, the relation of W_{r_1s}, the amplitude of the mechanical oscillator β and the maximum of the roll angle of the quasi-passive walker θ_{max} is investigated by ODE simulation to acquire W_{r_1s} based on β and θ_{max}.

From the viewpoint of dynamics of the lateral motion of the quasi-passive walker, the torque of the motor determines the lateral motions of the quasi-passive walker and the mechanical oscillator. The amplitudes of the lateral motion of the quasi-passive walker and the mechanical oscillator are indicated by θ_{max} and β, respectively. Moreover, W_{r_1s} is the path integral of the torque of the motor, and the integrating range is [0, β]. Therefore, the relation between W_{r_1s}, θ_{max} and β is connected by the torque of the motor, and thus it is possible to acquire W_{R_1s} by utilizing θ_{max} and β for experimental quasi-passive walker.

The relation between W_{r_1s}, θ_{max} and β is investigated in ODE simulation. The version 2 of the simulation model is used, as shown in Fig. 2-4, because the model has the same structure, size and mass distribution with the current experimental quasi-passive walker. In simulation, β is set to a constant value, the range of which is set to 6~12 degree and the coefficient of restitution of the flat ground is changeable so that θ_{max} changes as the coefficient of restitution changes. The data of W_{r_1s} versus θ_{max} and β acquired from the simulation are shown in Fig. 4-9, the three axes of which represent W_{r_1s}, θ_{max} and β, respectively. The function $W_{r\_1s}(\theta_{max}, \beta)$ is calculated by curve fitting based on least square method, and is expressed as

$$W_{r\_1s} = 0.6034 - 0.00049\beta - 0.00188\theta_{\max} + 0.00323\beta\theta_{\max}, \qquad (4.45)$$

which is shown in Fig. 4-10. Based on the Eq. (4.45), W_{r_1s} can be calculated by using β and θ_{max} in experiment. The amplitude of the quasi-passive walker θ_{max} can be measured by the 6-axis motion-tracking sensor.

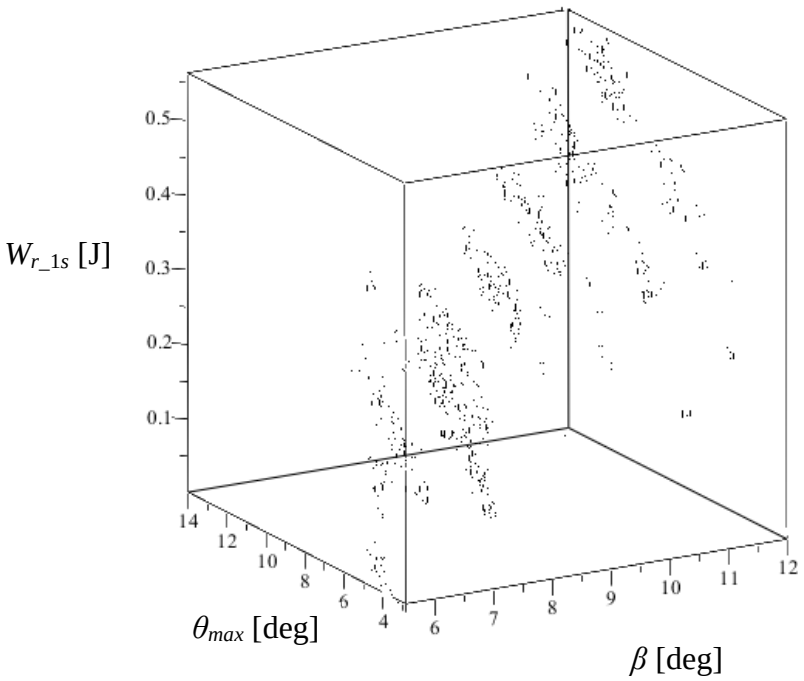

Fig. 4-9 Data of W_{r_1s} versus θ_{max} and β from the simulation

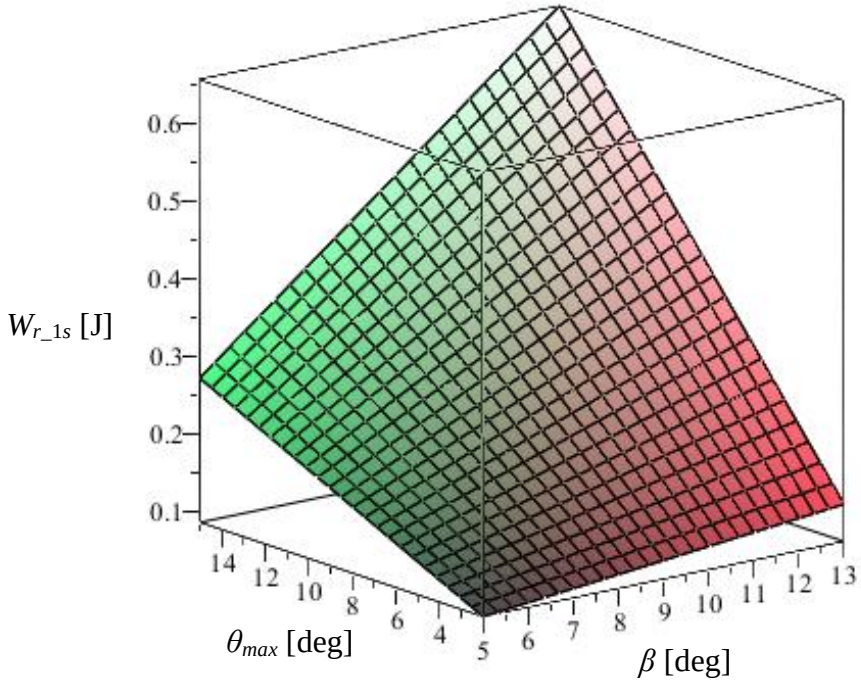

Fig. 4-10 W_{r_1s} as a function of θ_{max} and β

4.5.5 Determination of amplitude based on input energy

The input energy E_{N_1s} can be calculated from Eq. (4.40) in experiments, and by assuming that θ_w and θ have sufficiently close value to 0, the approximate linear relation between amplitude β and mechanical work W_r can be expressed by

$$\frac{\beta}{\beta'} = \frac{W_{r\_1s}}{W'_{r\_1s}} = \frac{E_{N\_1s}}{W'_{r\_1s}}, \tag{4.46}$$

which is also used in the direct method for the determination of amplitude, as shown in Eq. (4.32). Therefore, β can be calculated from Eq. (4.40) and Eq. (4.46) as follows

$$\beta = \frac{E_{N\_1s}}{W'_{r\_1s}}\beta' = \frac{W'_{r\_1s} - \Delta E'_{P\_roll\_1s} - \Delta E'_{K\_1s}}{W'_{r\_1s}}\beta'. \tag{4.47}$$

In actual experiments, the gait of the quasi-passive walker can be stabilized by using β, which is determined only by Eq. (4.47), so the integral T_{int} shown in Eq. (4.34) is not used in the indirect method.

4.6 Conclusion

In this chapter the energy balance equation of stable walking was defined based on the energy transformation during walking, and a stabilization method based on energy balance was proposed. A direct method based on energy balance for the determination of β is examined by simulation. However, the some error of required input energy in one step caused by the direct method exists, and the direct method cannot be realized in experiment. To solve the problems, a novel indirect method based on energy balance for the determination of β was proposed to decrease the error in the calculation of input energy and to realize the proposed stabilization method in experiment. There are several conclusions and findings.

First, in the proposed direct method and indirect method, the amplitude of mechanical oscillator β is determined by using the required input energy. The results of the simulation showed that the gait of the quasi-passive walker was stabilized by the proposed control method.

Second, the indirect method uses the information of energy transformation during the last one step to calculate the required input energy. It is expected that the accuracy in the calculation of required input energy could be increased by decreasing the error in the calculation of potential energy and dissipation energy.

Third, the required input energy for keeping steady walking can be calculated based on energy balance. The calculation of input energy is only based on the information of the gait, and does not rely on the information from external sensors.

Fourth, an estimation method of mechanical work performed by the quasi-passive walker W_{r_1s} was proposed and applied to the calculation of input energy E_{N_1s} and the amplitude β. To estimate W_{r_1s}, a 3D map was constructed based on the data of simulation, and W_{r_1s} was shown as a function of the amplitudes of the quasi-passive walker and the mechanical oscillator.

5. Examination of the environmental adaptability of the quasi-passive walker

5.1 Introduction

In chapter 4, a stabilization method based on energy balance was proposed to improve the environmental adaptability of the quasi-passive walker, and a direct and an indirect method based on energy balance were proposed to determine the amplitude of the mechanical oscillator. The environmental adaptability means that quasi-passive walkers can stably walk under variable ground conditions and adapt to the changing ground conditions such as different slope angles and coefficients of restitution. Therefore, in order to verify the environmental adaptability of the quasi-passive walker, the proposed method based on energy balance is examined under uncertain ground conditions including variable slopes and a path with different coefficients of restitution.

First, the stabilization method based on energy balance is examined under different ground conditions by ODE simulation in section 5.2. The direct method for the determination of the amplitude of the mechanical oscillator is used for the simulation model. Second, the stabilization method based on energy balance is examined under different ground conditions by using experimental quasi-passive walker in section 5.3. The indirect method for the determination of the amplitude of the mechanical oscillator is used in experiment.

5.2 Examination of the direct method for the determination of the amplitude by simulation

The direct method for the determination of the amplitude of the mechanical oscillator based on energy balance is proposed in section 4.4. In this section, the gait stabilization method based on the direct method and "stabilization control algorithm" is examined by ODE simulation. First, the stabilization method is examined on several slopes with constant inclination angle. Second, the stabilization method is examined on a slope with variable inclination angles. Third, the stabilization method is examined on a flat path with variable coefficients of restitution.

The version 1 of the simulation model shown in Fig. 2-1 is used for the ODE simulation. The center of masses of the feet is adjusted backward for 0.01 m to generate a rotation moment around hip axis (as shown in Fig. 2-3), so as to enable the swing leg to naturally swing forward even on a slight upward slope.

The gait of the quasi-passive walker is stabilized for 3 seconds by "stabilization control algorithm" introduced in the section 2.3 at the beginning of the simulations, and then the "stabilization control algorithm" is switched to the proposed method based on energy balance, because the proposed method can keep steady walking in the condition that the initial state of the gait of the quasi-passive walker is stable. The gain for β_2 in Eq. (4.35) K_S is set to 0.8, and the maximum amplitude β_{max} is set to 30 degree. The sampling period of the simulation is set to 0.01 s.

5.2.1 Walk on a constant angle slope

The proposed method is examined by simulation under different conditions with different slope angles, which are set to 1.5 degree, 1 degree, 0.5 degree, -0.5 degree, -1 degree and -1.5 degree. The downward slopes are represented by the negative value of the slope angles, and upward slopes are represented by the positive value of the slope angles. The period of lateral motion T_L and the period of swing leg motion T_S in the different ground conditions are shown in Fig. 5-1. The horizontal axis is time, and the vertical axis is period. The input energy E_{N_1s} and the mechanical work

performed by quasi-passive walker W_{r_1s} in one step under the different ground conditions are shown in Fig. 5-2. The horizontal axis is time, and the vertical axis is work and energy.

The average values of β in the each ground condition are shown in Fig. 5-3. The correlation coefficient R of the average values of β and the approximate straight line is equal to 0.984. The range of the correlation coefficient R is (0,1), and when R is equal to 1, the correlation is highest. The average values of β_1 determined based on energy balance and β_2 determined by the change of the period of swing leg ΔT_S are also shown in Fig. 5-3. As the slope angle increases, β_1 almost linearly increases, but β_2 almost linearly decreases. Moreover, β_1 is larger than β_2 except the ground condition of -1.5 degree slope, so the principal component of β is β_1, which is determined by the proposed method based on energy balance. Therefore, based on the proposed method, the amplitude of the mechanical oscillator β is changed automatically, and the desired energy is inputted into the quasi-passive walker so that the quasi-passive walker can walk stably.

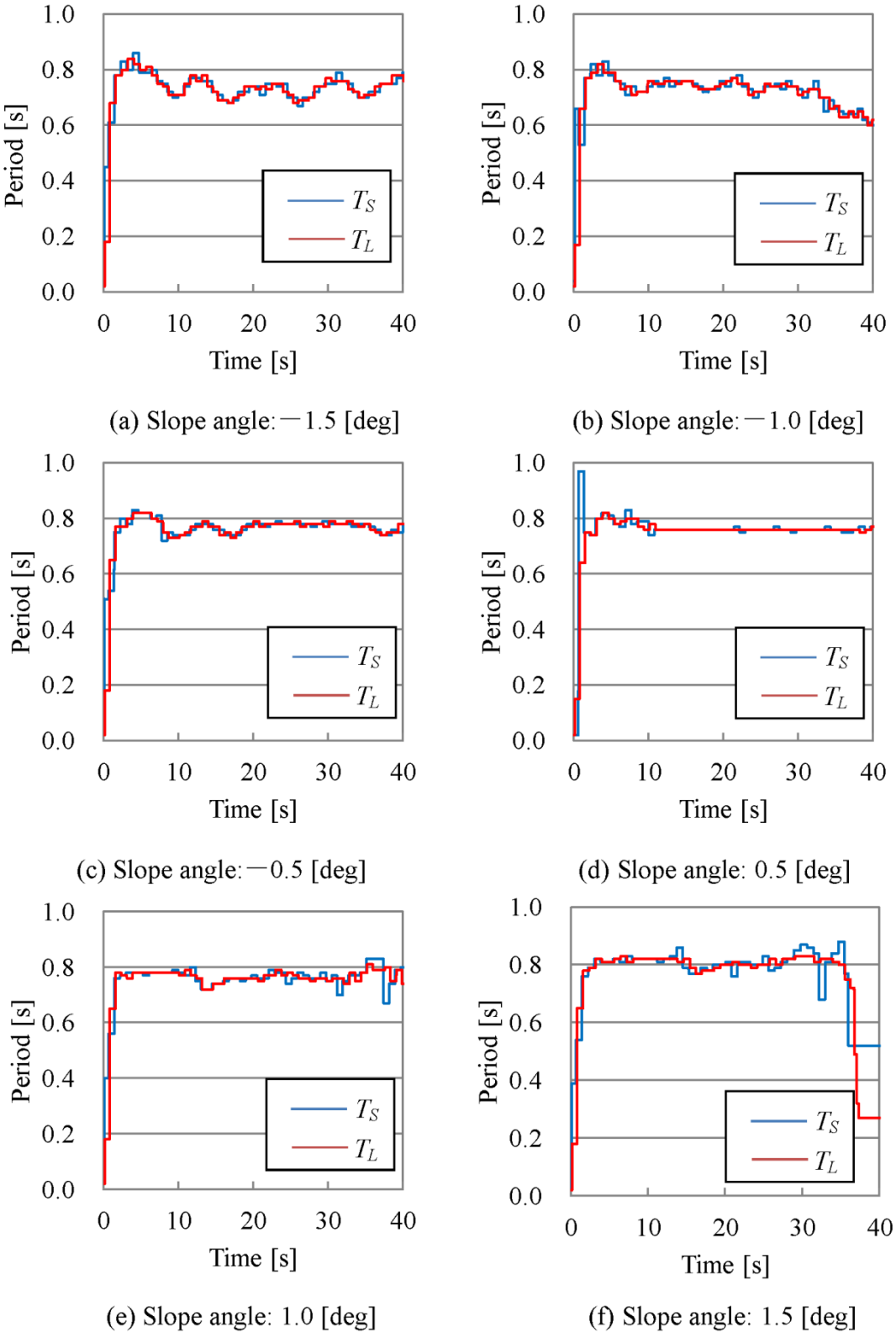

Fig. 5-1 The changes of the period of swing leg motion T_S and the period of lateral motion T_L under different ground conditions

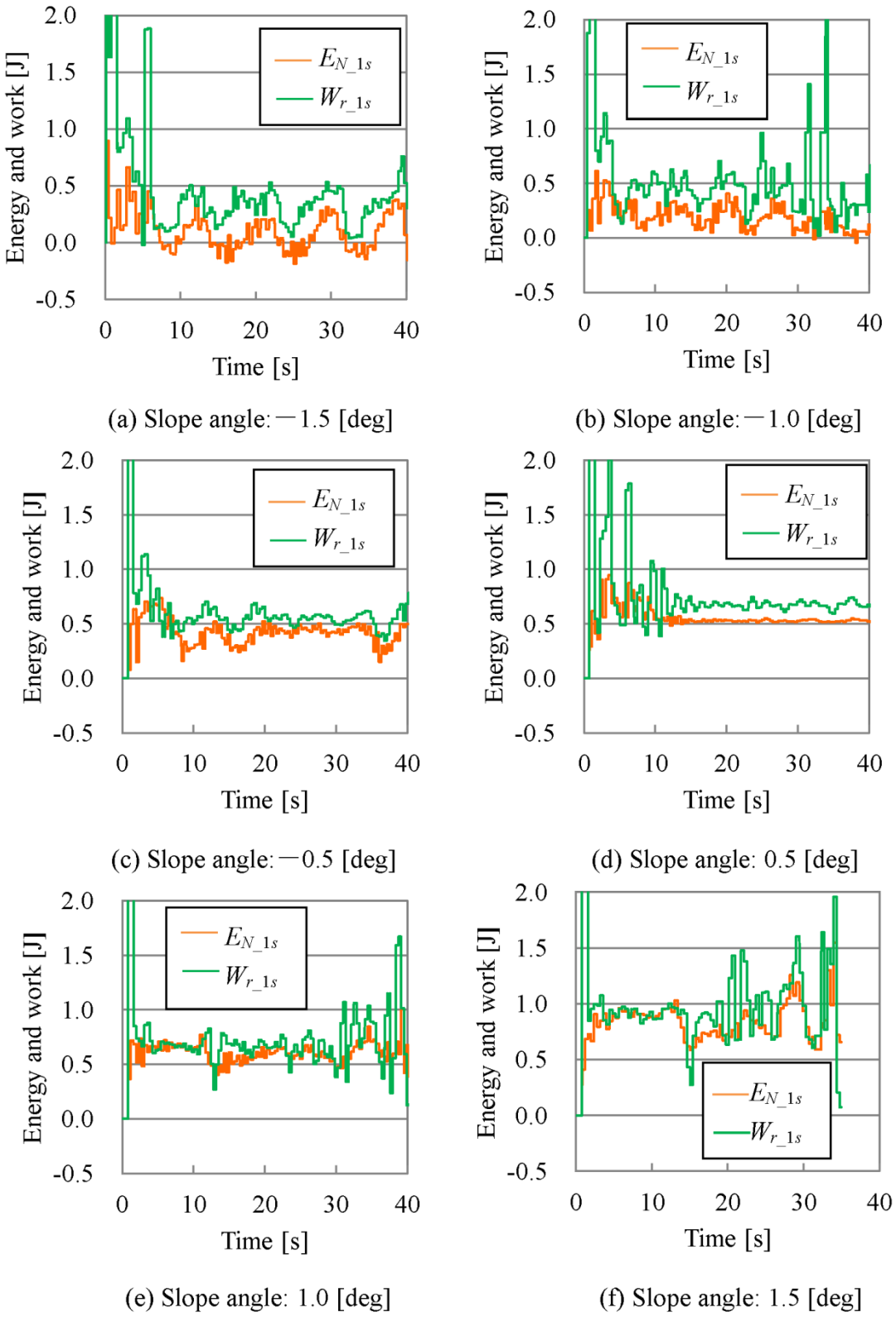

(a) Slope angle: −1.5 [deg]

(b) Slope angle: −1.0 [deg]

(c) Slope angle: −0.5 [deg]

(d) Slope angle: 0.5 [deg]

(e) Slope angle: 1.0 [deg]

(f) Slope angle: 1.5 [deg]

Fig. 5-2 The input energy E_{N_1s} and mechanical work performed by the quasi-passive walker W_{r_1s} under different ground conditions

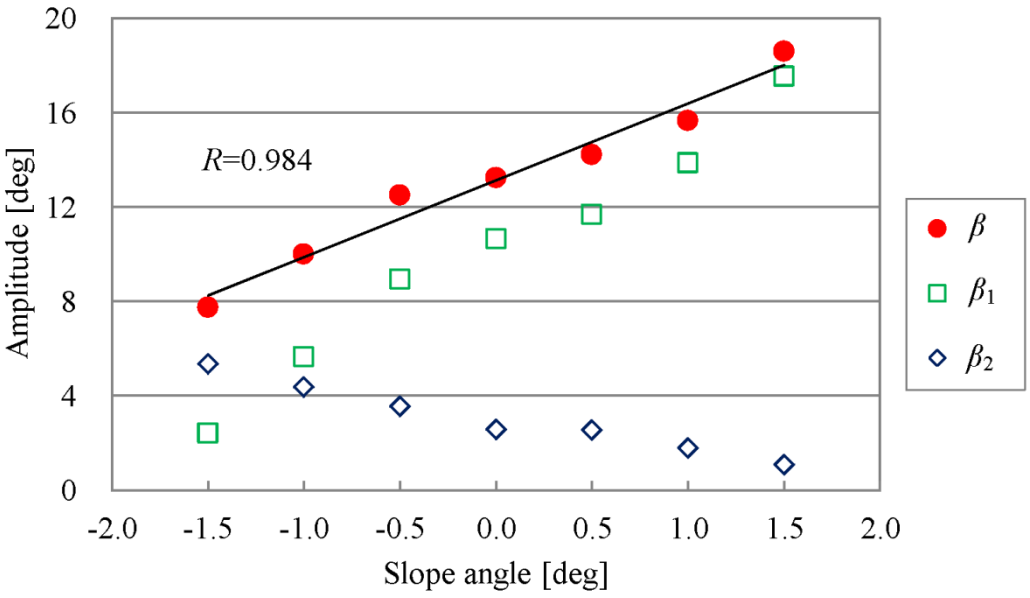

Fig. 5-3 Average values of β, β_1 and β_2 versus of slope angle

5.2.2 Walk on a changeable slope

The direct method for the determination of the amplitude of the mechanical oscillator is examined in ODE simulation in the condition of a changeable slope, the angles of which change in the sequence of 0 degree, -1.5 degree, 0 degree, 1.5 degree and 0 degree, as shown in Fig. 5-4(a). The length of the first 0 degree slope is 1.5 meter, and the length of the other slopes is 1 meter. The quasi-passive walker can walk stably on the changeable slope in simulation, and thus the proposed method is effective and can improve the environmental adaptability of the walker. The desired input energy E_{N_1s} and the mechanical work performed by the quasi-passive walker W_{r_1s} in the simulation are shown in Fig. 5-4 (b). The horizontal axis is time, and the vertical axis is energy and work. From the Fig. 5-4, W_{r_1s} can supplies the desired energy in one step so that the quasi-passive walker can walk stably even on changeable slopes. However, there are obvious differences between W_{r_1s} and E_{N_1s} during downhill and uphill walking, because the period of swing leg motion T_S changes during downhill and uphill walking, and the assistant component β_2 determined by T_S causes the additional input energy relative to E_{N_1s}.

The change of the kinetic energy of the quasi-passive walker in the simulation is shown in Fig. 5-5. According to energy balance, if E_{N_1s} is estimated correctly and supplied by W_{r_1s}, the kinetic energy of the quasi-passive walker changes periodically. However, the kinetic energy of the quasi-passive walker changes obviously as the change of the slope angles especially during downhill and uphill walking. There are two reasons for the problem. One reason is the estimation error of ΔE_{P_1s}, which is calculated based on the slope angle and walking distance in one step only with the consideration of the sagittal motion for simplicity. However, the lateral motion of the stance leg leads to estimation error of walking distance. Another reason is that the assistant component β_2 leads to additional energy input, but without β_2 it is difficult to stabilize the gait during uphill walking.

The change of the amplitude of the mechanical oscillator β in the simulation is shown in Fig. 5-6. The horizontal axis is time, and the vertical axis is the amplitude.

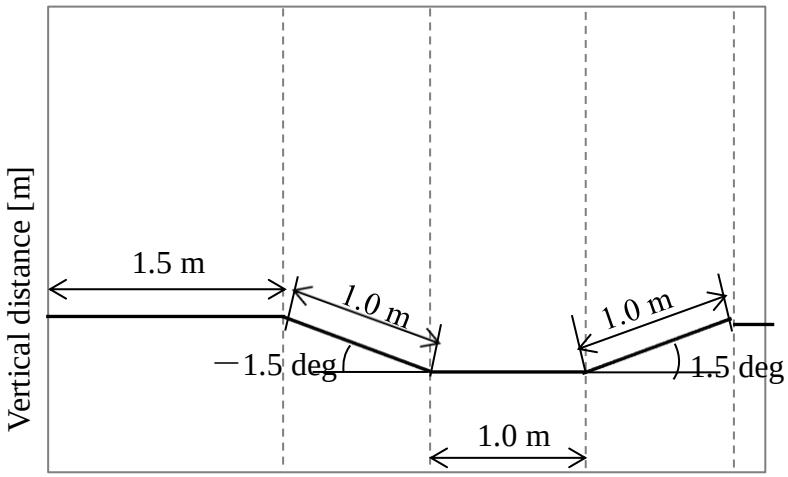

(a) Slope profile

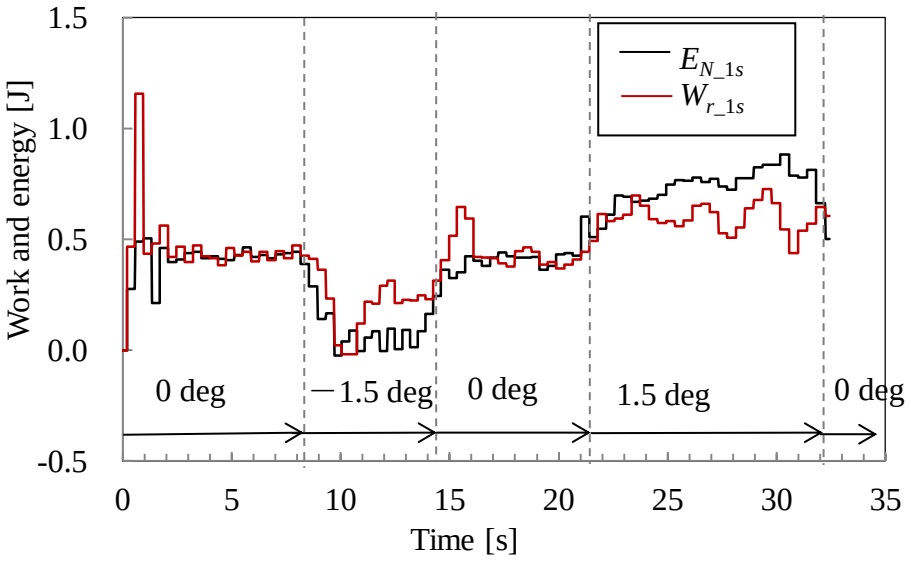

(b) The change of E_{N_1s} and W_{r_1s}

Fig. 5-4 The change of the input energy E_{N_1s} and the mechanical work performed by the robot W_{r_1s} on a changeable slope

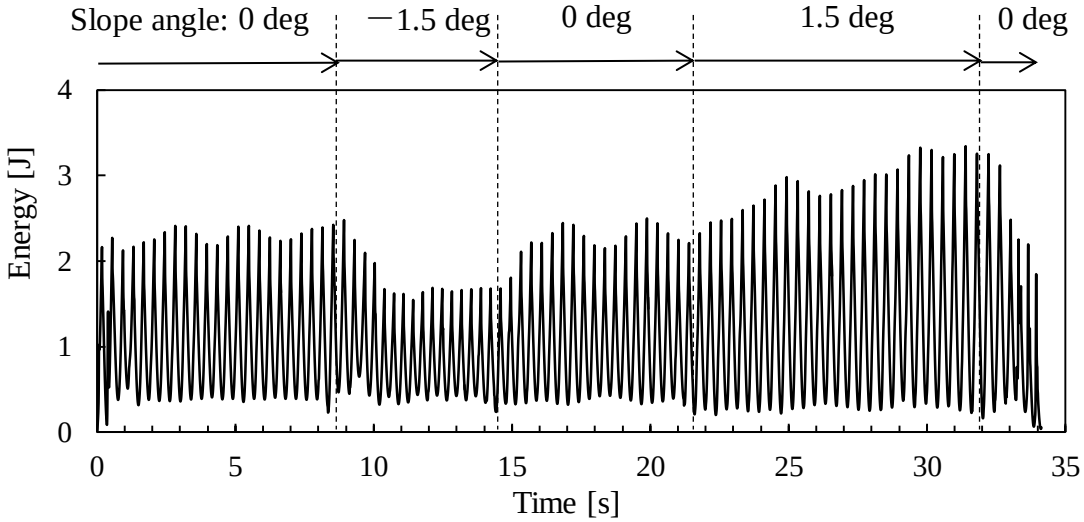

Fig. 5-5 The change of kinetic energy of the quasi-passive walker on a changeable slope in the control of the direct method

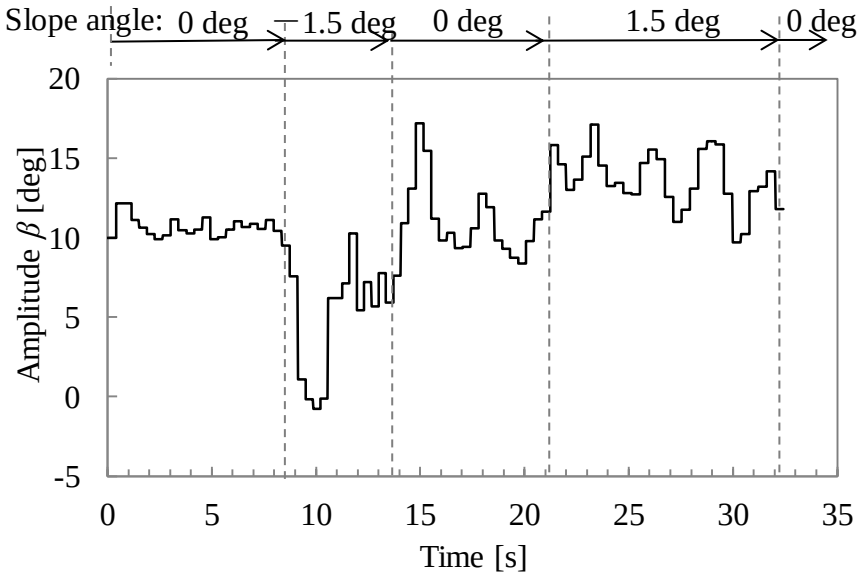

Fig. 5-6 The change of the amplitude of the mechanical oscillator β on a changeable slope in the control of the direct method

From the Fig. 5-6, the average value of β varies relative to the slope angles, because the change of slope angle causes the change of ΔE_{P_1s} and E_{N_1s}.

The change of the roll angle θ of the quasi-passive walker is shown in Fig. 5-7(a). Relative to the change of slope angles, the roll angle θ changes obviously. The limit cycle of the roll angle θ is shown in Fig. 5-7(b). The phase plane trajectory does not converge to the initial stable trajectory because of the estimation erorr of E_{N_1s}.

The change of pitch angle of the two legs is shown in Fig. 5-8, where γ_R and γ_L are the pitch angles of the right and left legs. The result shows that the gait varies as the change of slope angles.

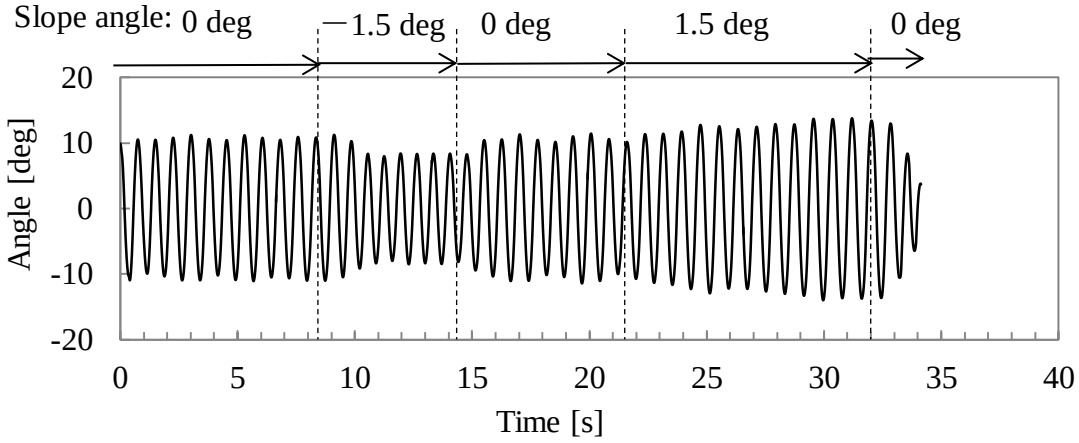

(a) Roll angle θ of the quasi-passive walker

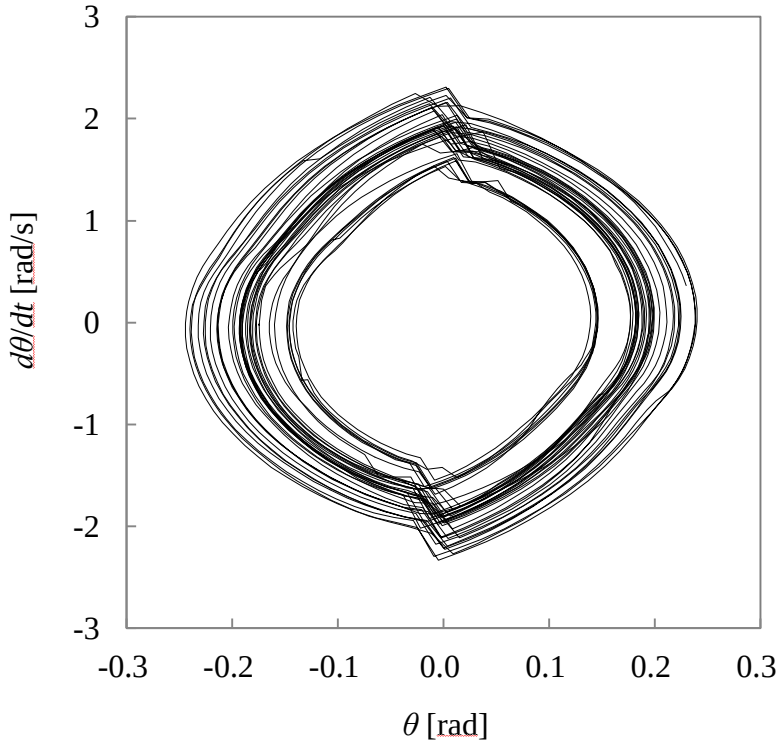

(b) Phase plane portraits of lateral motion of the quasi-passive walker

Fig. 5-7 The change of roll angle of the quasi-passive walker on a changeable slope in the control of the direct method

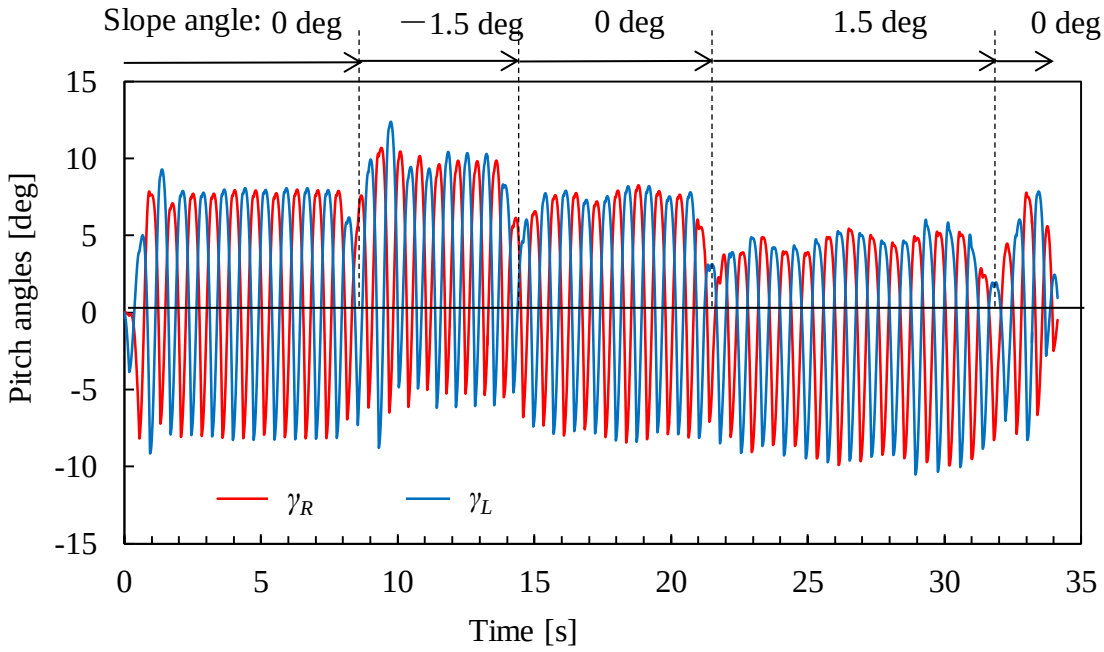

Fig. 5-8 The change of pitch angle of the two legs on a changeable slope in the control of the direct method

5.2.3 Walk on a flat ground with different coefficients of restitution

In this section, the direct method is examined by simulation on a flat path with different coefficients of restitution. The coefficients of restitution of each flat path is set to 0.1, 0.4, 0.1 and 0.4 in sequence, and the lengths of the each flat path is set to 1.5 m, 1.0 m, 1.0 m and 1.0 m in sequence, as shown in Fig. 5-9. In simulation the quasi-passive walker can adapt to the uncertain ground condition of different coefficients of restitution in the control of the direct method.

The input energy E_{N_1s} and the mechanical work performed by the quasi-passive walker W_{r_1s} in one step are shown in Fig. 5-10. The result shows that E_{N_1s} almost agrees with W_{r_1s}, so W_{r_1s} supplies the desired energy that enables the quasi-passive walker to walk stably. Moreover, the average values of E_{N_1s} and W_{r_1s} change according to the coefficients of restitution of the path, because the dissipation energy changes according to the coefficients of restitution of the path. There are differences between W_{r_1s} and E_{N_1s}, because the period of swing leg motion T_S changes according to the changes of coefficients of restitution of the ground, and the assistant component β_2 which is determined by the change of T_S causes the additional input energy relative to E_{N_1s}.

The change of the kinetic energy of the quasi-passive walker is shown in Fig. 5-11. In the control of direct method, the kinetic energy of the quasi-passive walker changes obviously as the change of the coefficients of restitution. The reason is that the estimation error of E_{N_1s} and the assistant component β_2 lead to additional energy input into the kinetic energy.

The change of the amplitude of the mechanical oscillator β is shown in Fig. 5-12. When the coefficients of restitution of the path change, the average values of the amplitude β change significantly, and thus the quasi-passive walker can adapt to the changing ground conditions.

The change of the roll angle θ of the quasi-passive walker is shown in Fig. 5-13. The roll angle θ changes as the change of slope angles because of the additional energy input caused by the assistant component β_2. The change of pitch angle of the

two legs is shown in Fig. 5-14, where γ_R and γ_L are the pitch angles of the right and left legs. The result shows that the gait changes as the change of slope angles.

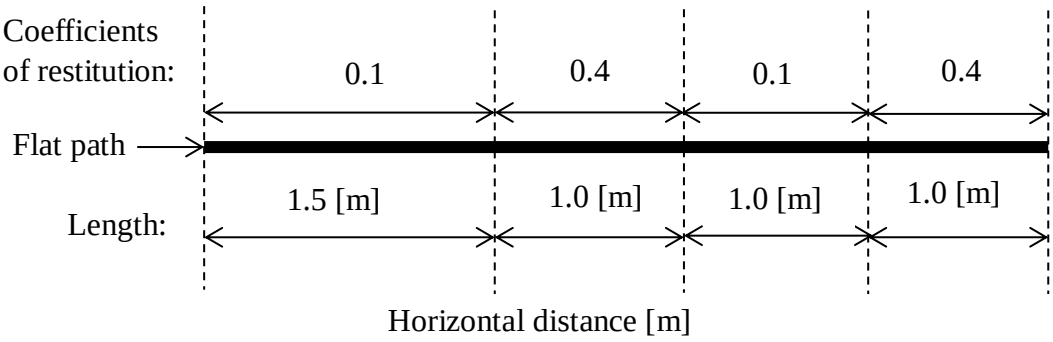

Fig. 5-9 Profile of a flat path with different coefficients of restitution

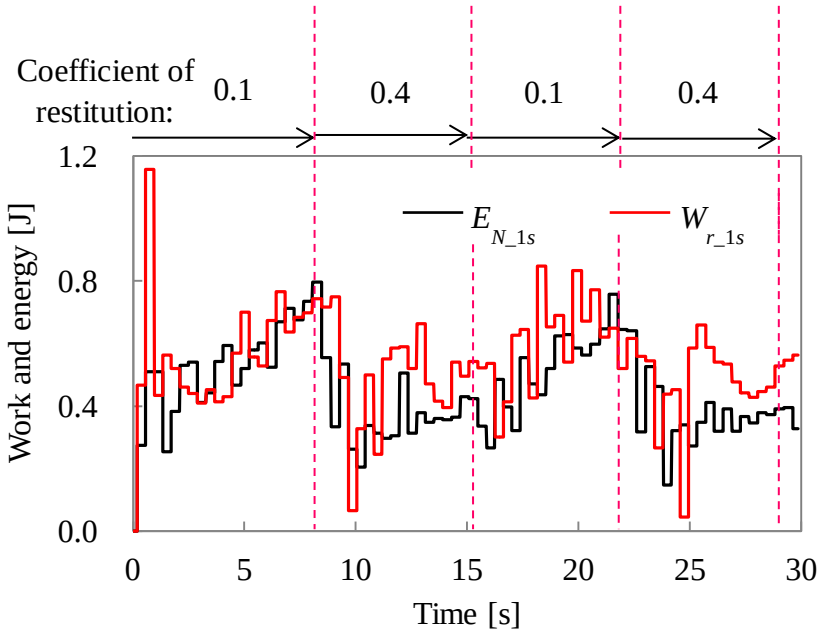

Fig. 5-10 The change of the input energy E_{N_1s} and the mechanical work performed by the robot W_{r_1s} on a flat path with different coefficients of restitution

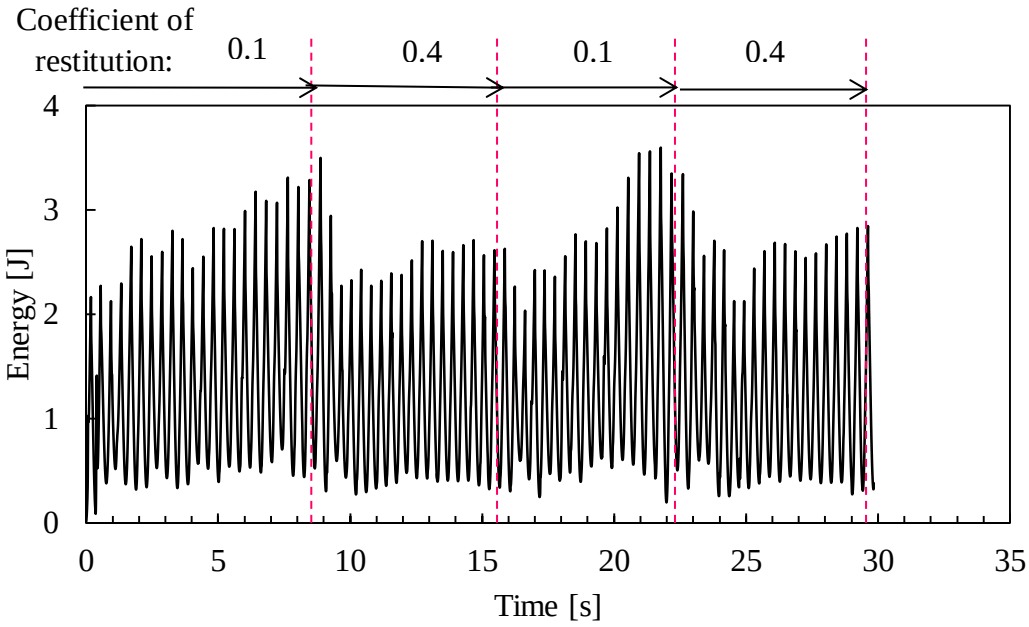

Fig. 5-11 The change of kinetic energy of the quasi-passive walker on a flat path with different coefficients of restitution

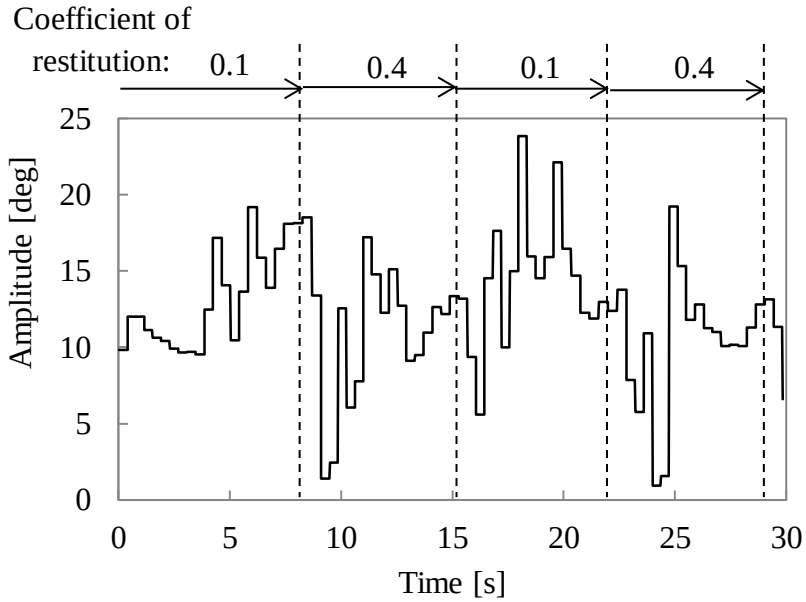

Fig. 5-12 The change of the amplitude of the mechanical oscillator β on a flat path with different coefficients of restitution

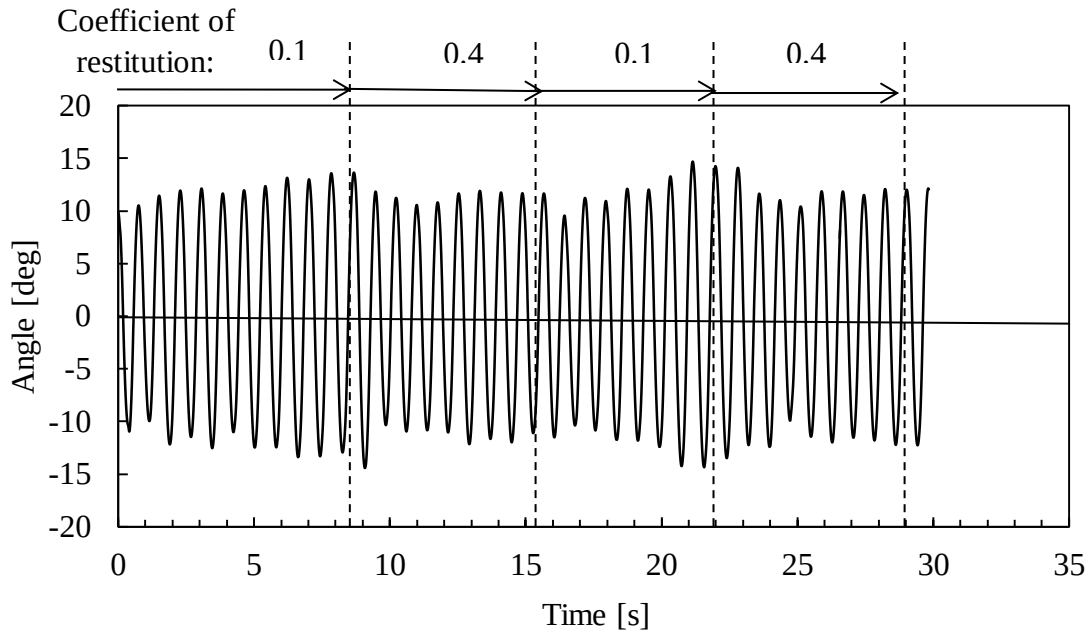

Fig. 5-13 The change of roll angle of the quasi-passive walker on a flat path with different coefficients of restitution

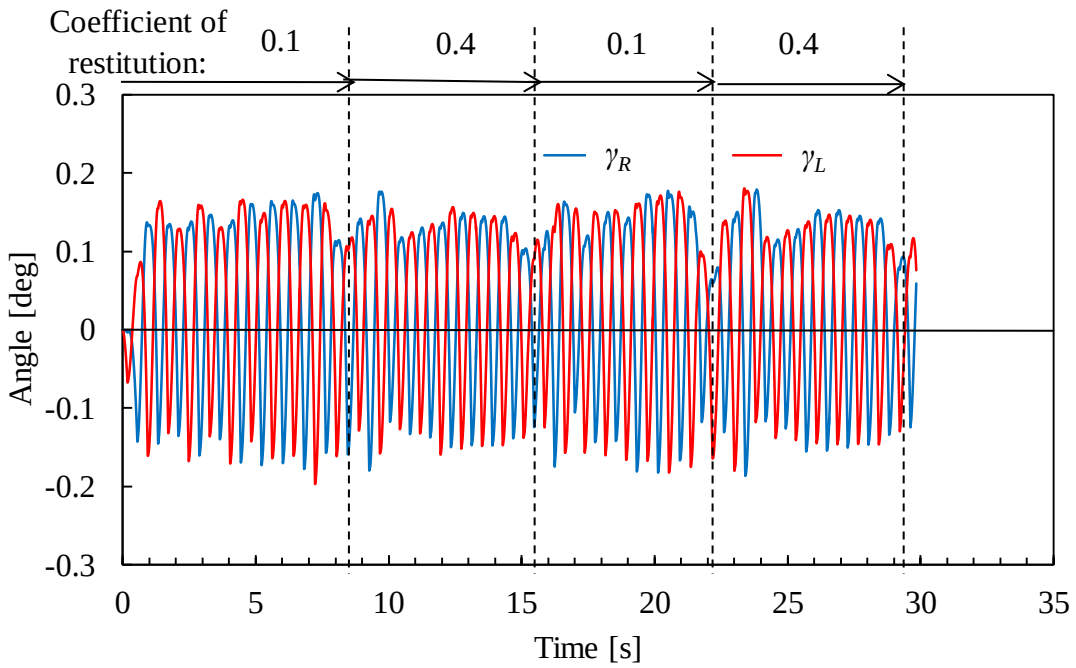

Fig. 5-14 The change of pitch angle of the two legs on a flat path with different coefficients of restitution

5.3 Examination of the indirect method for the determination of the amplitude by simulation

The indirect method for the determination of the amplitude of the mechanical oscillator based on energy balance is proposed in section 4.5. In this section, the gait stabilization method based on the indirect method is examined by ODE simulation. In order to compare the indirect method to direct method, the same simulation model and walking paths are utilized in simulation. First, the stabilization method is examined on a slope with variable inclination angles. Second, the stabilization method is examined on a flat path with variable coefficients of restitution.

The gait of the quasi-passive walker is stabilized for 3 seconds by "stabilization control algorithm" introduced in the section 2.3 at the beginning of the simulations, and then the determination method of the amplitude of the mechanical oscillator is switched to the indirect method. The maximum amplitude β_{max} is set to 30 degree. The sampling period of the simulation is set to 0.01 s.

5.3.1 Walk on a changeable slope

The changeable slope is shown in Fig. 5-15(a), and the slope angles the change in the sequence of 0 degree, -1.5 degree, 0 degree, 1.5 degree and 0 degree. The quasi-passive walker can walk stably on the changeable slope in simulation in the control of indirect method. The desired input energy E_{N_1s} and the mechanical work performed by the quasi-passive walker W_{r_1s} in the simulation are shown in Fig. 5-15 (b). The horizontal axis is time, and the vertical axis is energy and work. From the Fig. 5-15(b), W_{r_1s} almost supplies the desired energy in one step. In comparison to the direct method, there are fewer differences between W_{r_1s} and E_{N_1s} during walking, because the indirect method does not use the assistant component β_2 to determine the amplitude of the mechanical oscillator.

The change of the kinetic energy of the quasi-passive walker in the control of indirect method is shown in Fig. 5-16. According to energy balance, if E_{N_1s} is correctly estimated and supplied by W_{r_1s}, the kinetic energy of the quasi-passive

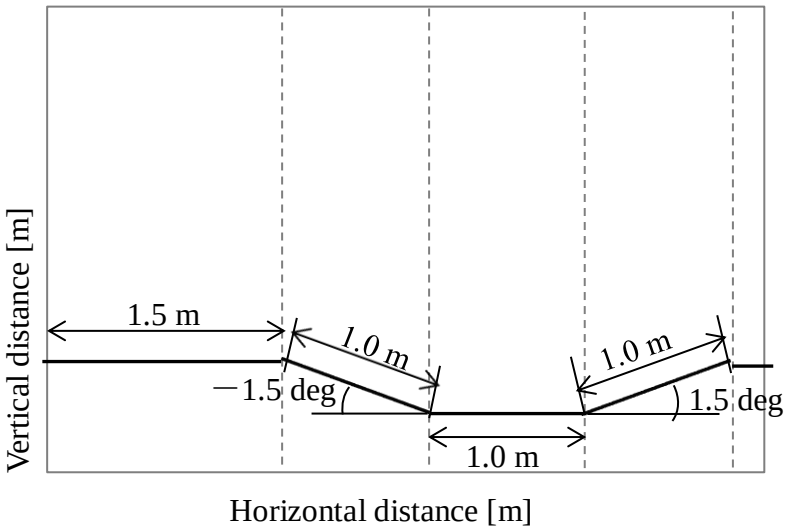

(a) Slope profile

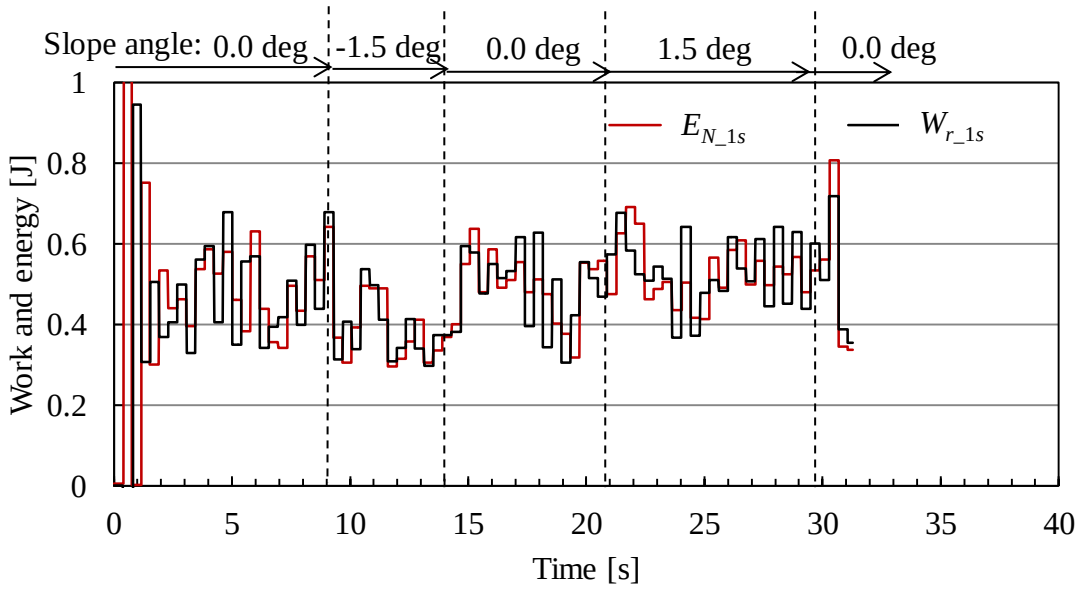

(b) The change of E_{N_1s} and W_{r_1s}

Fig. 5-15 The change of the input energy E_{N_1s} and the mechanical work performed by the robot W_{r_1s} on a changeable slope in the control of the indirect method

walker changes periodically. In comparison to the direct method, the indirect method makes the kinetic energy of the quasi-passive walker almost change periodically even during downhill and uphill walking. It is because that the indirect method utilizes the information of energy transformation during last one step to improve the estimation accuracy of E_{N_1s}.

The change of the amplitude of the mechanical oscillator β in the control of indirect method is shown in Fig. 5-17. From the Fig. 5-17, the average values of the amplitude β vary relative to the change of the slope angles, because the change of slope angle causes the change of E_{N_1s}.

The change of the roll angle θ of the quasi-passive walker is shown in Fig. 5-18(a). Relative to the change of slope angles, the roll angle θ does not change hugely. The limit cycle of the roll angle θ is shown in Fig. 5-18(b). The phase plane trajectory converges to the area near the initial stable trajectory. Therefore, the lateral motion of the quasi-passive walker is stabilized in the control of indirect method. In comparison to the direct method, the indirect method can enable the walker to walk more stably under uncertain ground conditions.

The change of pitch angle of the two legs is shown in Fig. 5-19, where γ_R and γ_L are the pitch angles of the right and left legs. In comparison to the lateral motion of the quasi-passive walker, the sagittal motion of the walker varies relative to the slope angles and can be still stabilized during walking.

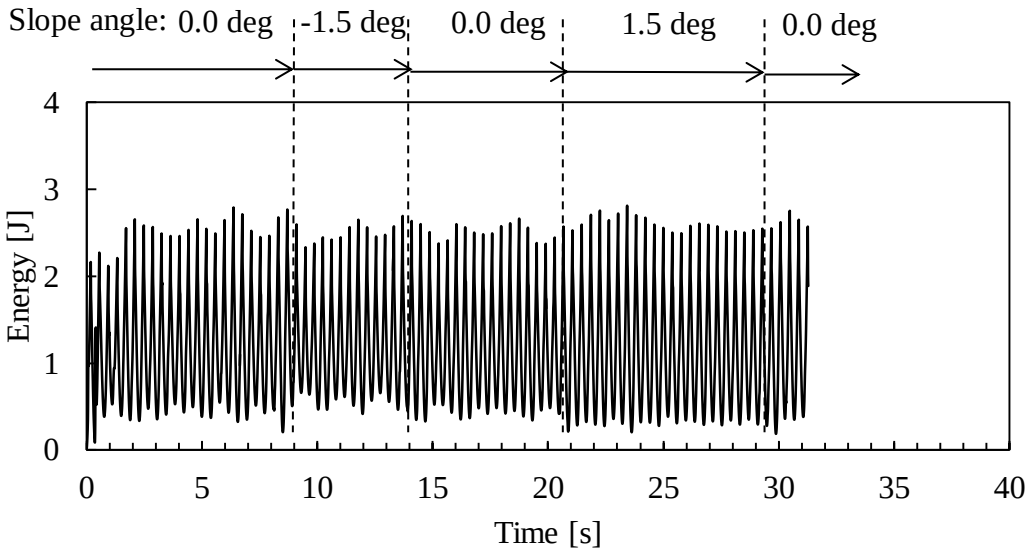

Fig. 5-16 The change of kinetic energy of the quasi-passive walker on a changeable slope in the control of the indirect method

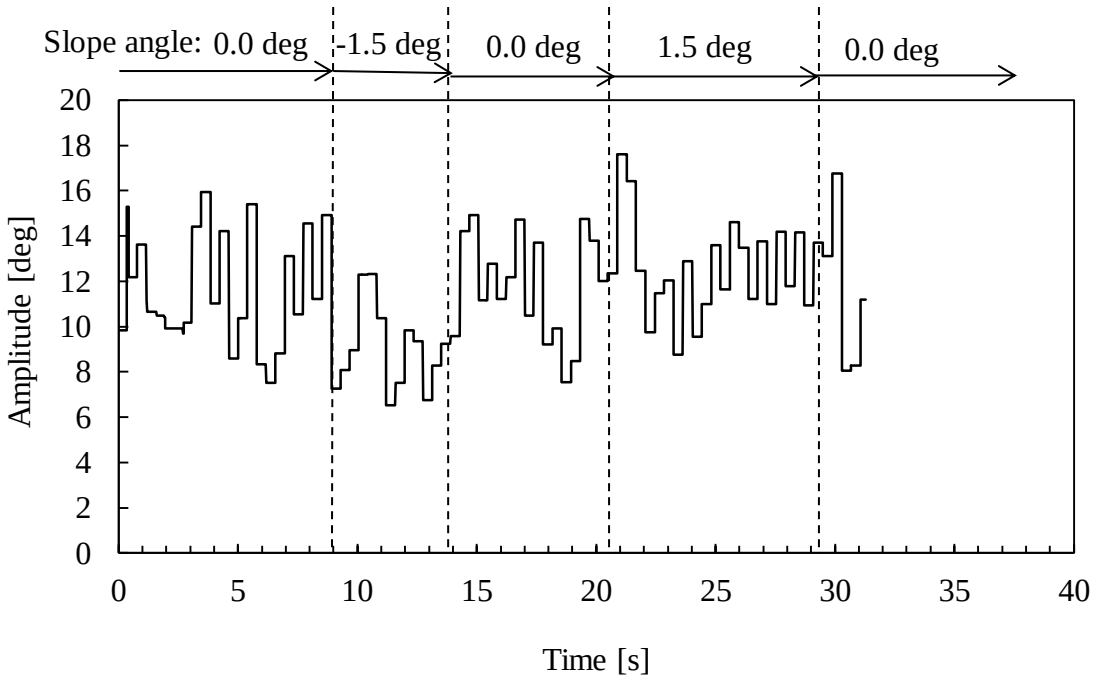

Fig. 5-17 The change of the amplitude of the mechanical oscillator β on a changeable slope in the control of the indirect method

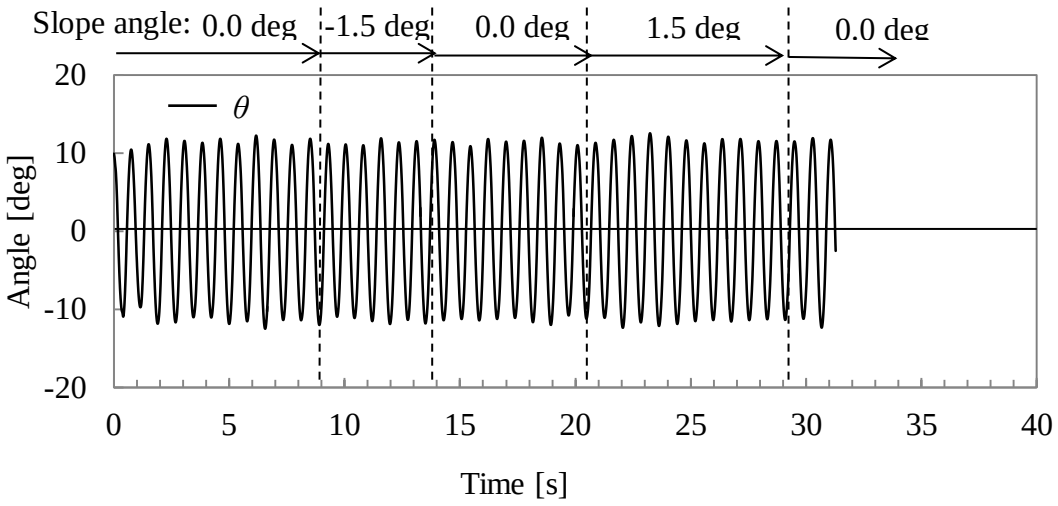

(a) Roll angle θ of the quasi-passive walker

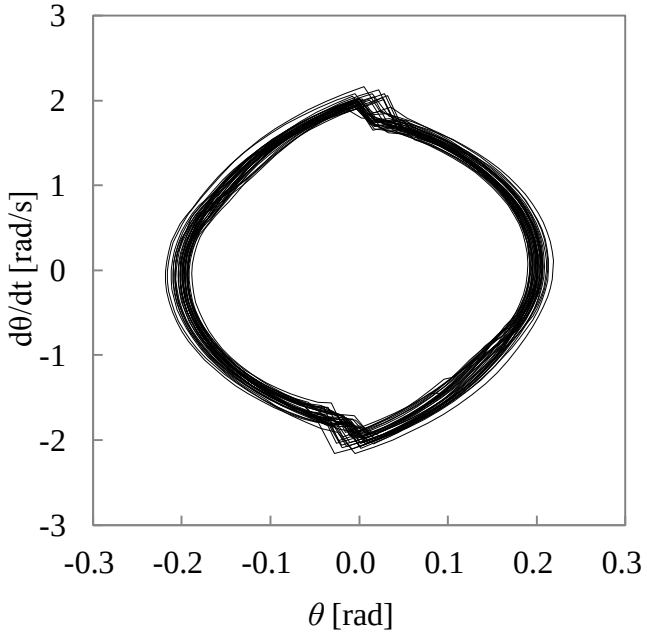

(b) Phase plane portraits of lateral motion of the quasi-passive walker

Fig. 5-18 The change of the roll angle of the quasi-passive walker on a changeable slope in the control of the indirect method

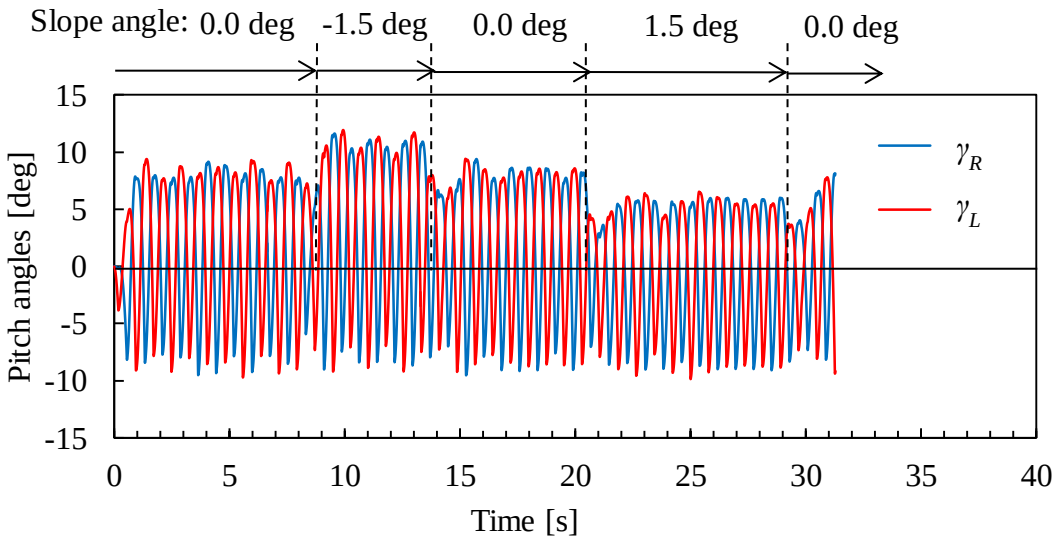

Fig. 5-19 The change of pitch angle of the two legs on a changeable slope in the control of the indirect method

5.3.2 Walk on a flat ground with different coefficients of restitution

In this section, the indirect method is examined by simulation on a flat path with different coefficients of restitution. In order to compare the indirect method with direct method, the same path is used as shown in Fig. 5-9. The coefficients of restitution of each flat path is set to 0.1, 0.4, 0.1 and 0.4 in sequence, and the lengths of the each flat path is set to 1.5 m, 1.0 m, 1.0 m and 1.0 m in sequence.

The desired input energy E_{N_1s} and the mechanical work performed by the quasi-passive walker W_{r_1s} in one step are shown in Fig. 5-20. The result shows that E_{N_1s} almost agrees with W_{r_1s}, so W_{r_1s} supplies the desired energy and enables the quasi-passive walker to walk stably. In comparison to the direct method, there are fewer differences between W_{r_1s} and E_{N_1s} during walking, because the indirect method does not use the assistant component β_2 to determine the amplitude of the mechanical oscillator.

The change of the kinetic energy of the quasi-passive walker is shown in Fig. 5-21. According to energy balance, if E_{N_1s} is correctly estimated and supplied by W_{r_1s}, the kinetic energy of the quasi-passive walker changes periodically. In comparison to the direct method, the indirect method makes the kinetic energy of the quasi-passive walker almost change periodically even when the coefficient of restitution of the path changes. It is because that the indirect method utilizes the information of energy transformation during last one step to decrease the estimation error of E_{N_1s}.

The change of the amplitude of the mechanical oscillator β is shown in Fig. 5-22. When the coefficients of restitution of the path change, the average value of the amplitude β does not change significantly in comparison to the condition of the changeable slope as shown in Fig. 5-17 even in the same control method. It is because that the change of slope angles causes more change of E_{N_1s} in comparison to the change of coefficients of restitution in this simulation condition.

The change of the roll angle θ of the quasi-passive walker is shown in Fig. 5-23. Relative to the change of coefficients of restitution, the roll angle θ does not change

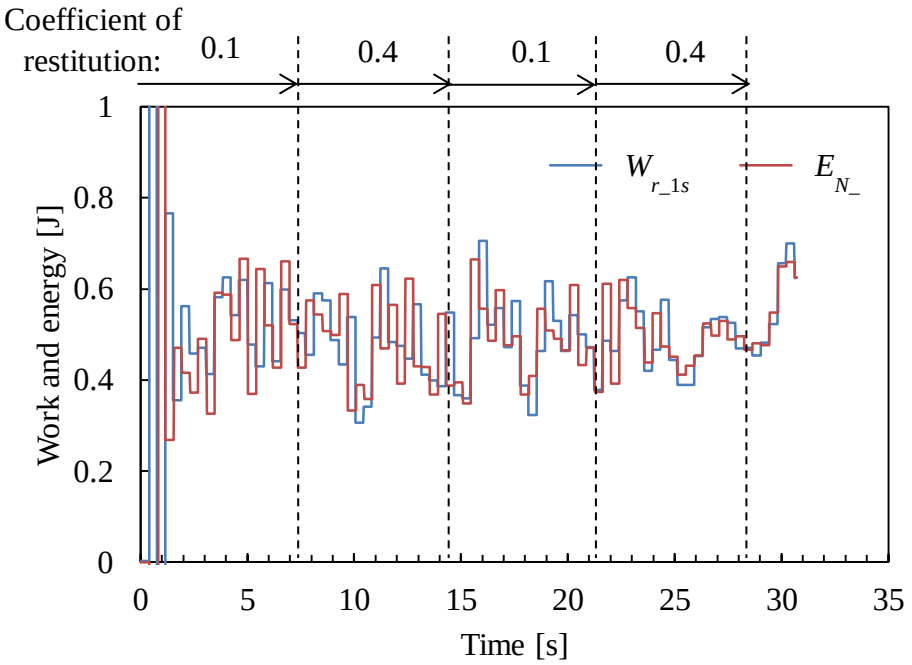

Fig. 5-20 The change of the input energy E_{N_1s} and the mechanical work performed by the robot W_{r_1s} on a flat path in the control of the indirect method

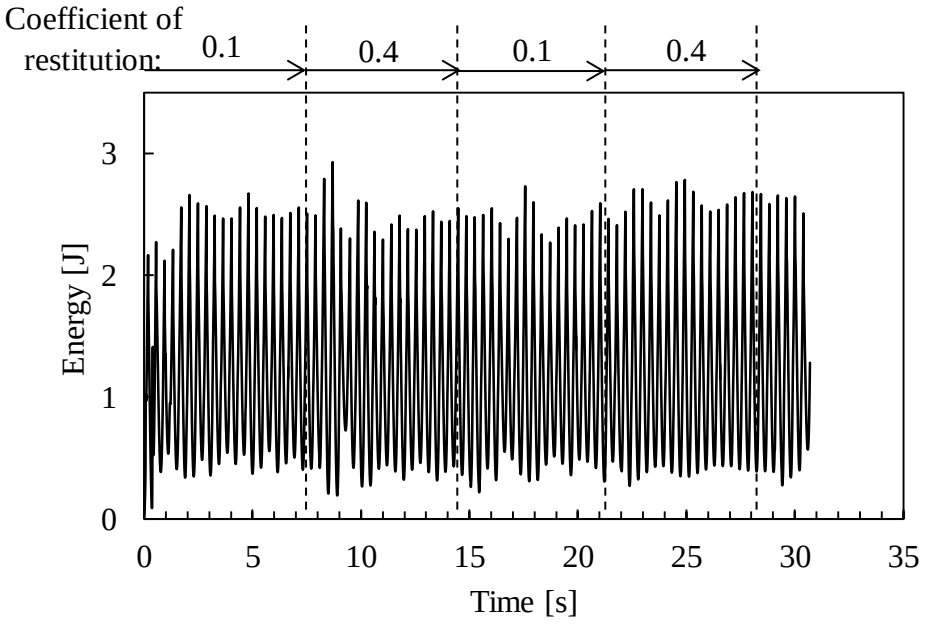

Fig. 5-21 The change of kinetic energy of the quasi-passive walker on a flat path with different coefficients of restitution in the control of the indirect method

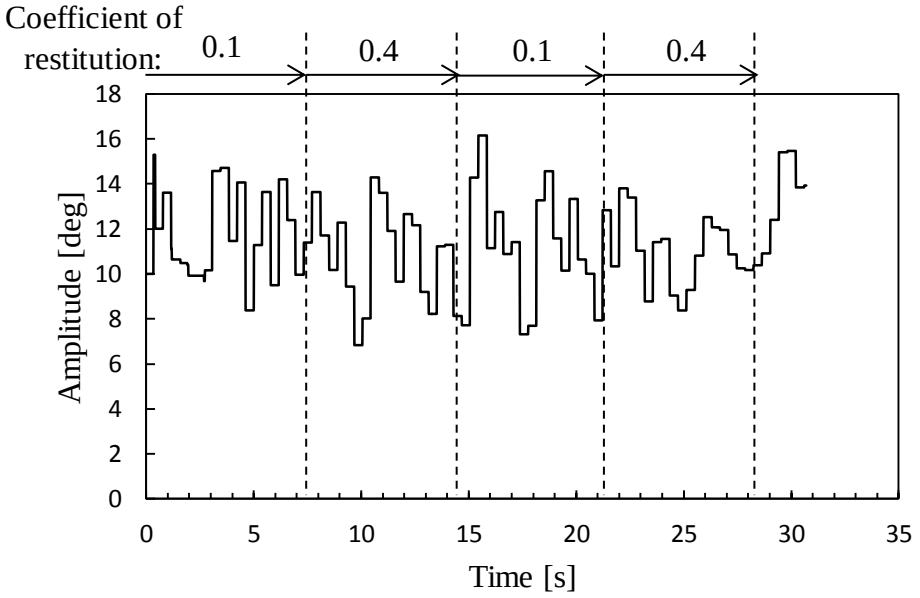

Fig. 5-22 The change of the amplitude of the mechanical oscillator β on a flat path with different coefficients of restitution in the control of the indirect method

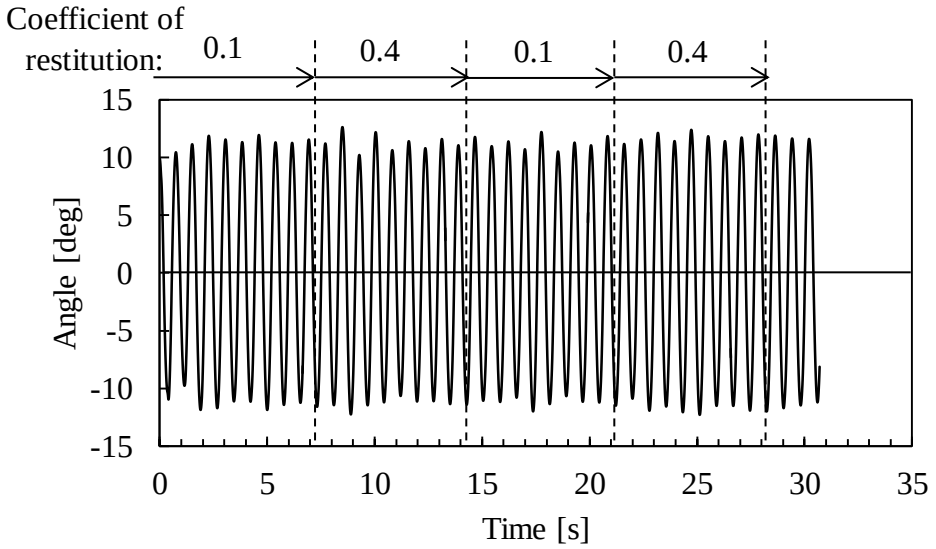

Fig. 5-23 The change of roll angle of the quasi-passive walker on a flat path with different coefficients of restitution in the control of the indirect method

hugely. Therefore, the lateral motion of the quasi-passive walker is stabilized in the control of the indirect method.

The change of pitch angle of the two legs is shown in Fig. 5-24, where γ_R and γ_L are the pitch angles of the right and left legs. The result shows that the gait does not change hugely relative to the change of coefficients of restitution in comparison to the change of slope angles.

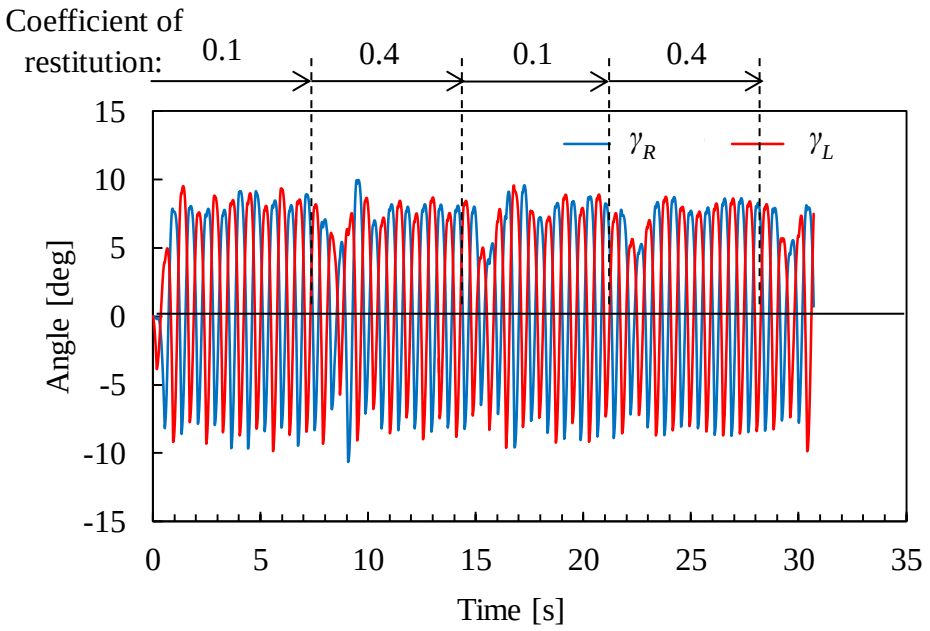

Fig. 5-24 The change of pitch angle of the two legs on a flat path with different coefficients of restitution in the control of the indirect method

5.4 Examination of the environmental adaptability by experiments

5.4.1 Hardware structure

The hardware structure of the control system of the quasi-passive walker is composed of a stepping motor, a motor driver, two microcomputers, two rotary encoders, and a 6-axis motion-tracking sensor, as shown in Fig. 5-25.

The microcomputer "H8/3052F" calculates the trajectory of the mechanical oscillator and sends control pulse to motor driver to actuate the stepping motor.

The 6-axis motion-tracking sensor "MPU 6050" can measure the roll, pitch, and yaw angle of the trunk, and the angular velocities around the three body axes of the sensor. The data from the sensor is send to the microcomputer "Arduino Uno" through I^2C, and "Arduino Uno" sends the data to the microcomputer "H8/3052F" through RS232. Here, the microcomputer "Arduino Uno" is used only for data communication.

The two rotary encoders can measure the pitch angles of the legs relative to the trunk. From the roll, pitch, and yaw angle of the trunk acquired from 6-axis motion-tracking sensor, the roll, pitch, and yaw angle of the legs can be calculated. The angular velocity of the legs can also be calculated in the same manner. Moreover, the period of the swing leg T_S can be measured by using the data from rotary encoders. The beginning of one period of the swing leg is judged when the pitch angles of the legs become the same.

The rotational kinetic energies of the trunk and legs and the change in potential energy of the quasi-passive walker $\Delta E_{P\_roll\_1s}$ caused by lateral motion can be calculated by using the data form the rotary encoders and the 6-axis sensor.

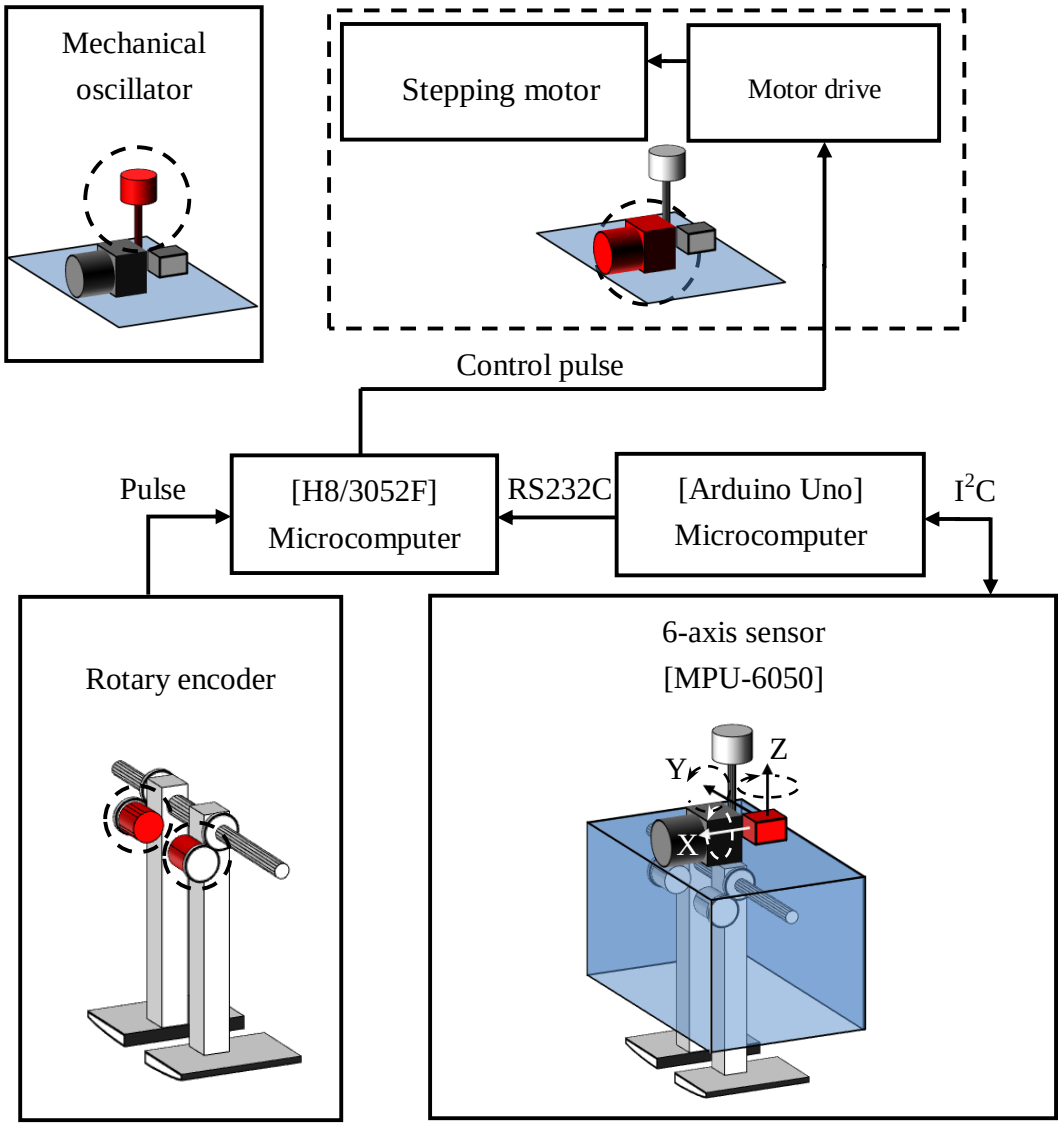

Fig. 5-25 Hardware structure of the control system

5.4.2 Experiment on a changeable slope

The indirect method proposed in section 4.8 is examined experimentally on a changeable slope in order to verify the environmental adaptability of the quasi-passive walker. The walking path with different slope angles is shown in Fig. 5-26. The slope angles are set to 1°, 0°, and $-1°$ in sequence, but the ground condition is unknown to the quasi-passive walker. The gait of the quasi-passive walker is stabilized by setting β to 10° for 8 seconds at the beginning of the experiment on the slope with the inclination of 1 degree. And then the determination method of β is switched to the indirect method based on energy balance proposed in section 4.8, because the proposed method can keep steady walking in the condition that the initial state of the gait is stable. Besides, the sampling period of the control system is 0.02 s.

The quasi-passive walker shows stable gait in the experiment as shown in Fig. 5-27, which indicates that the indirect method based on energy balance can also stabilize the gait of the quasi-passive walker even under uncertain ground conditions of different slope angles.

The period of lateral motion T_L and the period of swing leg motion T_S during walking is shown in Fig. 5-28. Since the stride of the quasi-passive walker is very small during uphill walking, it is difficult to judge the matching of the two legs by the sensors and to measure T_S correctly during uphill walking. Therefore, T_L does not agree with T_S during uphill walking before 26 s. However, T_L agrees with T_S during level- and downhill-walking after 26 s because the stride of the quasi-passive walker becomes larger. From the data during level- and downhill-walking after 26 s, T_L is synchronized with T_S.

The change of β during walking is shown in Fig. 5-29. Since the steady state gait of the quasi-passive walker is greatly changed when the slope angle changes, the required input energy E_{N_1s} is changed and thus β changes greatly at the moment. Besides, β shows different values during steady walking under different ground conditions. It means that the determination method of β based on energy balance is

effective and the proposed control method can stabilize the gait of the quasi-passive walker under uncertain ground conditions.

The change of required input energy E_{N_1s} and the mechanical work performed by the motor W_{r_1s} in one step is shown in Fig. 5-30. During steady walking E_{N_1s} almost agrees with W_{r_1s}. It means that the required input energy is provided by the motor so that the quasi-passive walker can keep steady walking.

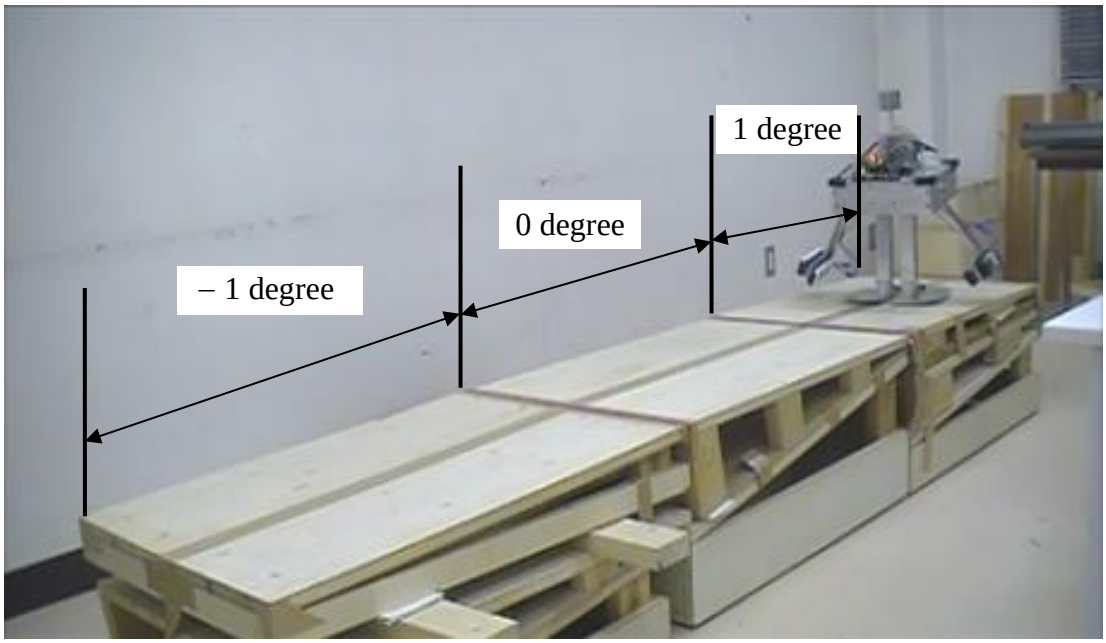

Fig. 5-26 The walking path for the experiment

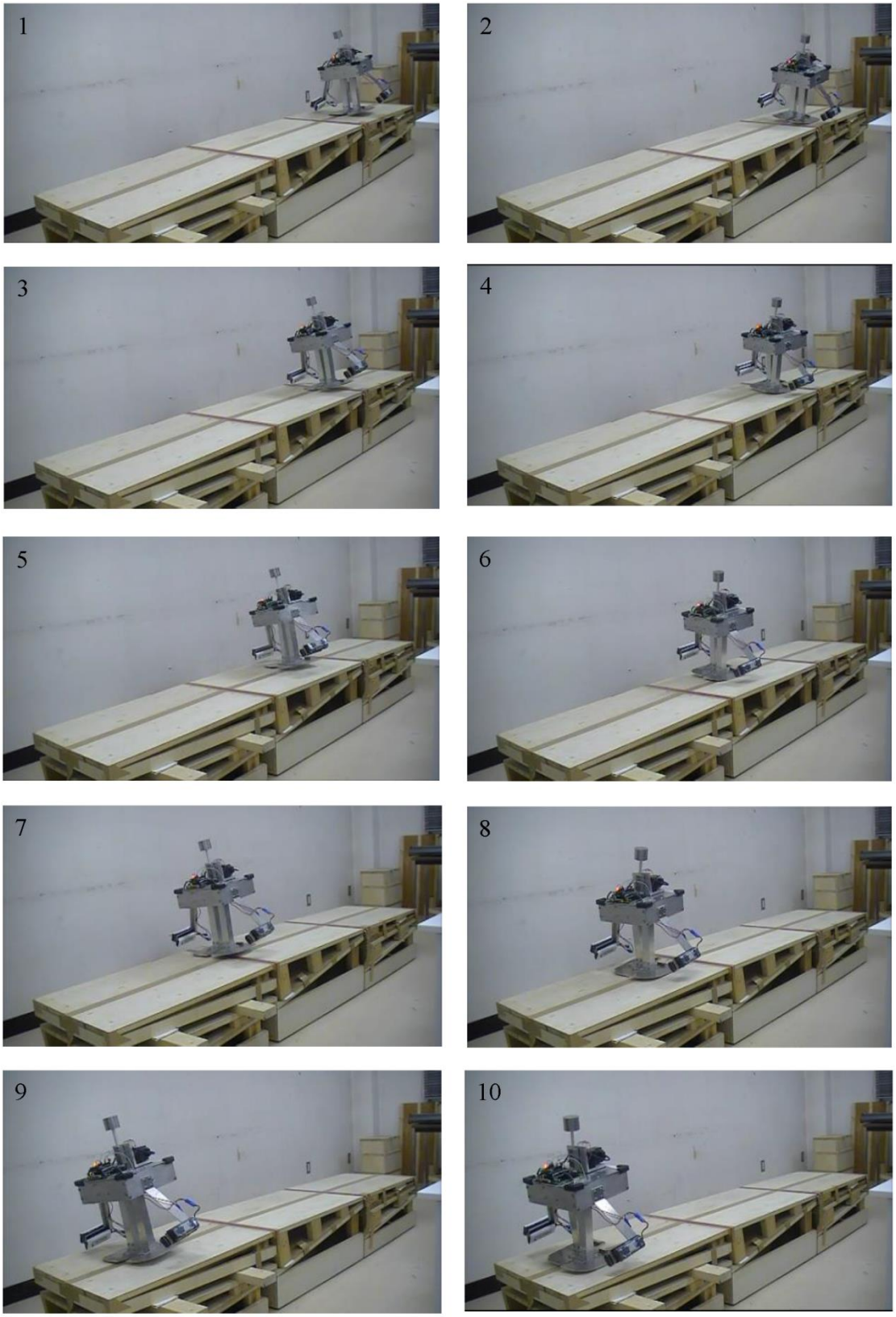

Fig. 5-27 The experiment of walking under uncertain ground conditions

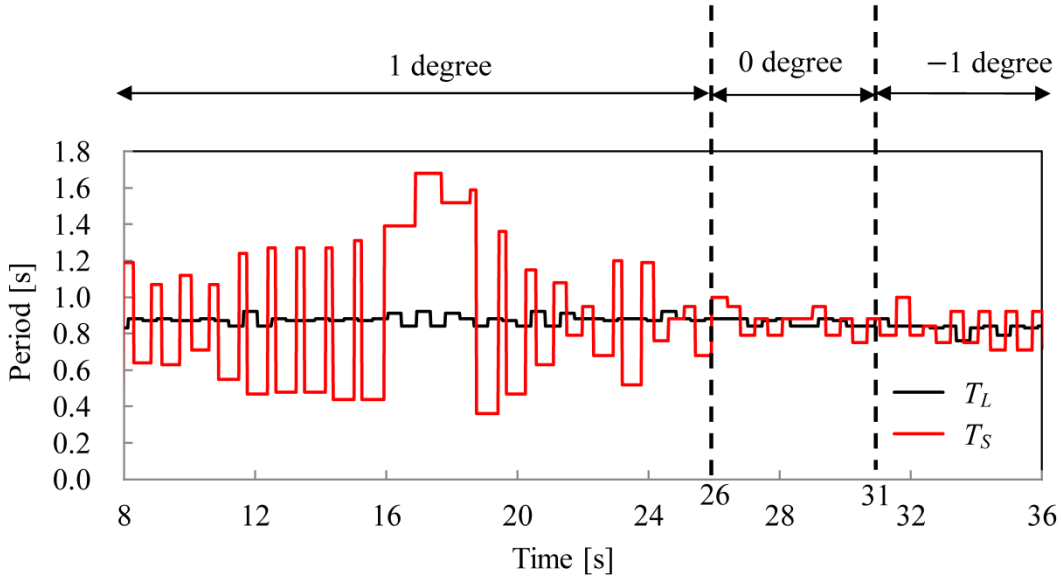

Fig. 5-28 The changes of the period of lateral motion T_L and the period of swing leg motion T_S on a variable slope

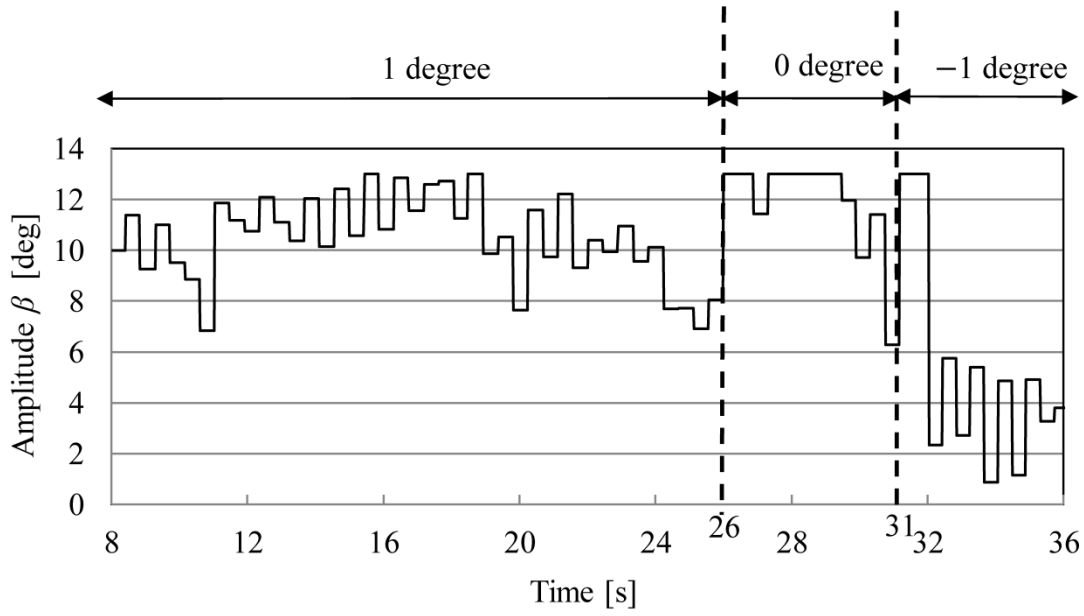

Fig. 5-29 The change of the amplitude of the mechanical oscillator on a variable slope

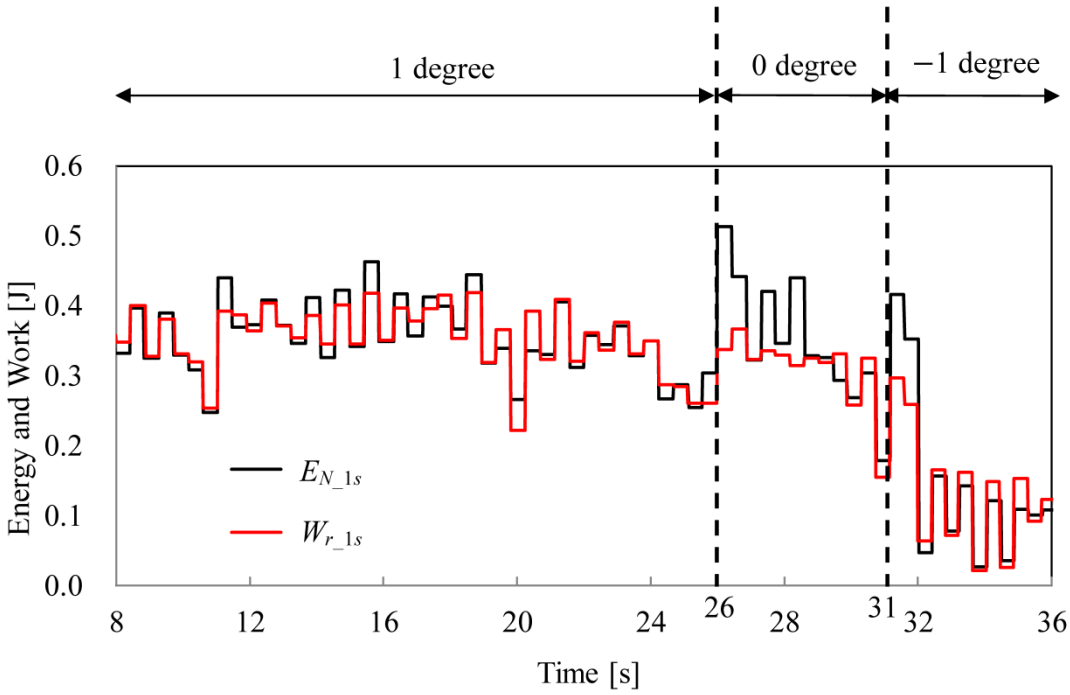

Fig. 5-30 The changes of the input energy E_{N_1s} and the mechanical work performed by the quasi-passive walker W_{r_1s}

5.4.3 Experiment on a flat ground with different coefficient of restitution

The indirect method is examined experimentally on a flat path with different coefficient of restitution to verify the environmental adaptability of the quasi-passive walker under different ground conditions. The walking path with different slope angles is shown in Fig. 5-31. The coefficient of restitution of the wooden path is 0.042, and the coefficient of restitution of the path covered by rubber blanket is 0.021. The gait of the quasi-passive walker is stabilized by setting the amplitude of the mechanical oscillator β to 10° for 8 seconds at the beginning of the experiment. And then the determination method of β is switched to the indirect method based on energy balance. Besides, the sampling period of the control system is 0.02 s.

The result shows that the quasi-passive walker can walk stably on a flat path with different coefficient of restitution, as shown in Fig. 5-32. The period of lateral motion T_L and the period of swing leg motion T_S during walking is shown in Fig. 5-33. The result shows that T_L almost agrees with T_S during walking, so the gait of the quasi-passive walker is stabilized by the proposed method. The walking path changes from wooden path to rubber path, so the gait of the quasi-passive walker becomes unstable at 16 second, but the T_L is synchronized with T_S after 20 second.

The change of β during walking is shown in Fig. 5-34. The amplitude β changes greatly after 16 second, because the steady state gait of the quasi-passive walker changes according to the coefficient of restitution. It means that the determination method of β based on energy balance is effective.

The change of required input energy E_{N_1s} and the mechanical work performed by the motor W_{r_1s} in one step is shown in Fig. 5-35. During steady walking E_{N_1s} almost agrees with W_{r_1s} even under the ground conditions of different coefficient of restitution. It means that the energy balance is satisfied so that the quasi-passive walker can keep steady walking. According to the experiment, the quasi-passive walker can adapt the changing ground condition of different coefficient of restitution.

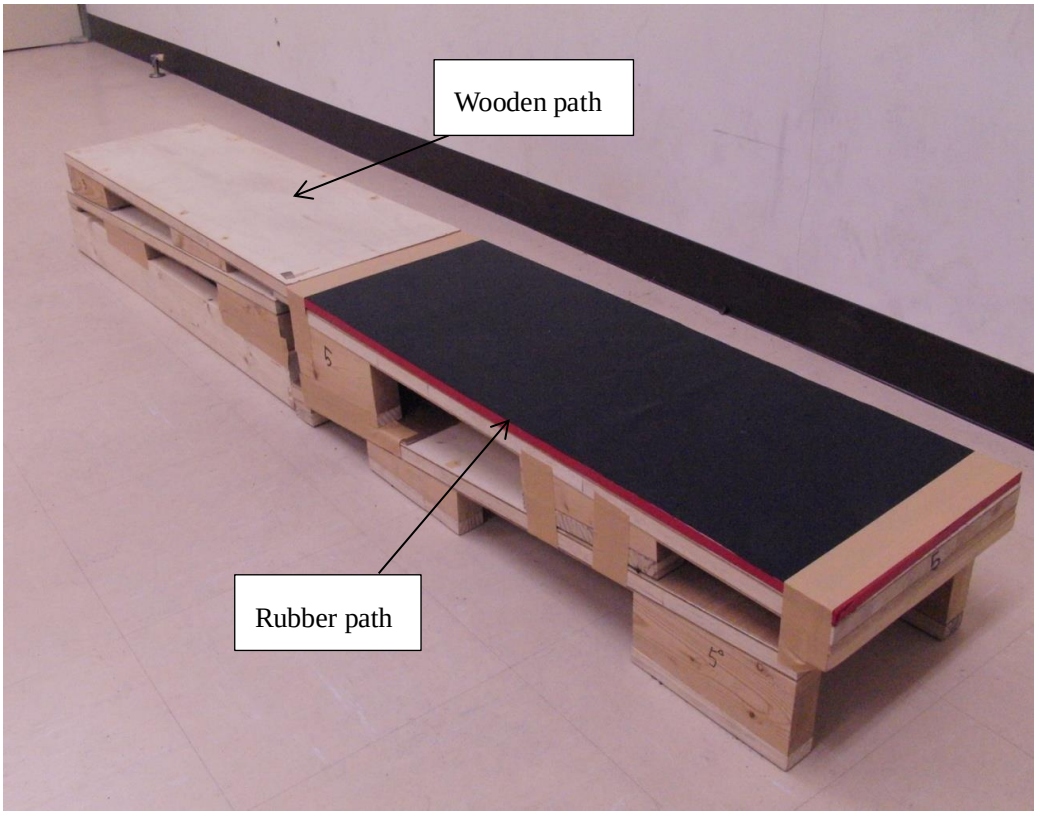

Fig. 5-31 The walking path with different coefficients of restitution for the experiment

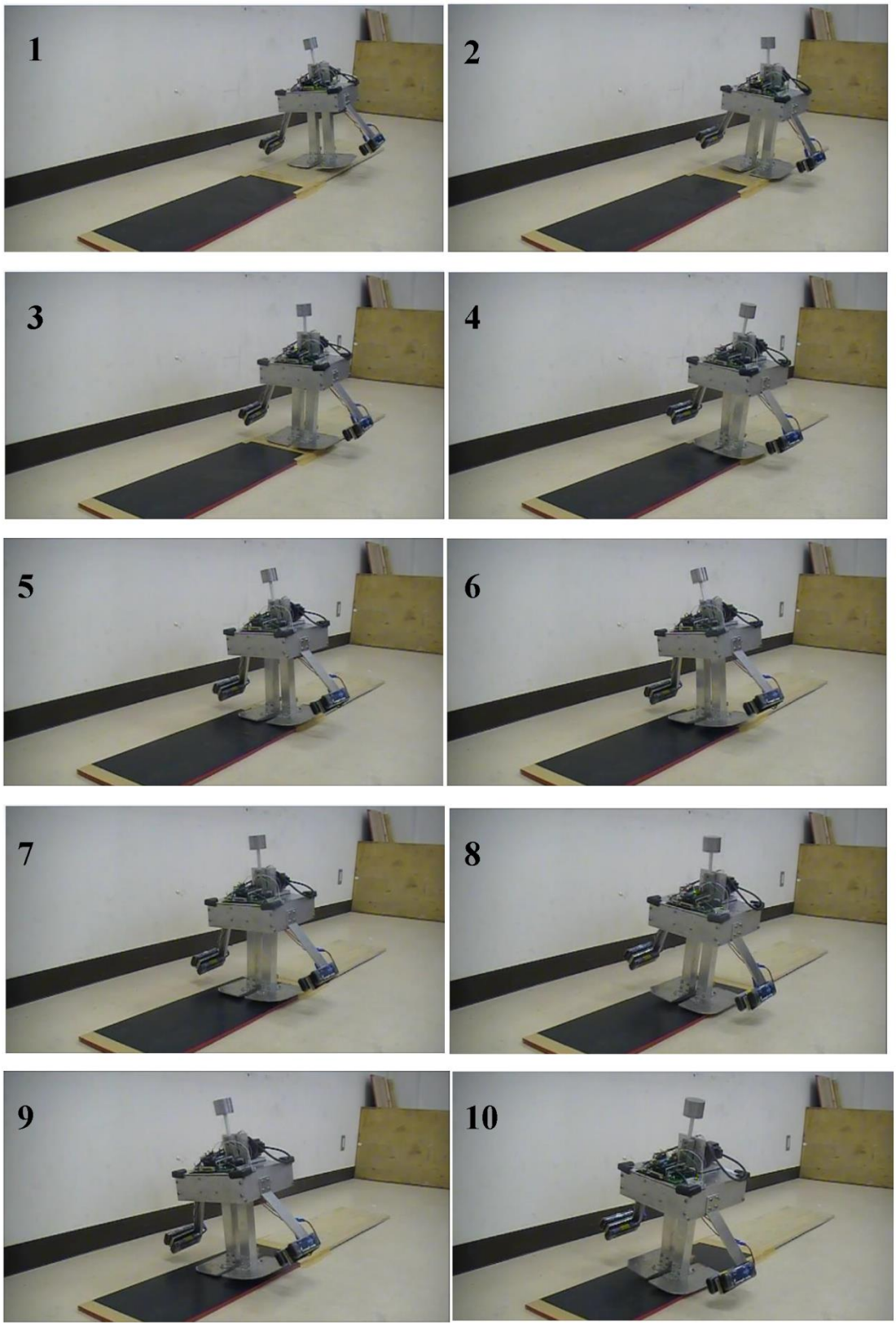

Fig. 5-32 The experiment of walking on a flat path
with different coefficients of restitution

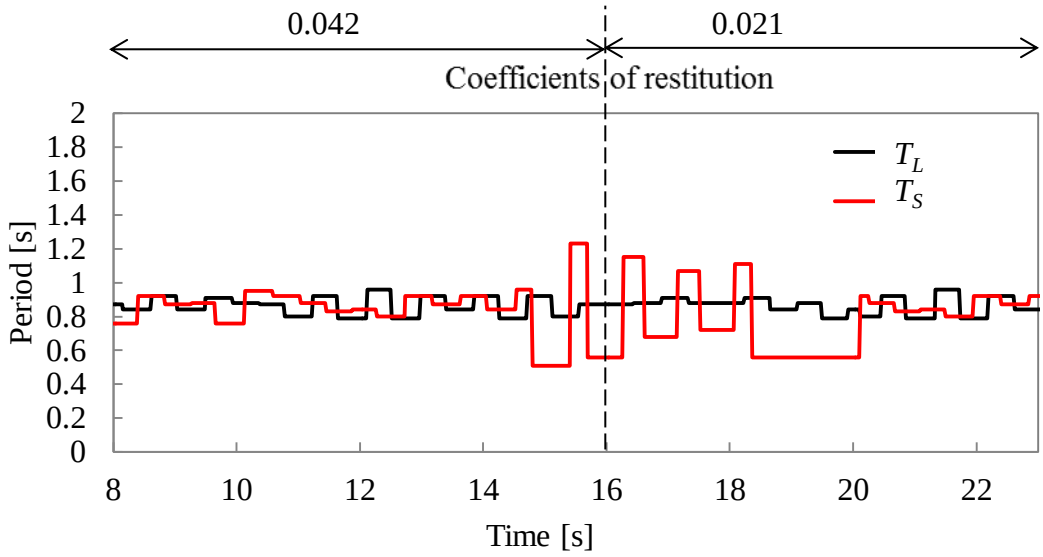

Fig. 5-33 The changes of the period of lateral motion T_L and the period of swing leg motion T_S on a flat path with different coefficients of restitution

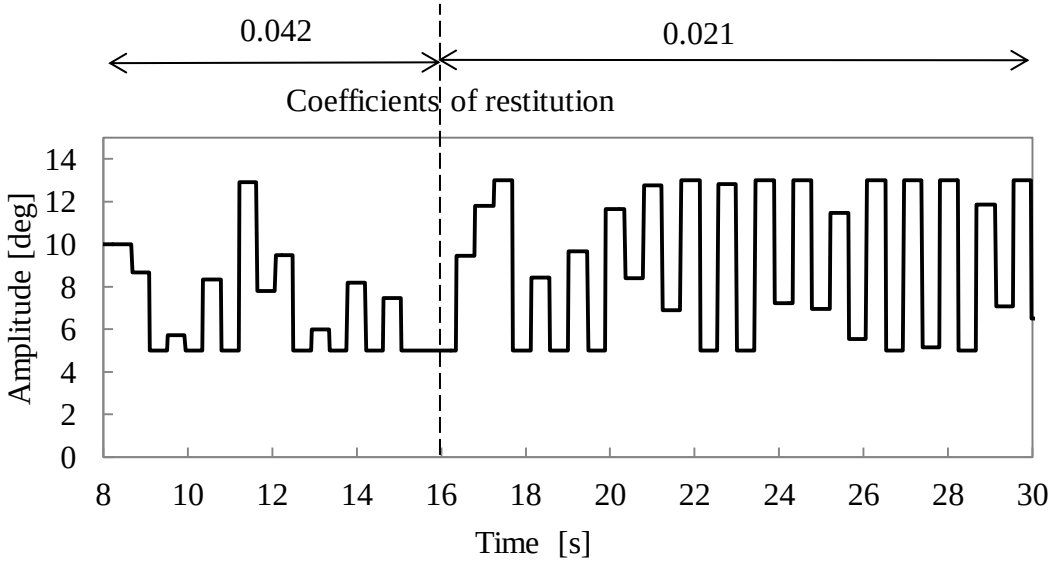

Fig. 5-34 The change of the amplitude of the mechanical oscillator on a flat path with different coefficients of restitution

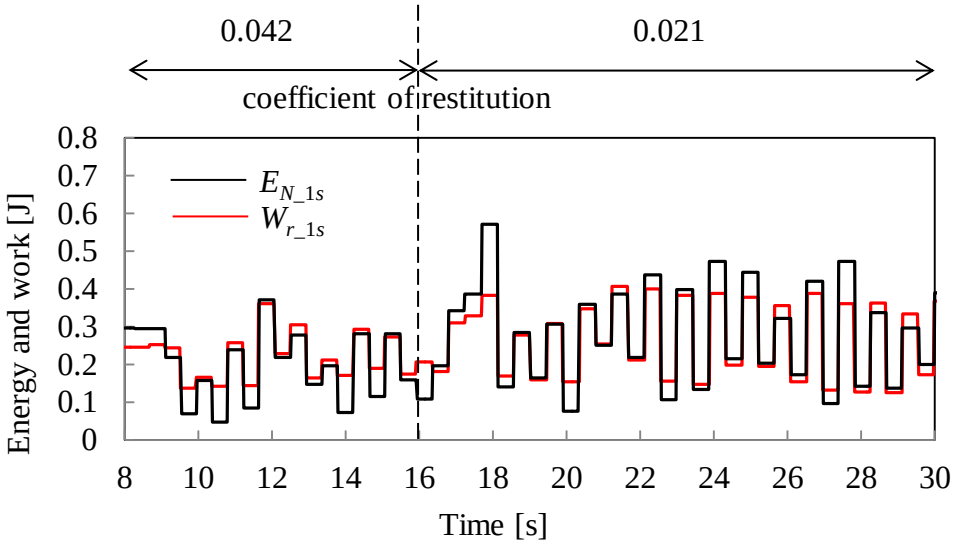

Fig. 5-35 The changes of the input energy E_{N_1s} and the mechanical work performed by the quasi-passive walker W_{r_1s} on a flat path

5.5 Conclusion

In this chapter the stabilization method based on energy balance was numerically and experimentally examined under uncertain ground conditions including different slope angles and coefficients of restitution. The direct and indirect method for the determination of β is examined by simulation. The results of the simulation showed that the environmental adaptability of the quasi-passive walker is significantly improved by the indirect method. The estimation accuracy of the desired input energy is improved by the indirect method.

Moreover, the indirect method for the determination of β was experimentally examined. The results of the experiments showed that the gait of the quasi-passive walker could be stabilized by the proposed stabilization method even under uncertain ground conditions including different slope angles and coefficients of restitution.

6. Conclusion

This research focuses on stabilizing the gait of a 3D quasi-passive walker based on energy balance to improve its environmental adaptability by utilizing the information of gait.

First，in order to improve the environmental adaptability of the quasi-passive walker under complex ground condition, the control methods for turn, uphill and level walking were proposed and examined numerically and experimentally. However, the problem of excess or deficiency of input energy exists because of the determination method of the amplitude of the mechanical oscillator based on "period stabilization condition". Besides, the quasi-passive walker and the control method based on forced entrainment were compared with two similar quasi passive walkers and their control methods based on sine oscillator by applying the sine oscillator to our quasi-passive walker in ODE simulation.

Second，energy efficiency of the quasi-passive walker was investigated and analyzed from the viewpoint of energy transformation. Moreover, energy transfer and transformation during walking were defined and analyzed qualitatively to further understand the mechanism of energy efficient gait of the quasi-passive walker.

Third, according to the energy transformation, energy balance equation in steady walking was proposed. Further, a stabilization algorithm based on energy balance was proposed and examined numerically and experimentally under uncertain ground condition.

Fourth, the dynamics of the lateral motion of the quasi-passive walker and the model of changing motion of stance leg were indicated. Since the approximate linear relationship between the amplitude of the mechanical oscillator β and mechanical work performed by the motor was used to calculate β, the approximate linear relationship was investigated based on the dynamics of the quasi-passive walker. Further, the energy balance equation of stable walking was defined, and a stabilization method based on energy balance was proposed.

Fifth, the stabilization method based on energy balance was numerically and experimentally examined under different ground conditions different slope angles and

coefficients of restitution. The results showed that the environmental adaptability of the quasi-passive walker was significantly improved by the indirect method.

There are several conclusions and finding in this thesis:

(1) Uphill and level walking of the 3D quasi-passive walker was realized on a changeable slope in ODE simulation by improving the determination method of the amplitude of the mechanical oscillator. It was demonstrated that passive gait could be realized even under changeable ground condition by appropriate actuation and control.

(2) In comparison to the control method based on sine oscillator, the control method proposed by this thesis made the quasi-passive walker more robust to initial conditions, because the control method proposed in this research utilized the information of gait. It is demonstrated that appropriate utilization of the information of the gait can improve the environmental adaptability of the quasi-passive walker.

(3) A novel turn control method based on passive walking was proposed and examined. This founding improved the possibility of application of quasi-passive walker under complex ground condition.

(4) The relation between energy utilization rate and energy efficiency of walking was investigated, and it was found that high energy utilization rate could improve the energy efficiency of walking.

(5) Energy transfer, transformation, input and dissipation from the quasi-passive walker to environments were analyzed. The constraint forces of joints transfer mechanical energy to the legs. This founding can explain why a quasi-passive walker with passive hip joints can walk on flat ground and even upward slope.

(6) The dynamics of lateral motion of a model with curved feet was indicated. The relation between the amplitude of the mechanical oscillator and the mechanical work performed by the quasi-passive walker was investigated and clarified based on dynamics.

(7) Energy balance equation in steady walking was proposed and defined according to the energy transformation. Energy balance equation is a necessary condition

of steady walking, and provides a possibility to stabilize the gait of the quasi-passive walker.

(8) A stabilization algorithm based on energy balance was proposed and examined numerically and experimentally. The required input energy of the quasi-passive walker in one step was calculated based on energy balance equation. The environmental adaptability of the quasi-passive walker is significantly improved by the indirect method. The estimation accuracy of the desired input energy is improved by the indirect method.

(9) Based on the idea that utilize the interaction between the quasi-passive walker and environment, the required input energy of the quasi-passive walker in one step can be calculated even under uncertain ground condition by using the information of the gait of the quasi-passive walker. It is because that the gait of the quasi-passive walker is the result of the interaction, and contains the information of uncertain ground conditions. Therefore, the idea was successfully extended to the stabilization control under uncertain ground conditions.

In future work, first, the energy balance of turn will be investigated, and the proposed method based on energy balance will be extended to turn control. Second, the disturbance of external force will be considered in the proposed method, because the disturbance changes the mechanical energy of the quasi-passive walker. Third, the proposed method will be examined in a more human-like quasi-passive walker, such as a quasi-passive walker model with knees. Fourth, the stabilization method based on energy balance can be also applied to stabilize periodic motion other systems.

Acknowledgement

I would like to thank my advisor, Professor Suzuki Soichiro, for his great advice, support, and enthusiasm and for creating an ideal research environment during my three years in the Bio-mechatronics Laboratory. Researching here has been funny and fruitful due to the advice, support, and respect that Professor Suzuki has given me. Professor Suzuki not only gave me advises about the direction of my research, but also let me know the importance of the philosophy for a research of Ph.D.

Thanks to assistant professor Hoshino Yohei for giving advices about my research and pointing out the many flaws and omissions in my researches and thesis. We often talked about my research together, and I learned many things from Professor Hoshino, such as academic theories and technologies.

Thanks to Professor Shibano Junichi, Professor Eisaka Toshino, Professor Sannami Atsuro and associate professor Watanabe Michiko for giving advises on my research and thesis. Based on their advice more examinations and discussions are added into my researches.

Thanks to Iwamoto Reina, Igami Shiyouhei, Sato Takahiko, Endo Yukari and Hashimoto Masaya for their cooperation in the research. They gave me help to build the hardware of the quasi-passive walker, to improve the simulation and experimental models, and complete the simulation and experiments.

Bibliography

[1] A. Tsukahara, Y. Hasegawa, Y. Sankai. Standing-up motion support for paraplegic patient with Robot Suit HAL. IEEE International Conference on Rehabilitation Robotics, Kyoto, Japan, 2009: 211-217.

[2] J. Yoon, R. P. Kumar, A. Özer. An adaptive foot device for increased gait and postural stability in lower limb orthoses and exoskeletons. International Journal of Control, Automation and Systems, 2011, 9(3): 515-524.

[3] C. J. Walsh, D. Paluska, K. Pasch, et al. Development of a lightweight, underactuated exoskeleton for load-carrying augmentation. IEEE International Conference on Robotics and Automation, Orlando, FL, United states, 2006: 3485-3491.

[4] A. M. Dollar, H. Herr. Lower extremity exoskeletons and active orthoses: Challenges and State-of-the-Art. IEEE Transactions on Robotics, 2008, 24(1): 144-158.

[5] S. Y. Okita, V. Ng-Thow-Hing, R. Sarvadevabhatla. Learning together: ASIMO developing an interactive learning partnership with children. IEEE International Symposium on Robot and Human Interactive Communication, Toyama, Japan, 2009: 1125-1130.

[6] Y. Sakagami, R. Watanabe, C. Aoyama, et al. The intelligent ASIMO: system overview and integration. IEEE International Conference on Intelligent Robots and Systems, Piscataway, NJ, USA, 2002: 2478-2483.

[7] K. Hirai, M. Hirose, Y. Haikawa, et al. Development of Honda humanoid robot. IEEE International Conference on Robotics and Automation, Piscataway, NJ, USA, 1998: 1321-1326.

[8] M. Vukobratović, J. Stepanenko. On the stability of anthropomorphic systems. Mathematical Biosciences, 1972, 15(1): 1-37.

[9] M. Vukobratović, B. Borovac. Zero-moment point—thirty five years of its life. International Journal of Humanoid Robotics, 2004, 1(01): 157-173.

[10] S. Kajita, M. Morisawa, K. Miura, et al. Biped walking stabilization based on linear inverted pendulum tracking. IEEE/RSJ International Conference on

Intelligent Robots and Systems (IROS), Taibei, 2010: 4489-4496.

[11] T. Ishida. Development of a small biped entertainment robot QRID. International Symposium on Micro-Nanomechatronics and Human Science, New York, NY, USA, 2004: 23-28.

[12] S. H. Collins, A. Ruina, R. Tedrake, and M. Wisse. Efficient bipedal robots based on passive dynamic walkers, Science Magazine, 2005, 307, 1082-1085.

[13] T. McGeer. Passive dynamic walking, International Journal of Robotics Research, 1990, 9(2), 62-82.

[14] T. McGeer. Passive walking with knees. IEEE International Conference on Robotics and Automation, Cincinnati, OH, USA, 1990: 1640-1645.

[15] T. McGeer. Passive dynamic biped catalogue. Proc. of the 2nd International Symposium of Experimental Robotics. New York,1991,190: 463-490.

[16] A. Goswami, B. Espiau, A. Keramane. Limit cycles and their stability in a passive bipedal gait. IEEE International Conference on Robotics and Automation, Minneapolis, 1996: 246-251.

[17] M. Wisse. Essentials of dynamic walking: Analysis and design of two-legged robots. Delft University, PhD dissertation, 2004.

[18] M.Wisse, R.Q.van der Linde. Delft pneumatic bipeds. Springer Transactions on Advanced Robotics, 2007.

[19] M. Wisse, D. G. E. Hobbelen, A. L. Schwab. Adding an upper body to passive dynamic walking robots by means of a bisecting hip mechanism. IEEE Transactions on Robotics, 2007, 23(1): 112-123.

[20] M. Wisse, D. G. E. Hobbelen, et al. Ankle springs instead of arc-shaped feet for passive dynamic walkers. IEEE-RAS International Conference on Humanoid Robots, Genova, 2006: 110-116.

[21] A. Gosiwami, B. Espiau, A. Keramane. Limit cycles in a passive compass gait biped andpassivity-mimicking control laws. Autonomous Robots, 1997, 4(3): 273-286.

[22] M. W. Spong, F. Bullo. Controlled symmetries and passive walking. IEEE Transactions on Automatic Control, 2005, 50(7): 1025-1031.

[23] M. W. Spong, J. K. Holm, D. Lee. Passivity-based control of bipedal locomotion. IEEE Robotics and Automation Magazine, 2007, 14(2): 30-40.

[24] S. Collin, A. Ruina. A bipedal walking robot with efficient and human-like gait. IEEE International Conference on Robotics and Automation, Barcelona, Spain, 2005: 1983-1988.

[25] R. Tedrake, T. W. Zhang, M. Fong, et al. Actuating a simple 3D passive dynamic walker. IEEE International Conference on Robotics and Automation, New Orleans, LA, United states, 2004: 4656-4661.

[26] R. Tedrake, T. W. Zhang, H. S. Seung. Stochastic policy gradient reinforcement learning on asimple 3D biped. Proceedings of IEEE/RSJ International Conference on Intelligent Robotsand Systems,2004.2849-2854.

[27] M. Wisse. Three additions to passive dynamic walking; actuation, an upper body, and 3D stability. IEEE-RAS International Conference on Humanoid Robots, 2004. 113–132.

[28] Y. Ikemata, A. Sano, K. Yasuhara, et al. Dynamic effects of arc feet on the leg motion of passive walker. IEEE International Conference on Robotics and Automation, 2009: 2755-2760.

[29] M. J. Coleman, A. Ruina. An uncontrolled walking toy that cannot stand still. Physical Review Letters, 1998, 80(16): 3658-3661.

[30] M. J. Coleman, M. Garcia, K. Mombaur, et al. Prediction of stable walking for a toy that cannot stand. Physical Review E, 2001, 64(2): 022901-1 - 022901-3.

[31] S. Collins, M. Wisse, A. Ruina. A three-dimensional passive-dynamic walking robot with two legs and knees. International Journal of Robotics Research, 2001, 20(7): 607-615.

[32] S. Suzuki, M. Hachiya. Experimental Study on Stabilization of a Three Dimensional Biped Passive Walking Robot. Journal of the Society of Biomechanisms. 2008, 32(4): 239-246. (Japanese)

[33] H. Dankowicz, J. Adolfsson, A. Nordmark. Existence of stable 3d-gait in passive bipedal mechanisms. Biomechanical Engineering. 1999, 123(1), 40-46.

[34] P. Piiroinen, H. Dankowicz, A. Nordmark. Breaking symmetries and constraints:

Transitions from 2D to 3D in passive walkers. Multibody system dynamics, 2003, 10(2): 147-176.

[35] P. Piiroinen, H. Dankowicz, A. Nordmark. On a normal-form analysis for a class of passive bipedal walkers. International Journal of Bifurcation and Chaos, 2001, 11(09): 2411-2425.

[36] M. J. Coleman, M. Garcia, A. Ruina, et al. Stability and chaos in passive-dynamic locomotion. IUTAM Symposium on New Applications of Nonlinear and Chaotic Dynamics in Mechanics. Springer Netherlands, 1999: 407-416.

[37] A. Smith, M. Berkemeier. Passive dynamic quadrupedal walking. IEEE International Conference on Robotics and Automation, 1997: 34-39.

[38] M. Garcia, A. Ruina, A. Chatterjee, M. Coleman. The simplest walking model: stability, complexity, and scaling. ASME Journal of Biomechanical Engineering, 1998, 120(2):281-288.

[39] M. Garcia, A. Chatterjee, A. Ruina. Speed, efficiency, and stability of small-slope 2-D passive dynamic bipedal walking. IEEE International Conference on Robotics and Automation, Leuven, Belgium, 1998, 3: 2351-2356.

[40] M. Garcia, A. Chatterjee, A. Ruina. Efficiency, speed, and scaling of two dimensional passive-dynamic walking. Dynamics and Stability of Systems, 2000, 15(2): 75-99.

[41] J. W. Grizzle, G. Abba, F. Plestan. Asymptotically stable walking for biped robots: analysis via systems with impulse effects. IEEE Transactions on Automatic Control, 2001, 46(1): 51-64.

[42] C. Chevallereau, J. W. Grizzle, C. L. Shih. Asymptotically stable walking of a five-link underactuated 3-D bipedal robot. IEEE Transactions on Robotics, 2009, 25(1): 37-50.

[43] A. Chatterjee, M. Garcia. Small slope implies low speed for McGeer passive walking machines. Dynamics and Stability of Systems, 2000, 15(2): 139-157.

[44] M. Coleman, A. Chatterjee, A. Ruina. Motions of a rimless spoked wheel: A simple three-dimensional system with impacts. Dynamics and Stability of Systems,

1997, 12(3): 139-159.

[45] A. L. Schwab, M. Wisse. Basin of attraction of the simplest walking model. Proceedings of the ASME Design Engineering Technical Conference. 2001, Vol. 6: 531-539.

[46] M. Wisse, A. L. Schwab, F. C. T. Van Der Helm. Passive dynamic walking model with upper body. Robotica, 2004, 22(6): 681-688.

[47] D. Owaki, K. Osuka, A. Ishiguro. Understanding the common principle underlying passive dynamic walking and running. IEEE/RSJ International Conference on Intelligent Robots and Systems. 2009: 3208-3213.

[48] Y. Harata, F. Asano, Z. W. Luo et al. Biped gait generation based on parametric excitation by knee-joint actuation. Robotica, 2009, 27(7): 1063-1073.

[49] T. McGeer. Dynamics and control of bipedal locomotion. Journal of Theoretical Biology, 1993, 163(3), 277-317.

[50] T. Narukawa, M. Takahashi, K. Yoshida, “Efficient walking with optimization for a planar biped walker with a torso by hip actuators and springs”, Robotica, 2010, 29(04), 641-648.

[51] A. D. Kuo, Stabilization of lateral motion in passive dynamic walking, International Journal of Robotics Research, 1999, 18(9), 917-930.

[52] M. Hachiya, S. Suzuki. Stabilization of a Biped Quasi Passive Walking Robot via Periodic Input. Journal of the Society of Biomechanisms, 2009, 33(1), 57-63. (Japanese)

[53] S. Suzuki, M. Takada, Y. Iwakura. Stability Control of a Three-Dimensional Passive Walker by Periodic Input Based on the Frequency Entrainment. Journal of Robotics and Mechatronics, 2011, 23(6), 1100-1107.

[54] D. Nakanishi, Y. Sueoka, Y. Sugimoto, et al. Emergence and motion analysis of 3D quasi-passive dynamic walking by excitation of lateral rocking. IEEE/RSJ International Conference on Intelligent Robots and Systems, 2012, 2769-2774.

[55] S. Suzuki, Y. Cao, M. Takada, K. Oi. Climbing and turning control of a biped passive walking robot by periodic input based on frequency entrainment. Advanced Engineering Forum, 2011, 2(3), 48-52.

[56] Russell Smith, “Open dynamics engine v0.5 user guide”, 2006. http://ode.org

[57] R. Rand, “Lecture Notes on Nonlinear Vibrations”, 2012. http://ecommons.library.cornell.edu/handle/1813/28989

[58] D. G. E. Hobbelen, M. Wisse. Limit Cycle Walking. Humanoid Robots, Human-like Machines, 2007, Chapter 14. (I-Tech Education and Publishing, Vienna, Austria).

[59] M. Srinivasan, A. Ruina. Computer optimization of a minimal biped model discovers walking and running. Nature, 2005, 439, 72–75.

[60] J. M. Donelan, R. Kram, A. D. Kuo. Simultaneous positive and negative external mechanical work in human walking. Journal of Biomechanics, 2002, 35(1), 117-124.

Publications and presentations

Publications

1. S. Suzuki, Y. Cao, M. Takada, K. Oi: Climbing and Turning Control of a Biped Passive Walker by Periodic Input Based on Frequency Entrainment, Advanced Engineering Forum—Mechatronics and Information Technology, Vol.2, No.3, pp. 48~52 (published 2012)
2. Y. Cao, S. Suzuki, Y. Hoshino: Turn Control of a Three-Dimensional Quasi-Passive Walking Robot by Utilizing a Mechanical Oscillator, Engineering, Vol.6 No.2, pp.93~99 (published 2014)
3. Y. Cao, S. Suzuki, Y. Hoshino: Uphill and level walking of a three-dimensional biped quasi-passive walking robot by torso control, Robotica (Accepted)

Presentations

1. Y. Cao, S. Suzuki, Y. Hoshino, "Turn Control of a Three-Dimensional Quasi-Passive Walking Robot Based on Forced Entrainment", 2013 IEEE/SICE International Symposium on system Integration, Kobe, Japan. (Dec. 2013)
2. Y. Cao, S. Suzuki, "Energy Transformation and Transfer of a Three-Dimensional Quasi-Passive Walker in Climbing", 日本ロボット学会第 30 回学術講演会 (International session), 4D2-3. (Sep. 2012)
3. S. Suzuki, Y. Cao, M. Takada, K. Oi, "Climbing and Turning Control of a Biped Passive Walker by Periodic Input Based on Frequency Entrainment", Proceedings of ICMIT 2011, Shenyang, China. (Dec. 2011)